International Atomic Energy Agency

INDC(GDR)-34/GI
INT(85)-8

INDC INTERNATIONAL NUCLEAR DATA COMMITTEE

TECHNIQUES OF MEASUREMENTS, ANALYSIS AND INSTRUMENTATION FOR 14 MEV NEUTRON NUCLEAR CROSS SECTIONS

Compiled by
D. Seeliger
Technical University Dresden, German Democratic Republic

October 1985

IAEA NUCLEAR DATA SECTION, WAGRAMERSTRASSE 5, A-1400 VIENNA

INDC(GDR)-34/GI
INT(85)-8

TECHNIQUES OF MEASUREMENTS, ANALYSIS AND INSTRUMENTATION FOR 14 MEV NEUTRON NUCLEAR CROSS SECTIONS

Compiled by
D. Seeliger
Technical University Dresden, German Democratic Republic

October 1985

Reproduced by the IAEA in Austria
October 1985

85-05306

Foreword

This report contains the text of contributed papers reported during the working group sessions of the 13th International Conference on Nuclear Physics - Fast Neutron Reaction held and organized by the Physics Section of the Technical University of Dresden at Gaussig - GDR, during 21-25 November 1983 concurrently with the First Research Co-ordination meeting of the IAEA's Coordinated Research Programme on measurement and analysis of 14 MeV neutron nuclear data needed for fission and fusion reactor technology. The first paper was an invited review paper and the rest were contributed papers (six other invited review papers are already published in a separate INDC report - INDC(NDS)-173/GI). The texts of the papers are directly reproduced from the unedited manuscripts submitted by the authors. It is expected that this report will be useful to those laboratories who are already active in fast neutron nuclear measurements, and especially to those new laboratories where a neutron generator was installed recently and who are planning new neutron nuclear measurement programmes.

Table of Contents

COMMENTS ON (N,CHARGED PARTICLE) REACTIONS AT E_n = 14 MEV *)

Robert C. Haight
Lawrence Livermore National Laboratory, University of California

ABSTRACT

The study of charged particles produced by bombarding materials with 14 MeV neutrons is important for the development of fusion reactors and for biomedical applications as well as for the basic understanding of nuclear reactions. Several experimental techniques for investigating these reactions are discussed here. The interpretation of the data requires the consideration of several possible reaction mechanisms including equilibrium and preequilibrium particle emission and, for light nuclei, sequential particle emission, final state interactions, and the effect of resonances.

I. INTRODUCTION

By the term "(n,charged particle) reaction" we mean those reactions of neutrons with nuclei that result in light charged particles, namely protons, deuterons, tritons, ^{3}He and ^{4}He. For 14 MeV neutrons incident on typical target nuclides, several of these reaction channels are possible. For example, the ^{56}Fe (n,charged particle) reactions at 14 MeV include the (n,p), (n,n'p), (n,d), and (n, alpha) reactions, each with significant cross sections, and the (n,t) and (n,^{3}He) reactions with smaller cross sections. The emitted charged particles have energies from about 1 to 14 MeV. Thus it is expected that the required measurement techniques, the theoretical analyses, and the effects in applications are broad-ranging.

Although these reactions have been investigated for many years, experimental data of high quality are not abundant. The reason is that the experiments are difficult due to low neutron source strengths (even for present-day sources), the short range of the charged particles in matter, and the difficulty of shielding the charged-particle detector from the source neutrons and other background radiation. To obtain data of acceptable quality, most experiments have been optimized so that only one type of charged particle is detected and only a portion of the charged-particle energy

*) Invited Review Paper

spectrum (usually the high end) is measured. Thus even where reasonably good data exist, they are usually incomplete in the energy range of the charged particles and in the particle type.

The present report is not intended to be a comprehensive review of (n,charged particle) reactions. Instead it is a commentary on some facets that are of current interest. Selected experimental methods are listed to point the reader to certain approaches considered successful by the author. The types of physics issues that are crucial to an understanding of the data are discussed.

II. EXPERIMENTAL METHODS

The methods of investigating (n,charged particle) reactions may be grouped into two classes: those that employ the detector material itself as the target and the more general techniques where the target and detector are separate entities. This distinction is useful to indicate which approaches are especially suited to low intensity neutron sources (the former) and which require higher neutron fluxes (the latter).

A. Target = Detector

Because of the short range in matter of charged particles with energies of interest here (about 1 to 20 MeV), a significant increase in the counting rate can be made if the target is not required to be a thin foil from which the charged particles escape but rather a much thicker sample where the particles can be detected internally. Photographic emulsions, scintillators, cloud chambers, and semiconductor detectors have been used as these thicker samples. Of course the materials that can be investigated are those that are major constituents of the detectors or those that can be heavily loaded into them.

Photographic emulsions have many advantages when used as a target-detector combination. They have no dead-time, they allow investigations of many-body decays in kinematically complete experiments, they can be used with broad-spectrum neutron sources in selected experiments, and they are simple yet well characterized, having been used for decades. Of particular note are the experiments on the $^{12}C(n,n')3$ alpha reaction, both old[1] and new.[2] The difficulties of using emulsions include the problems of measuring short tracks (particles of low energy), of kinematically confusing events where two particles have nearly identical directions, and of reactions on other elements in the emulsion. Proton recoils from n-p elastic scattering, for example, are

an unavoidable background. If the element to be studied is not a major component of the emulsion, then it may be difficult to load the emulsion with enough of the element to obtain a good signal-to-background ratio.

Scintillators have been used in the study of (n,charged particle) reactions on ^{6,7}Li, Na, CsI and other materials. Innovative experiments by Bartle[3-5] showed that not only is it possible to measure the energy spectra of the out-going charged particles, but one can in favorable cases also deduce the angular distribution.

Cloud chambers were used many years ago in the study of (n,alpha) reactions on oxygen, nitrogen, and argon.[6] To the author's knowledge no further work is being done with this technique. The time required to analyze the data from many photographs has deterred further experiments of this type.

Semiconductor detectors have been used to measure (n,alpha) and (n,p) reactions on silicon for example.[7] Because of the good resolution available in such detectors, it is possible to resolve individual states populated in the residual nucleus. The recoiling nucleus does carry away some energy and the resolution is consequently worsened. Certain tricks, such as the use of two detectors in coincidence, help overcome this problem.

For all of these approaches where the pulse-time can be recorded (e.g. all except the emulsions and cloud chambers), a coincidence may be made with a pulsed beam or with an associated particle from the neutron source reaction. These coincidences help reduce the background from scattered neutrons, and they can be used to indicate the neutron energy.

B. Target ≠ Detector

To investigate other target nuclides, one must use an approach where the target and the detector are different entities. Many of the types of detectors mentioned above can be used, but in this case they must be shielded from the neutron source lest the (n,charged particle) reaction take place in them rather than in the target. In addition the target must be thin, for example, a thin foil so that the charged particles can escape and pass to the detector.

Data of high quality have been obtained using photographic emulsions as detectors (e.g. Ref. 8) and individual counter telescopes (e.g. Refs. 9). A recent innovative approach to measuring the complete angular distribution of the emitted charged particles has recently been reported.[10]

To improve the signal-to-background ratio in these experiments, three laboratories have developed charged-particle transport schemes to conduct the charged-particle reaction products from the target foil to detectors far away

that can be shielded well from the background radiation.[11-14] Most of these schemes use magnetic quadrupole lenses to focus the charged particles, but not the background neutrons and gamma rays, onto energy-sensitive detectors (Fig. 1). Electrostatic transport is also possible.[12] These transport approaches reduce the background typically by two orders of magnitude and thereby allow the detection, reliably, of charged particles with energies as low as 1 MeV.

III. PHYSICS ISSUES

A rich variety of physical effects have been inferred from (n,charged particle) data at 14 MeV neutron energy. To interpret future data the relative strengths of each of these contributions must be quantified.

For targets of very light nuclei, the reaction mechanism in many cases is not obvious from the charged particle emission data. For example, the alpha-particle emission spectrum from the $^{12}C(n,n')$ 3 alpha reaction has been used to infer a 3-body breakup, 4-body breakup, or sequential two-body break-up. In addition, final state interactions may be important in the multi-body breakup channels. Finally, resonances in the incident channel may confuse the interpretation of the energy dependence of the data, unless data points at many energies are obtained.

For heavier nuclei, say in the range of $20 < A < 70$, the charge-particle emission is dominated by compound nuclear, statistical evaporation. The competition between neutron and charged-particle emission is crucial here, and thus one needs reliable level densities and transmission coefficients derived from the optical model. The energies and spins of low-lying levels can also be important when only a few channels are open for charged-particle emission. In cases where the neutron emission is energetically impossible, one may also require information on the competing gamma-ray decay widths. In many cases, a Hauser-Feshbach calculation that uses state-of-the-art parameters can reproduce the compound-statistical emission (e.g. Ref. 15, see Fig. 2).

Precompound emission of charged particles is evident in some cases near mass 60 and becomes more obvious for heavier nuclides where the compound-statistical contribution is less. With the hybrid formulation of Blann,[16] some of the pre-compound emission data are well described[15] (see Fig. 2) whereas in the molybdenum isotopes significant discrepancies remain between experiment and calculation (Fig. 3).[17] Because the cross sections for (n,charged particle) reactions generally decrease with increasing target mass, measurement of targets heavier than molybdenum is difficult and only a

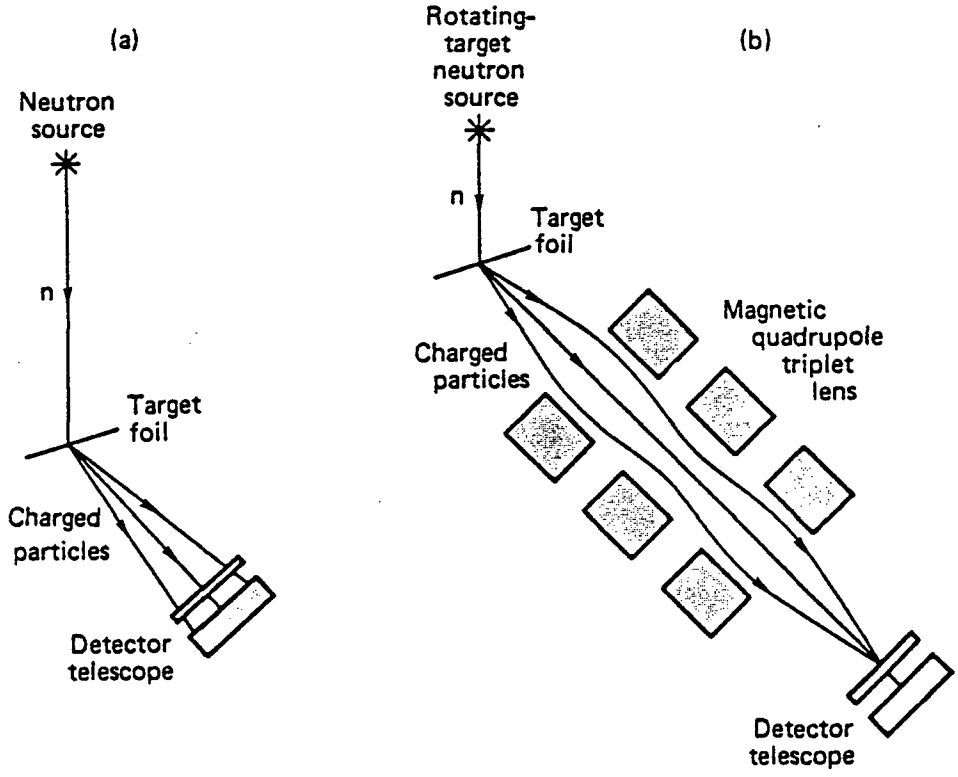

1. Two methods of studying (n,charged particle) reactions: (a) Traditional method; (b) Newly developed method employing a magnetic quadrupoles for transporting the charged particles from their point of production (the target foil) to detectors located in a region of low background.

few groups have attempted such work. Yet with these heavier targets, the ratio of precompound to compound charged-particle emission increases and thus such studies are of great importance in understanding the precompound mechanism.

Direct (n,charged particle) reactions have been studied at 14 MeV in relatively light nuclides (e.g. in the 2s-1d shell and 1-p shell). Charged-particle-induced reaction studies have for many years indicated that the reaction mechanism is complicated at these energies by the contributions of compound mechanisms, multi-step processes, and severe distortion by coulomb effects and the nuclear optical potential. Thus one may prefer to go to higher energies to enhance the direct effects. In any case, for targets of medium and heavy nuclides, the level density in the residual nuclide is often so high that very few states can be separated with the available experimental resolution (150 keV would be considered very good). Thus it is unlikely that much more work will be carried out soon in this area of reaction studies with 14 MeV neutrons. Certain questions, for example of of M1 strength, can be in principle be tackled best by (n,p) investigations, but again the higher incident energy is preferred.

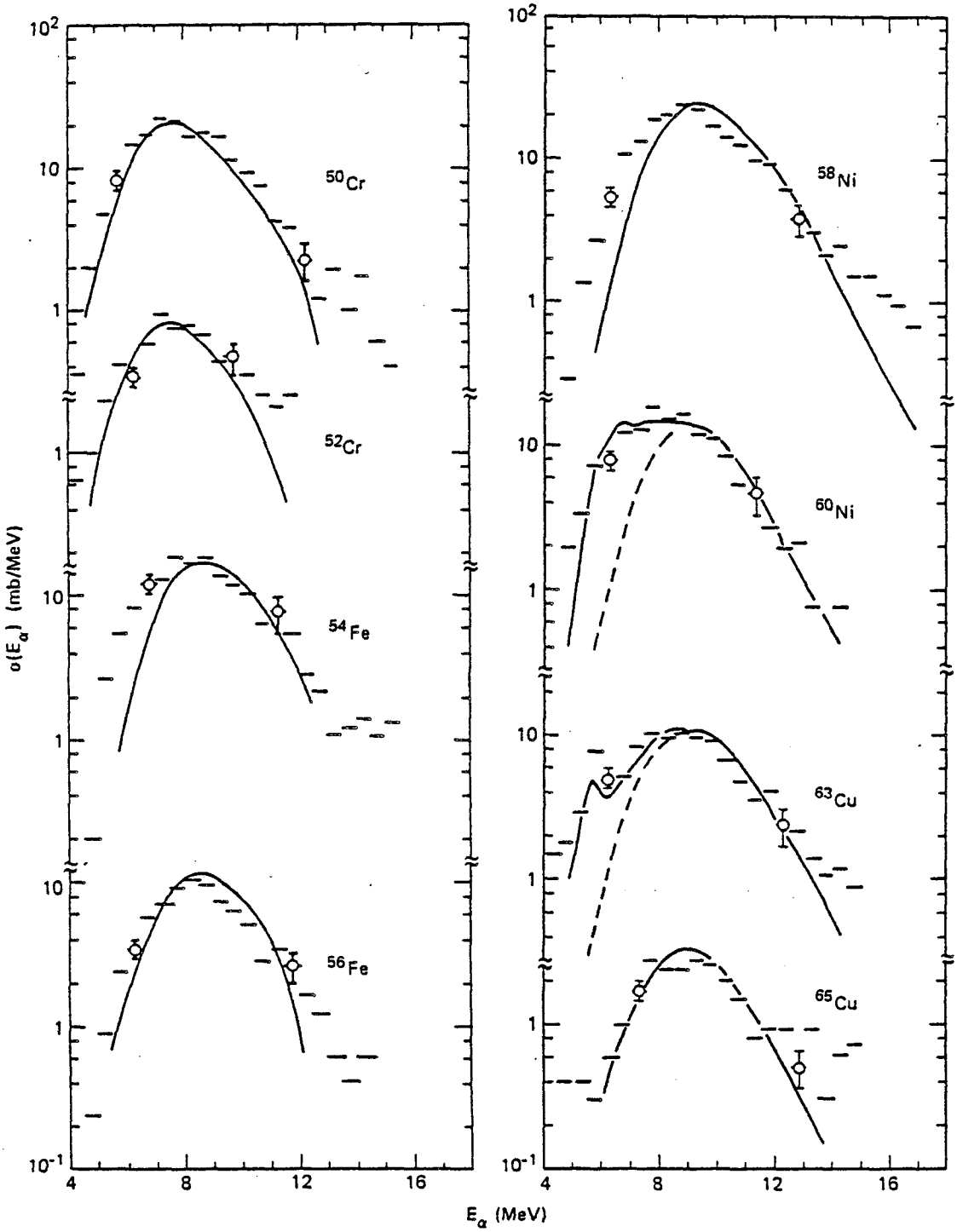

2. Alpha-particle emission spectra compared with Hauser-Feshbach calculations.

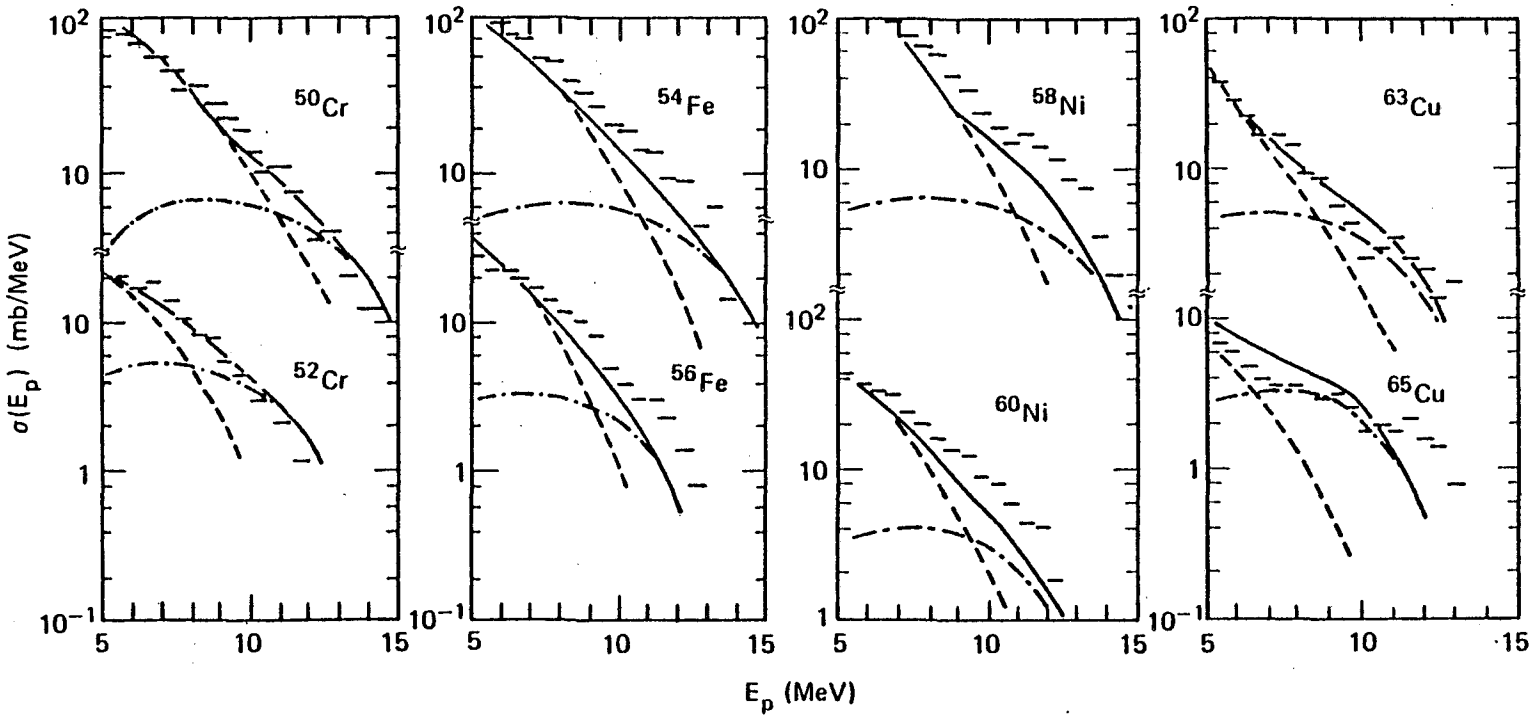

3. Upper end of the proton emission spectra for mass $\tilde{=}$ 60 targets compared with Hauser-Feshbach calculations (dashed curves) and preequilibrium calculations according to the hybrid model (dot-dashed curves). The sums of the model calculations are given by the solid curves.

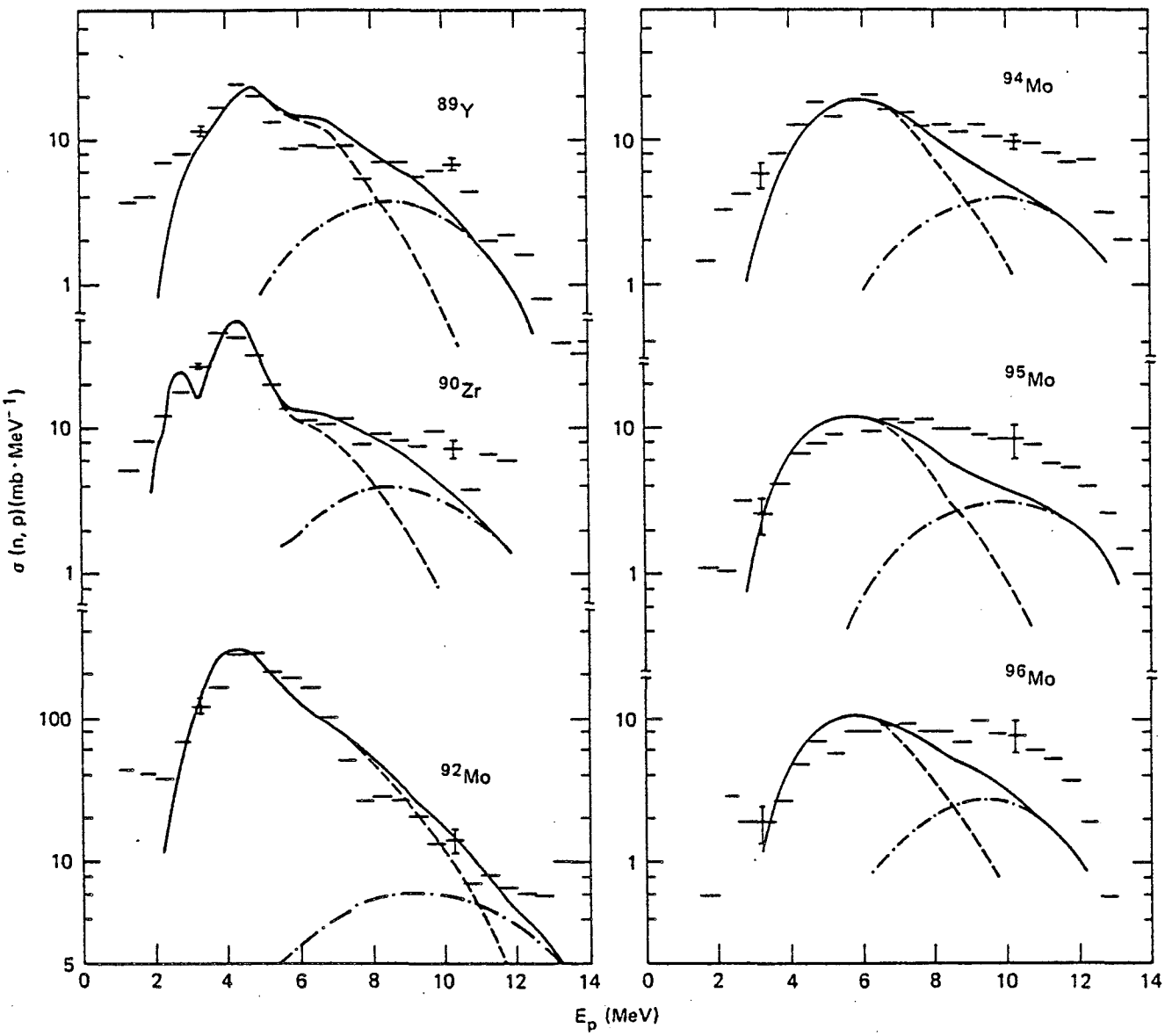

4. Proton emission spectra for mass ≅ 90 targets compared with multi-step Hauser-Feshbach (dashed curves) and hybrid-model (dot-dashed curves) calculations. The sums of the calculations are given by the solid curves.

IV. SUMMARY

Recent developments in experimental techniques are being used to obtain data of much improved quality for (n,charged particle) reactions at 14 MeV. The new data put nuclear reaction models to more stringent tests. In particular our understanding of the compound-statistical model and of precompound particle emission is increasing as a result of these new comparisons between theory and experiment. This increased understanding leads to increased confidence in the data, provided by a combination of experiment and theory, for applications such as in fusion reactor development and medicine.

Work performed under the auspices of the U.S. Department of Energy by the Lawrence Livermore National Laboratory under contract number W-7405-ENG-48.

REFERENCES

1. G. M. Frye, L. Rosen, and L. Stewart, Phys. Rev. 99, 1375(1955).
2. B. Antolkovic, I. Slaus, D. Plenkovic, P. Macq, and J. P. Meulders, Nucl. Phys. A394, 87 (1983).
3. C. M. Bartle, Nucl. Phys. A330, 1 (1979).
4. C. M. Bartle, Nucl. Instr. and Methods 124, 547 (1975).
5. C. M. Bartle, Proc. Conf. on Nuclear Cross Sections and Technology, Washington, DC, NBS Special Publication 425, p. 688 (1975).
6. Y.-C. Hsu, C.-Y. Huang, and C.-C. Chang, Nucl. Phys. A104, 677 (1967).
7. S. M. Grimes, Nucl. Phys. A124, 369 (1969).
8. D. L. Allan, Nucl. Phys. 24, 274 (1961).
9. E. Wattecamps, H.Liskien, and F. Arnotte, Proc. Int. Conf. on Nuclear Data for Science and Technology, Antwerp, 1982, ed. K. Boeckhoff, p. 156 (1983).
10. H. Vonach, this symposium.
11. K. R. Alvar, H. H. Barschall, R. R. Borchers, S. M. Grimes, and R. C. Haight, Nucl. Instr. and Methods 148, 303 (1978).
12. R. C. Haight, R. M. White, and S. J. Zinkle, Proc. Int. Conf. on Nuclear Data for Science and Technology, Antwerp, 1982, ed. K. Boeckhoff, p. 849 (1983).
13. S. M. Grimes, private communication (1983).
14. G. Vourvopoulos, E. Kossionides, and T. Paradellis, Proc. Int. Conf. on Nuclear Data for Science and Technology, Antwerp, 1982, ed. K. Boeckhoff, p. 854 (1983).
15. S. M. Grimes, R. C. Haight, K. R. Alvar, H. H. Barschall, and R. R. Borchers, Phys. Rev. C 19, 2127 (1979).
16. M. Blann, Nucl. Phys. A213, 570 (1973).
17. R. C. Haight, S. M. Grimes, R. G. Johnson, and H. H. Barschall, Phys. Rev. C 23, 700 (1981).

DISCLAIMER

A 14 MEV TIME-OF-FLIGHT SPECTROMETER FOR PRECISE DETERMINATION OF ANGULAR DEPENDENCES AND MEASUREMENT OF NEUTRON EMISSION SPECTRA FROM Pb AND C

T. Elfruth, L. Loska[+]), J. Pöthig, D. Seeliger, K. Seidel, S. Unholzer
Section of Physics, Technical University Dresden, G.D.R.

After extensive study of nuclear reaction mechanisms occuring before the compound nucleus stage of the process by the hand of energy spectra of emitted particles and excitation functions, models have been developed which include the angular distribution of outgoing particles. To test the different approaches, the angular dependence of differential cross sections must be measured carefully.

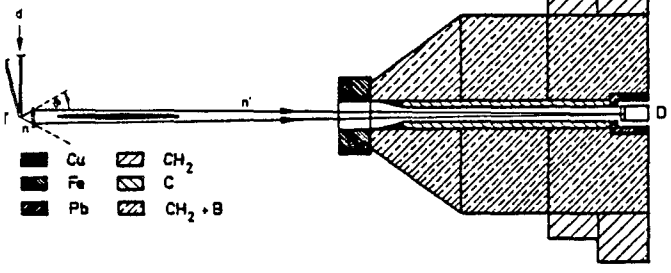

Fig. 1:
Geometrical arrangement of the spectrometer. The distance between tritium target (T) and neutron detector (D) is 5 m

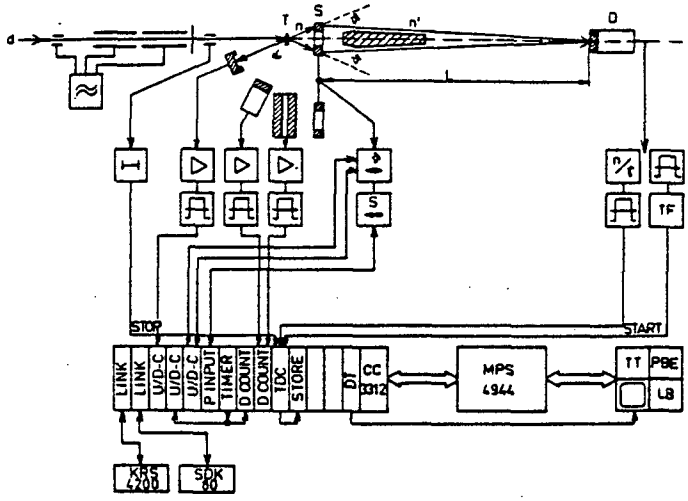

Fig. 2:
Block scheme of the spectrometer. (S - sample changer, ϑ angle alteration, n/γ - neutron-gamma discrimination, CC - controller of the CAMAC crate, U/D - up-and down-counter, TDC - time-analog and analog-digital-converter, DT - display driver, MPS - microcomputer, TT - teletype)

Therefore, a neutron time-of-flight spectrometer with ring-scatterer was arranged perpendicularly to the deuteron axis of the neutron generator. In this way, the neutron incidence energy depends minimal on the scattering angle ϑ and is not asymmetric to $\vartheta = 90^{\circ}$. Furthermore, the spectrometer is controlled by a microcomputer with free-programmable angle alteration and sample changing as well as

[+])fellowship of the IAEA, University of Mining and Metallurgy, Krakow, Poland

data inspection and correction after each run. A run is determined by the number of α-counts choosen so that statistical uncertainties are equal for all ϑ. The data inspection includes the counts in a given range of the time-of-flight spectrum, time drift of the spectrum, the counts of three monitors (α-counter, neutron monitor with plastic scintillator, long-counter like neutron monitor) and timer signals. A spectrum is accumulated only if the inspected values are within a given interval. So, a sequence of scattering angles can be covered many times with almost equal experimental conditions, and instabilities and drifts are eliminated to some degree.
Neutron emission spectra were measured in steps of 15° for Pb and C in the whole angle range. The used samples with inner diameter of 8.0 cm and outer of 12.0 cm had thicknesses of 1.0 cm and 1.5 cm in the case of Pb and of C (pressed powder) respectively so that absorption and multiple scattering were small and equal among each other, inclusively the H-scatterer which is used for normalization. Figs. 3 and 4 show two examples.

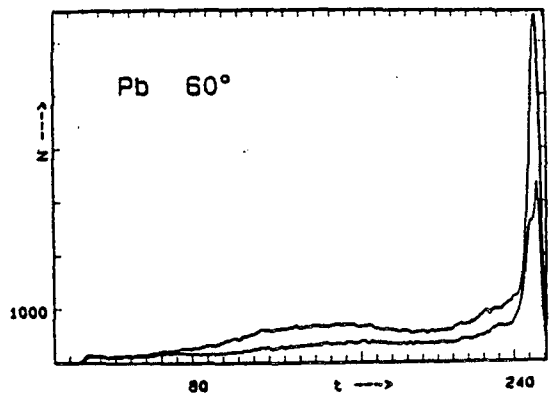

Fig. 3:
Time-of-flight spectrum from Pb, with and without scatterer

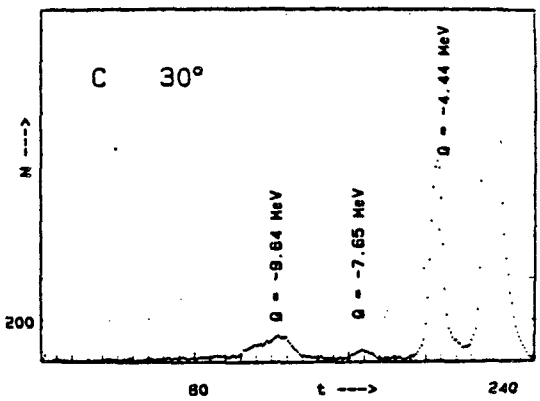

Fig. 4:
Time-of-flight spectrum from C after background subtraction

PULSING SYSTEM OF A 14 MEV NEUTRON GENERATOR FOR TIME-OF-FLIGHT SPECTROSCOPY

H. Helfer, L. Loska[+]), W. Pinkert, D. Seeliger, K. Seidel,
S. Unholzer
Section of Physics, Technical University Dresden, G.D.R.

The time-of-flight method joints high energy resolution with good intensity of the spectrometer. In the fast neutron field, two methods are used which differ in the start time determination. Either the neutron source is pulsed (p.s.) or a charged particle associated with the source neutron gives a pulse (a.p.m.). To compare both methods, the neutron flux available at the detector $d^2N/(dt \cdot dF)$ shall be used as done to characterize the spectroscopic quality of white neutron sources /1/. Taking into account that background coincidences limit the source intensity of the a.p.m., the ratio of fluxes

$$\left(\frac{d^2N}{dt \cdot dF} \right)_{p.s.} \Big/ \left(\frac{d^2N}{dt \cdot dF} \right)_{a.p.m.} \approx \frac{\dot{N}_o \cdot \delta t}{\Delta E / E}$$

where $\dot{N}_o$ is the intensity of the pulsed source, δt is the time resolution and $\Delta E/E$ is the relative energy resolution of the spectrometer. With $\delta t \approx 10^{-9}$s and $\dot{N}_o = \varkappa \cdot 10^9 s^{-1}$, it can be written as $\frac{\varkappa}{\Delta E/E}$. By supplementing of a pulsing system to a usual neutron generator, intensities of some $10^9 s^{-1}$ or more are attainable at time resolutions of 1...2 ns, and such a system must not be expensive /2/. One oscillator (5MHz in our case) feeds the deflection plates of the beam chopper and the tubes of the three-gap buncher. The distance between buncher and target determines the amplitude for the velocity modulation of the deuterons, and the distance between deflection plates and buncher tubes synchronizes both systems. Only if the deuteron energy shall be veried in a wide range or several pulse repetition rates are desirable, the chopper must be fed by an additional oscillator which is synchronized with the buncher oscillator. We want to regist with a flight-path of 5 m emitted neutrons also in the energy range lower than 2 MeV. To

---

[+])fellowship of the IAEA, University of Mining and Metallurgy, Krakow, Poland

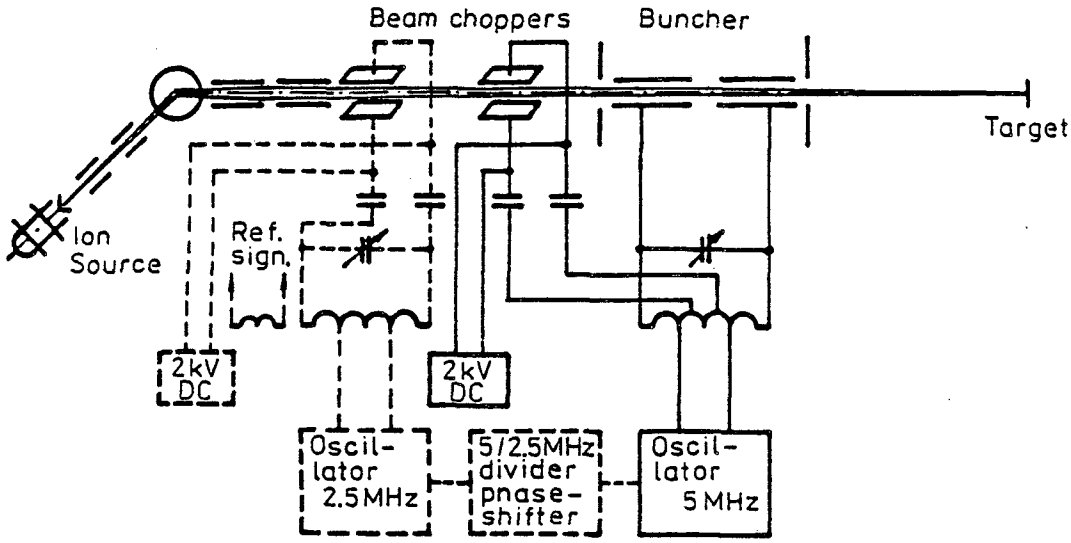

Fig.: Scheme of the pulsing system in basic (——) and extented (---) version

enlarge the neutron source pulse interval from 200 ns to 400 ns, the 5 MHz oscillation is divided and over a phase shifter fed in a 2.5 MHz oscillator. This extended system is in operation but must be further optimized.

References

/1/ S. Cierjacks, Neutron Sources, Pergamon Press, 1983

/2/ D. Seeliger, K. Trützschler, Nucl. Instr. Meth. 66 (1968) 157

DATA PROCESSING OF DIFFERENTIAL NEUTRON EMISSION SPECTRA FROM Pb AND C

T. Elfruth, W. Grimm, L. Loska[+]), J. Pöthig, D. Seeliger, K. Seidel, S. Unholzer
Section of Physics, Technical University Dresden, G.D.R.

Measured neutron time-of-flight spectra contain parts with overlapping levels as well as resolved regions or neutron groups which are to handle as monoenergetic. These parts and neutron peaks among one another must be separated before differential respectively double-differential cross sections are computed. It is convenient to fit peaks and to model background as well as contributions from neighbouring peaks or unresolved parts, in a dialogue via graphic display. A programme consisting of modules which are activated in a dialogue is useful also for the other procedures of data processing. That is realized with the code ISOKON. Besides separation procedures with asymmetric Gaussian functions, it contains background subtraction, dead-time and nonlinearity correction, time scale computation, transformation time-to-energy, normalization to H-scattering and/or monitor counts, consideration of detector efficiency and source anisotropy, correction of finite sample size, cross section computation and transformation from laboratory to center-of-mass system. The formulas were taken from Ref. /1/.

The following figures show examples of differential cross sections in the laboratory system obtained for the indicated neutron groups.

[+])fellowship of the IAEA, University of Mining and Metallurgy, Krakow, Poland

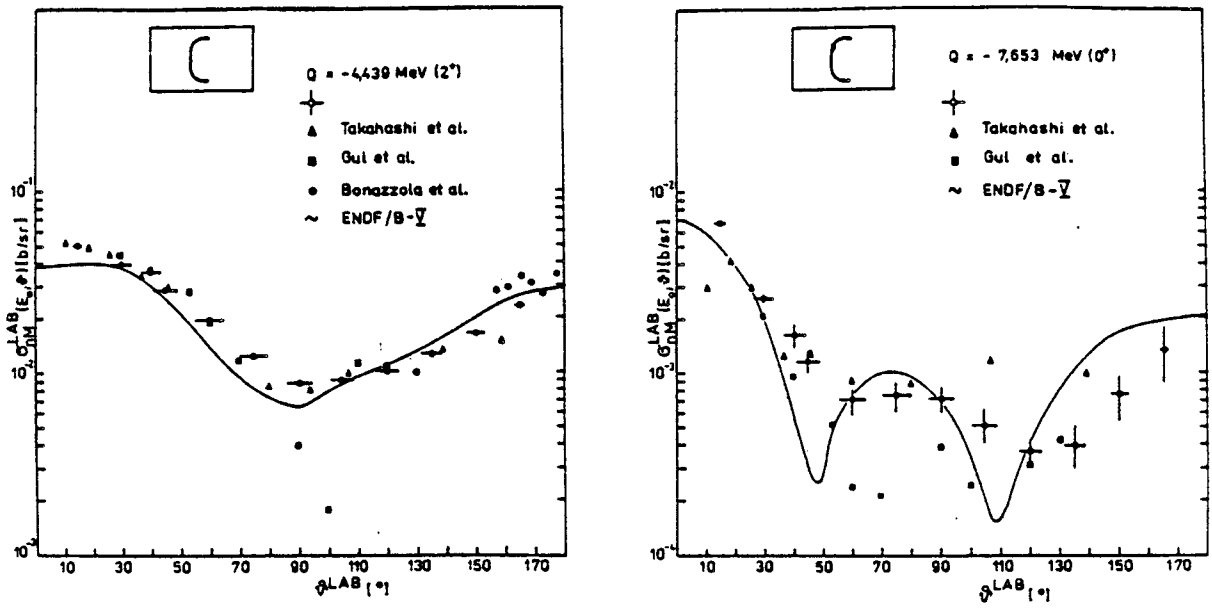

Carbon: The angular distributions are found to be in reasonable agreement with the data of Takahashi et al./2/ and Bonazzola et al. /3/. A neutron group interpreted for the first time by Gul et al. /4/ as $^{12}C(n, n)$ reaction, seems to appear in the whole angle range.

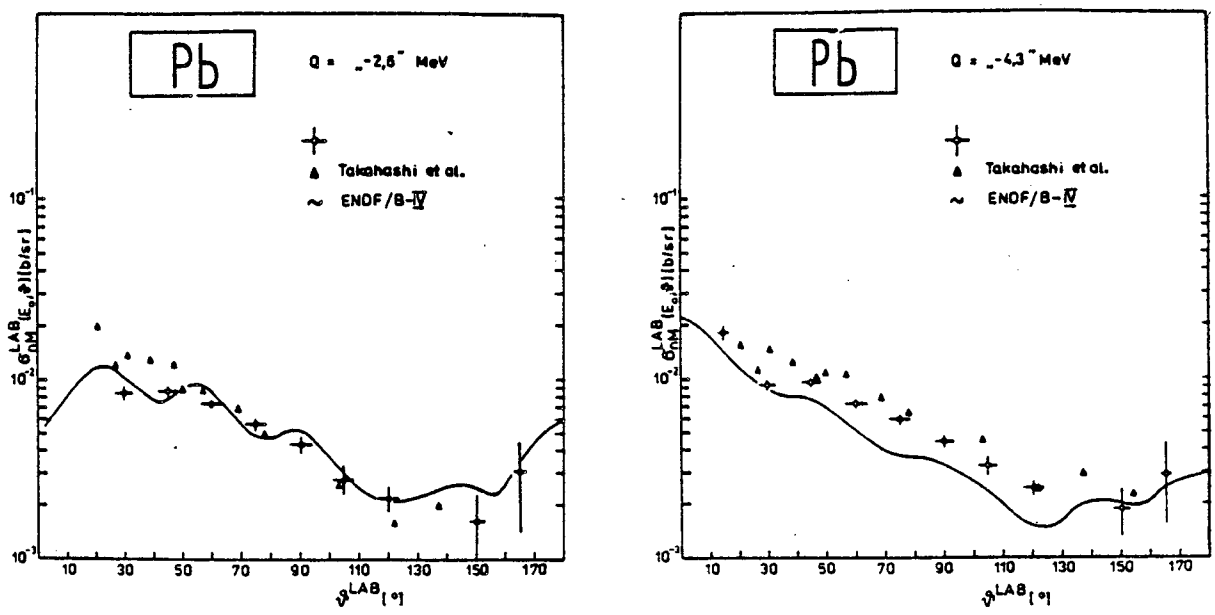

Lead: Good agreement is found with the data reported by Takahashi et al./2/ as well as with the evaluated data of ENDF/B-IV.

References

/1/ H.D. Giera et al., Kernenergie 14 (1971) 115
/2/ A. Takahashi et al., Int. Conf. on Nuclear Data for Science and Technology, Antwerp, 1982
/3/ C. Bonazzola et al., Lettre al Nuovo Cimento 3 (1972) 99
/4/ K. Gul et al., Phys. Rev. 24 (1981) 2458

ON PHENOMENOLOGICAL CALCULATIONS OF CONTINUOUS PARTICLE SPECTRA BY GEM AND DI

D. Hermsdorf, H. Kalka, D. Seeliger
Technical University of Dresden, Department of Physics,
GDR - 8027 Dresden, Mommsenstr. 13

Abstract:

An attempt has been undertaken for a complete description of continuous spectra of inelastically scattered fast neutrons in terms of phenomenological models.

Deviations from systematical description by GEM appear in the region of double-magic nuclei only.

1. Models

After capturing of a fast neutron, the excited nucleus will occupy different states during its time-evolution . If the nucleus is considered to be a degenerated Fermigas, the excited states can be subdivided in an adiabatic approximation into two groups: the pure quasi-particle states (exciton-states) and the collective states respectively.

Whereas the excitation of low-lying collective states are assumed to be fast (or direct) processes, the description of quasi-particle excitations can only be treated by statistical methods. A purely microscopical treatment of them has been given in Feshbach's MSDR and MSCR formalism /1/ in the representation of the Fermigas-Model. The derivation of MSDR and MSCR was done in RPA including states of different complexity starting from the 2p-1h-doorway state up to the so-called CN. Therefore, an addition of excitations of internal degrees of freedom introduced in direct reactions is not necessary.

In contrast to the very complicated MSDR and MSCR formalism the phenomenological Exciton-Model can be solved by convenient numerical methods. Basing on the time-dependent perturbation theory and other crude assumptions, the fundamental equations of the Exciton -Models show a similar structure as the MSDR/MSCR. Exciton-Models can't distinguish MSD and MSC processes because of the application of William's state densities /2/ which account for all states belonging to bound particles as well as particles in the continuum.

For a simulation of MSDR and MSCR an Exciton-Model has to include pre-equilibrium and equilibrium emissions within an unified formalism. Therefore, any solution can't be given by "Closed-Form-Models" but only by a "master-equation-approach" integrating the master-equations from $t = 0$ to $t = \infty$. This is done in GEM exactly /3/.

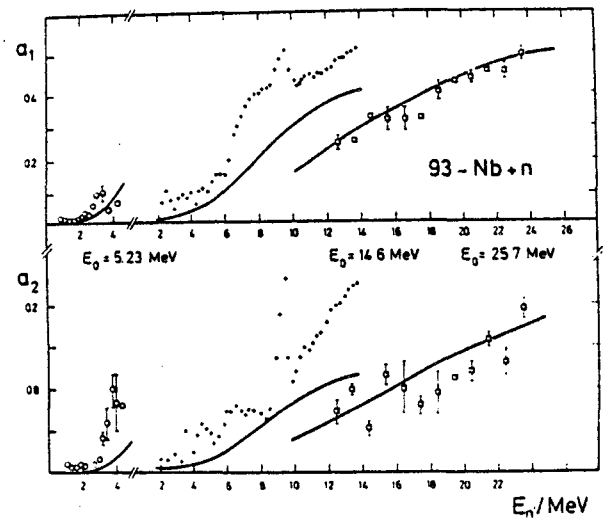

Fig. 1
Relative Legendre coefficients a_1 and a_2 for ^{93}Nb. Experimental data taken from Lovchikova et al. (5.23 MeV), Hermsdorf et al. (14.6 MeV) and Marcinkowski et al. (25.7 MeV) are compared with calculations by AMAPRE (solid lines) /5/.

Whereas the GEM for spectra integrated over solid angle includes MSDR as well as MSCR, angular distributions calculated in terms of the formalism of the "leading particle" /4/ can only be compared with MSDR. Neglecting MSCR-contributions having symmetrical angular distributions all even coefficients of Legendre-polynomial series will be underestimated by the GEM. With increasing incidence energy the increase of MSDR-component is expected yielding better agreements with experiments as demonstrated in fig. 1.

The total emission spectrum has to be incoherently superimposed from spectra

- of excitation of low-lying collective states calculated by DWBA or CCBA models as a one-step-process using ß-parameters and
- of quasi-particle excitations estimated by GEM using code AMAPRE.

Table 1: Input parameter and other quantities of GEM (accuracy in the order of 10 %).

	$\frac{E_0}{MeV}$	$\frac{g}{MeV^{-1}}$	$\frac{g_1}{MeV^{-1}}$	$\frac{\lvert M\rvert^2}{MeV^2 \cdot 10^6}$	$\frac{K}{MeV^3}$	$\frac{\lambda^+}{s^{-1} \cdot 10^{22}}$	$\frac{B_n}{MeV}$
Nb	5.23	6.5	6.8	97	1000	0.4	7.2
	7.23	6.5	6.8	84	1000	0.5	7.2
	14.6	6.5	6.8	56	1000	0.8	7.2
	25.7	6.5	6.8	37	1000	1.2	7.2
Bi	7.75	7	6	74	8500	0.4	4.7
	14.6	9	8.5	23	4100	0.7	4.7
	25.7	10	10	7	2100	0.8	4.7
Pb	14.6	10	8	16	3000	0.75	5.5

g = single state density in the composite nucleus
g_1 = single state density in the 1st residual nucleus
B_n = neutron binding energy in the composite nucleus

2. Calculations

Investigations have been carried out for Nb, Bi and Pb for neutron incidence energies ranging from 5 to 25 MeV /5/.

Angular distributions are represented by the normalized coefficients of Legendre-polynomial series

$$\sigma_{n,n_1}(E_o;E_n,\vartheta) = \sigma_{n,n_1}(E_o;E_n)\left[1+\sum_{l=1}(2l+1)\,a_l(E_o;E_n)\,P_l(\cos\vartheta)\right]/4\pi.$$

The coefficients for l = 1,2,3,4 are calculated by the code AMAPRE using the Correlated-Emission-Model /6/ which is an improved version of GEM.

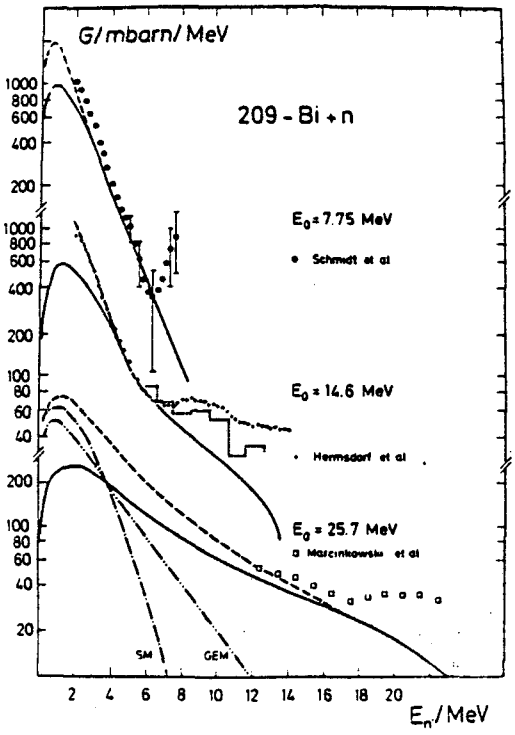

Fig. 2
Description of neutron emission spectra by the GEM and DI for ^{209}Bi. Calculations in terms of DI have been carried out by Ignatyuk et al. /5/.

The first group of input-data for AMAPRE demands inverse cross sections, binding energies for neutrons and the eigenvalues $/u_l$ of intranuclear scattering corrected for the Fermi-motion and Pauli-principle /7/. These data kept fixed for all calculations concerning an individual nucleus.

Other, individual properties of nuclei are described in the second input-data group consisting of the single particle state densities g and the matrixelement for the two-body-interaction $|M|^2$.

Whereas $|M|^2$ is the only free parameter in the case of Nb, for Bi and Pb also the state densities g had to be fitted additionaly to achieve a satisfactory agreement. Some results of all calculations /5/ are summarized in table 1 and shown in figs. 1 and 2.

Instead of $|M|^2$, the transition rate λ^+ from initial exciton state can be used as adjustable parameter referring to the relation $\lambda^+ \sim g^3 |M|^2$.

3. Conclusions

Comparisons with experimental results clearly demonstrate the success of calculations by use of GEM and DI in description of the double-differential cross section for fast neutron nonelastic scattering processes.

In contrast to the nuclei lying far off closed shells (Nb), the nuclei in the double magic region (Pb, Bi) can't be interpreted with a state density g = A/13 resulting from systematics. An energy dependence of g has been observed explainable by means of a phenomenological level density formula derived by Ignatyuk /8/.

References

/1/ H. Feshbach, A. Kerman, S. Koonin, Ann. Phys. 125 (1980) 429

/2/ F.C. Williams Jr., Nucl. Phys. A166 (1971) 231

/3/ J.M. Akkermans, H. Gruppelaar, G. Reffo, Phys. Rev. C22 (1980) 73

/4/ G. Mantzouranis, D. Agassi, H.A. Weidenmüller, Phys. Lett. 57B (1975) 220, Z. Phys. A276 (1976) 145

/5/ D. Hermsdorf, H. Kalka, D. Seeliger, A.V. Ignatyuk, V.P. Lunev, Proc. Conf. Kiev of Neutron Physics, 1983, in press

/6/ C. Costa, H. Gruppelaar, J.M. Akkermans, Phys. Rev. C28 (1983) 587

/7/ Sun Ziyang et al., Z. Phys. A305 (1982) 61
J.M. Akkermans, ECN-121 (1982)

/8/ A.V. Ignatyuk, Phys. and Appl. Vol. 10, Proc. Conf. Smolenice, 1982, p. 211

THE USE OF A ^{252}Cf SOURCE FOR NEUTRON DETECTOR CALIBRATION

H. Märten, D. Neumann and D. Seeliger
Technische Universität Dresden, GDR

^{252}Cf sources are widely used for neutron detector calibration at energies between about 0.5 and 8 MeV, i.e. the spectrum range with a sufficiently high emission probability N(E). In particular, neutron time-of-flight (TOF) spectrometers may be calibrated (or checked) regarding

i) the efficiency curve $e_d(E)$ for a fixed bias energy B,
ii) the $e_d(E,B)$ field on the base of a two-dimensional (TOF,LO)-measurement [6] (LO - light output of the scintillation detector),
iii) the accurate determination of B, i.e. the LO threshold of the spectrometer [7].

An IAEA Consultants' Meeting on the ^{252}Cf fission neutron spectrum [1] was held to summarize recent precise measurements with improved experimental techniques and analysis procedures (concerning data correction). A new evaluation was strongly recommended. The application of ^{252}Cf sources for calibration purposes requires the consideration of secondary annoying effects or their avoidance by special arrangements (Table 1). The ^{252}Cf fission neutron spectrum measured by the use of TOF spectrometers is influenced by the non-isotropic fragment detection (timing signal) due to the absorption in the sample plane or geometrical conditions. As an alternative to the Monte Carlo study by Chalupka [2], we calculated the measurable distribution $G(E,\beta)$ (β - angle of neutron emission with regard to the sample plane normal) analytically [4]. Fig. 1 shows the ratio $G(E,\beta)/N(E)$ in the case of a 5 % inefficiency (1-e) of the fragment detector. At an angle of about 60 deg, this ratio is nearly constant and amounts to about e. The fragment detector efficiency e can be determined by the measurement of neutron-fragment coincidences or appropriate measurements of $G(E,\beta)$. For instance, the integral anisotropy ratio for a given neutron detector bias B is

$$G_B(90\ \text{deg})/G_B(0\ \text{deg}) = 1 - m(B) \cdot (1 - e) \qquad (1)$$

with a B dependent parameter m as shown in Fig. 2.

TABLE 1

Annoying factors in fission neutron spectrum measurements and their consideration (avoidance, data correction)

Annoying factor	Consideration	Ref.
Scattering and absorption of fission neutrons (detector materials, air, collimator etc.)	Correction on the base of i) theoretical calculations, ii) appropriate measurements (concerning scattering)	5 2
Associated alpha-activity of the Cf source	Use of appropriate fragment detectors (ionization chamber, gas scintillator, avalanche detector)	2
Non-correlated timing signals	i) electronic pile-up rejector ii) analytical correction	5 3
Dead-time losses	analytical correction	-
Time resolution	TOF spectrum unfolding on the base of an E dependent time resolution function (due to neutron detector dimensions)	-
Non-isotropic fragment detection	analytical correction (see text)	2,4

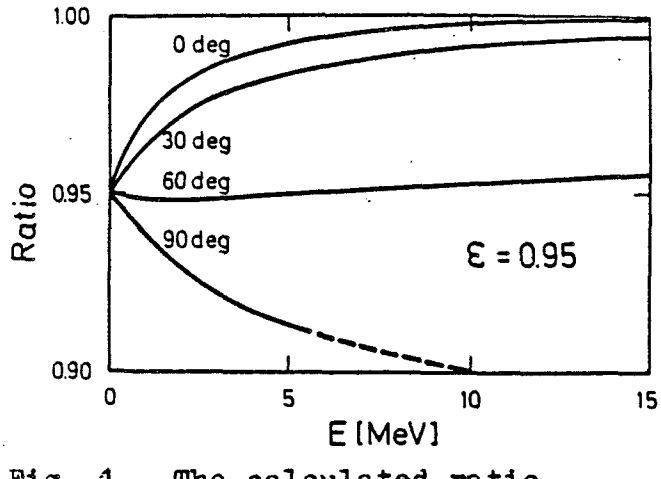

Fig. 1 The calculated ratio G(E,ß)/N(E) at selected ß

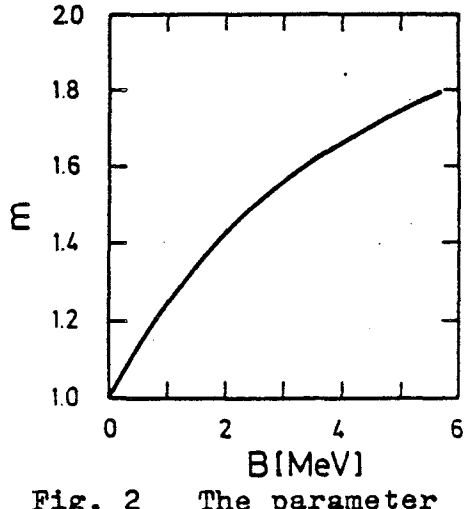

Fig. 2 The parameter m(B) of Eq. 1 (calc.)

References

1 - Proc. IAEA Cons. Meet. on the Californium-252 Fission-Neutron Spectrum, Smolenice, 1983, in press
2 - A. Chalupka et al., ibid.
3 - H. Klein et al., ibid.
4 - H. Märten et al., ibid.
5 - O.I. Batenkov et al., ibid.
6 - H. Märten et al., INDC(GDR)-17/L
7 - R. Franke et al., Nucl. Instr. Meth. 198(1982)311

TENDENCY OF DIRECT EXCITATION BY NEUTRONS SCATTERING AT BOMBARDING ENERGIES BELOW 15 MEV ON LIGHT NUCLEI

M. Adel-Fawzy, H. Förtsch, D. Schmidt, D. Seeliger, T. Streil
Technical University of Dresden, Department of Physics,
GDR - 8027 Dresden, Mommsenstr. 13

1. Introduction

The direct excitation is known to give an essential contribution to the reaction mechanism in neutron scattering on low-lying collective states in the target nucleus.

The aim of the present work in the theoretical analysis of the experimental data, obtained under same conditions with a consistent set of parameters in a wide energy range and including higher-excited states to get more information about the reaction mechanism and also the nuclear structure. The light even-even nuclei ^{24}Mg, ^{28}Si, and ^{32}S have been selected because they are known to have a quite different nuclear structure.

2. Experimental procedure

The differential cross sections were measured with the tandem facility in the CINR Rossendorf. The measurements were carried out with a computer-coupled multi-angle TOF-detector system consisting of eight detectors /1,2/.

3. Analysis of the experimental data and some conclusions

The excitation mechanism for the low-lying excited states in even-even light nuclei is described in the present work by an incoherent sum of two components: the emission from the compound nucleus treated within the Hauser-Feshbach-Moldauer theory and the direct excitation calculated within the collective model using the coupled channels method. The models used influence each other because in both models the reaction channels which are not treated explicitely are considered as an absorption term. It is discussed in detail how one has to fix the absorptive potential $W_S(E)$ in ref. 2.

It could be demonstrated that from the investigation of the first 2^+ state only, we cannot conclude definitely the energy dependence of W_S, therefore the description of higher-lying states has to be included. In the case of ^{32}S this was inpossible because of the experimental conditions. For the energy-dependent absorption term W_S we found the following values:

^{32}S : W_S = 8.50 MeV;
^{24}Mg: W_S = 0.5·E $\leq$ 5.43 MeV;
^{28}Si: W_S = 0.6·E

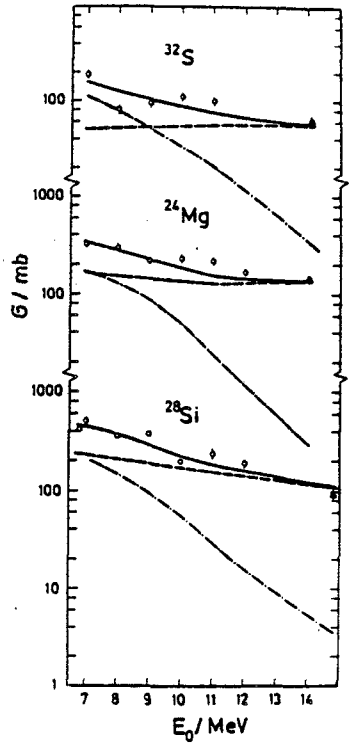

Fig. 1
Angle-integrated cross sections to the first 2^+ states; -·- HF, --- CC, —— HF+CC, see also text; data ϕ, ϕ, ϕ taken from refs. 3,4,5.

The other optical model parameters were taken from literature and tested by the comparison with the first 2^+ angular distribution.

Fig. 1 shows the competition of both components in the reaction mechanism at all bombarding energies investigated. In general the direct excitation of the first 2^+ states in these three even-even nuclei doesn't change rapidly with the bombarding energy between 7 and about 15 MeV. The small differences: rising curve for ^{32}S, decreasing curve for ^{28}Si, intermediate behaviour for ^{24}Mg are caused by the different energy dependence of W_S only. The compound nucleus contribution decreases rapidly with increasing energy due to the growing number of open channels for the compound nucleus decay. In this way the direct excitation dominates at bombarding energies higher than 10 MeV.

Fig. 2
Angular distributions from inelastic scattering on ^{24}Mg; data □ taken from ref. 4.

Fig. 2 shows that for 7 MeV the shape of the angular distribution is inprinciple symmetrically and the structure is small. Compound nucleus contribution and direct one are in the same order. But for 14 MeV the shape of the angular distribution will be forward peaked and the compound nucleus will be very small.

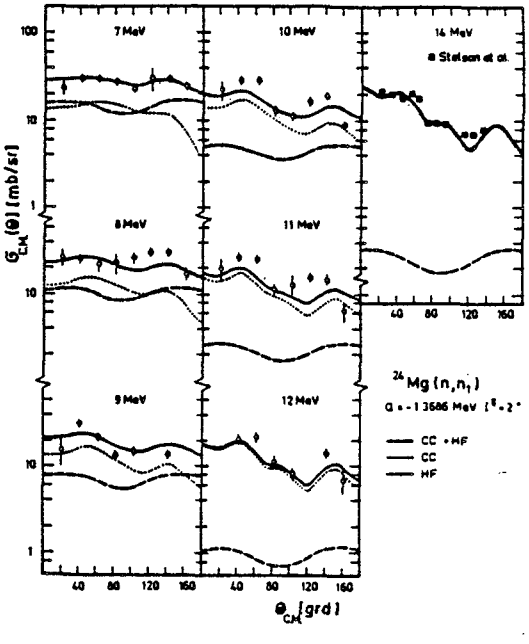

References

/1/ P. Eckstein et al., Nucl. Instr. Meth. 169 (1980) 533
/2/ M. Adel-Fawzy et al., submitted to Nucl. Phys.
/3/ R.L. Clarks and W.G. Cross, Nucl. Phys. 53 (1964) 177
/4/ P.H. Stelson et al., Nucl. Phys. 68 (1965) 97
/5/ J. Höhn, H. Pose and D. Seeliger, Nucl. Phys. A134 (1969) 289

ABSOLUTE FISSION CROSS-SECTIONS AT 14.7 MeV, 4.5 MeV AND 18.8 MeV NEUTRON ENERGIES

R.Arlt, H.Bohne, C.M.Herbach, M.Josch, G.Musiol, H.G.Ortlepp, G.Pausch, W.Wagner, Technical University of Dresden (TUD)

I.D.Alkhazov, L.V.Drapchinsky, A.V.Fomichev, O.I.Kostochkin, V.I.Shpakov, Chlopin-Radiuminstitute Leningrad (RIL)

During the last years the Time-Correlated Associated Particle Method (TCAPM) was used to determine absolute fission cross-sections. A review of our results at 2.6 MeV, 8.5 MeV and 14.7 MeV up to the end of 1982 including a correlation analysis of the uncertainties was given in /1/. The particular corrections applied to the ^{233}U and ^{242}Pu TUD measurements at 14.7 MeV were not published until now and are shown in tab.1. The procedure to determine these corrections typical for the TCAPM was described earlier /2/. Particular problems of the ^{233}U and ^{242}Pu measurements were connected with the contents of other nuclides in the sample material. The areal densities of the fission foils were determined by low geometry alpha counting. The half-life uncertainties, especially for the short lived components of the ^{242}Pu sample, caused considerable errors. The experimental data of the ^{242} Pu TUD measurement were reanalysed using more recent half-lifes /3/, and the resulting cross-section became smaller by about 3 % compared with the value published earlier. Following the recommendations of the IAEA Consultants Meeting in Smolenice /4/ first TCAPM measurements were performed at the tandem van-de-Graaff accelerator of the CBNR Rossendorf at 4.5 MeV and 18.8 MeV neutron energies. The uncertainties of the preliminary results (tab. 1) are due mainly to the poor statistics of the relatively short runs; longer measurements are in preparation. Further investigations are necessary to reduce the relatively high background in the associated particle channel at 18.8 MeV.

/1/ V.N.Dushin, et al., IAEA Consult. Meeting, Smolenice, Czech., March 28 - April 1, 1983

/2/ R.Arlt, et al., Kernenergie 24 (1981) p.48

/3/ Proposed Recommendet List of Transactinium Isotope Decay Data, Part I. Half-Lifes (December 1980 Edition): INDC (NDS)-121/NE

/4/ Conclusions and Recommendations of Working Group on the U-235 Fast Fission Cross-Section; IAEA Consult. Meeting, Smolenice, Czech., March 28 - April 1, 1983

Tab. 1: Corrections and uncertainties of the fission cross-section measurements on ^{233}U and ^{242}Pu at 14.7 MeV and on ^{235}U at 4.5 MeV and 18.8 MeV neutron energies

	^{233}U at 14.7 MeV		^{242}Pu at 14.7 MeV		^{235}U at 4.5 MeV		^{235}U at 18.8 MeV	
Source of Error	Correct.	Part. Error	Correct.	Part. Error	Correct.	Part Error	Correct.	Part. Error
Sample weighting		0.8 %		0.8 %		0.93 %		0.93 %
Sample inhomogenity		0.7 %		1.5 %		0.72 %		0.72 %
Sample composition and neutron scattering	7.63 %	0.8 %	2.61 %	0.25 %		0.7 %+)		0.7 %+)
Fission chamber efficiency								
- Extrapolation to zero pulse hight	1.69 %	0.35 %	4.10 %	0.65 %	0.74 %	0.3 %	1.38%	0.27 %
- Fragment absorption in the fissile layer (s)	0.33 %	0.2 %	0.82 %	0.4 %	2.04 %	0.6 %	1.73%	0.38 %
Counting of coincidences								
- Statistics		1.0 %		1.0 %		2.52 %		2.24 %
- Random coincidences	5.07 %	0.3 %	6.29 %	0.4 %	0.55 %	0.2 %	2.38 %	0.52 %
Counting of associated particles								
- Statistics		0.01 %		0.01 %		0.01 %		0.01 %
- Background	0.30 %	0.1 %	0.30 %	0.1 %	0.10 %	0.3 %	8.1 %	2.43 %
Total error		1.74 %		2.17 %		2.97 %		3.64 %
Result σ_f/ barn	2.244 ± 0.039		2.078 ± 0.045		1.047 ± 0.031		2.146 ± 0.078	
E_n / MeV	14.7 ± 0.15		14.7 ± 0.15		4.5 ± 0.2		18.8 ± 0.3	

+) Preliminary estimate

APPLICATION OF THE TIME-CORRELATED ASSOCIATED PARTICLE METHOD (TCAPM) TO ABSOLUTE FISSION CROSS-SECTION MEASUREMENTS

H.G.Ortlepp, G.Pausch, Technical University of Dresden

During the last years absolute fission cross-section measurements were performed by the Chlopin-Radiuminstitute Leningrad / Technical University of Dresden cooperation, using the TCAPM /1/. A cone of neutrons, belonging to the associated particles (AP's) registered within a fixed solid angle, is defined completely by the reaction kinematics. A homogeneous fission foil, with a known number n of atoms per unit of area, great enough to cover the cone completely, is placed perpendicular to the cone /2/. If fission events (N_f) are counted in coincidence with the AP's only, the fission cross-section can be determined by replacing the neutron flux at sample position and the total sample mass by the number of counted associated particles (N_{AP}) and the areal density of the fission foil, respectively:

$$\sigma_f = \frac{N_f}{N_{AP} \cdot n} \qquad (1)$$

There is no need to determine the AP detection efficiency or any geometrical factor. Bachground induced events are strongly suppressed by the coincidence condition. These advantages give rise to apply the TCAPM to other neutron induced reactions too.
The formula (1) is very simple, but several small corrections have to be applied /3,4/. The experimental set-up, is designed to keep these corrections as small as possible, and to collect sufficient data to determine them. Specific electronic devices were developed to process the AP amplitude informatinn within 0.1-1 µs, depending on the AP detection system. The AP timing signal is gated by the selected amplitude information before it is used to generate the coincidence timing spectrum. Because of the ns time resolution a coincidence resolving time of 10 ns became possible, leading to a low random coincidence rate. Amplitude spectra of the parallel plate ionization fission chamber and the AP detection system are collected to correct for loosed fission events and background underlying the AP peak, respectively. Using individual target/AP-detector combinations the TCAPM was applied to determine absolute fission cross-sections at five neutron energy points in the 2-20 MeV range (tab.1). At 14.7 MeV the specific error contributions of the TCAPM are believed to be below 0.5 % and a total error of about 1 % was reached for ^{235}U /1/.

Tab.1: Parameters of the experimental arrangements used for absolute fission cross-section measurements

E_n/MeV	2.6	4.5	8.5	14.7	18.8
Reaction	D(d,n)^{3}He			T(d,n)^{4}He	
E_d/MeV	0.12	5.0	9.5	0.13	6.0
Accelerator	NG (TUD)	TA (CINR)	TA (CINR)	NG (RIL, TUD)	TA (CINR)
AP detect. angle	90°	38°	42°	165°	68°
AP detector	Si-SB	Si-SB ΔE-E detector telescope		thin NE 102 scint.	Si-SB ΔE-E detector telescope
Target	Ti-D on cu	$(CD_2)_n$-foil		Ti-T on cu	Ti-T self-supporting
Ap rate 10^3/s	10	2	2	100	3
Number of fission foils	2	5	5	1	5

NG: 150 KV Cockroft-Walton neutron generator
TA: 5 MV tandem van-de-Graaff accelerator of the CINR Rossendorf (GDR)

In our 14.7 MeV experiments an upper limit of the neutron flux was given by the increasing amount of random coincidences due to fissions caused by low energy background neutrons. The AP detection system allows counting rates up to some millions per second /5/. The corresponding effective rate of neutrons penetrating the sample then becomes comparable with that of usual pulsed neutron sources, whereas the fast AP timing uncertainty is < 1 ns, and the timing background caused by scattered off-cone neutrons is "white".

/1/ R.Arlt, et al., Proc. Intern. Conf. Nuclear Cross Sections for Technology; Knoxville, USA, Oct. 22-26, 1979; NBS Spec. Publ. 594, p. 990, 1980

/2/ I.D.Alkhazov, et al., II.Conf.on Neutr.Phys., Kiev 1973, Vol. 4, p. 13

/3/ R.Arlt, et al., Kernenergie 24 (1981) p. 48

/4/ R.Arlt, H.G.Ortlepp, Proc. IAEA Consult.Meeting; Smolenice, Czech., March 28 - April 1, 1983

/5/ R.Arlt, et al., TUD Preprint 05-3-78, Dresden, 1978

TWO APPROACHES TO THE DESCRIPTION OF PREEQUILIBRIUM ANGULAR DISTRIBUTIONS

P. Mädler and R. Reif
Technische Universität Dresden, Sektion Physik,
DDR - 8027 Dresden

Abstract: Two models recently developed to describe preequilibrium angular distributions are briefly reviewed and compared with alternative models as well as with experimental data.

1. Introduction: To perform a quantum mechanical calculation of multi-step processes leading to nucleon emission in the framework of the FKK formalism /1/ is still a quite complicate and time consuming task /2/. In this approach the double-differential cross section for nucleon emission is reduced to DWBA matrix elements utilizing appropriate statistical assumptions. The resulting angular distributions in agreement with experimental data averaged over a certain emission energy interval show a rather smooth and strongly forward-peaked behaviour. With increasing bombarding energy this trend becomes more and more pronounced. This indicates that simple phase space considerations combined with the conservation laws of energy, linear and angular momentum can give a reasonable lowest order description of spectra and angular distributions even if neglecting the dynamics of the process (matrix elements).
A simple extension of the exciton model in which this statement is basically used /3/ is described in section 2.
Section 3 deals with a more sophisticated non-equilibrium statistical operator approach which takes into account a two-body residual interaction in a simple Fermi gas model governing the equilibration process /4/.

2. Generalized exciton model: In the generalized exciton model of ref./5/ only the leading particle carries memory of the incident direction. The incident energy,however, is equally shared by all excitons. Furthermore, this model uses the standard partial level densities without accounting for the fact that the leading particle is considered to move in an explicitly described direction. The concept of a leading par-

ticle is questionable for comparably low bombarding energies and for more complex exciton states which in turn exclusively determine backward angle emission.

To overcome at least partially this problems in /3/ we have proposed an approach which in some sense is alternative to that of ref. /5/ . It is assumed that at each stage the memory of the incident momentum (direction and energy) is equally shared among all excitons. A simple closed-form expression for the preequilibrium fraction of the double-differential cross section is written as

$$\frac{\partial^2\sigma}{\partial\varepsilon'\partial\Omega} \sim \varepsilon' \sigma_{inv}(\varepsilon') \sum_{\substack{n=n_0 \\ \Delta n=2}}^{\bar{n}} \frac{\rho_{p-1,h}(U,\bar{P}_{\parallel},\bar{P}_{\perp})}{\rho_{p,h}(E,P_{\parallel},0)} \qquad (1)$$

with σ_{inv} being the inverse cross sections. The quantities $\rho_{p,h}$ are the partial level densities evaluated in an extended phase space. The energy E as well as the total linear momentum $\vec{P} = (P_{\parallel}, P_{\perp})$ are considered as conserved quantities of the exciton gas. The averaged matrix element of the exciton model which determines the decay times of each exciton state is assumed not to depend on the exciton number and put into the normalization constant. This factor was chosen to fit one appropriate experimental point at a high emission energy in forward direction.

If applied to 14 MeV (n,n') data (compare /3,6/) this model yields results very close to those of ref. /5/. The scattering into backward angles is systematically underestimated. This is because angular momentum conservation, distortion effects and individual properties of the target at low residual excitation energy are not taken into account.

A surprisingly good agreement with experimental data of ref. /7/ as well as with a two-step DWBA calculation of ref. /8/ is found at higher incident energy. Fig.1 shows the corresponding results for the reaction ^{27}Al(p,p'), E_p = 62 MeV. The slight underestimation of the cross section at forward angles in the highest energy bins possibly can be related to the neglect of the leading particle effect in the direct (first) step of the reaction. The Fermi energy and the normalization constant are the only parameters of the model.

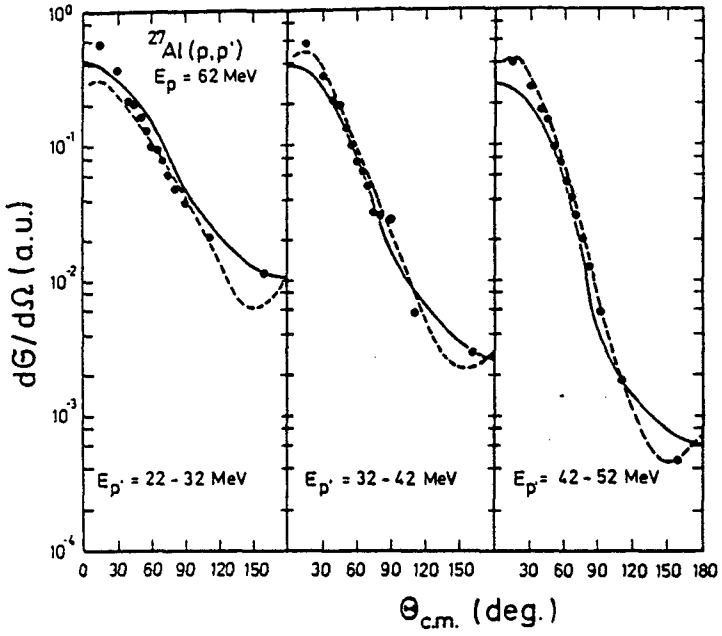

Fig. 1 :
Differential cross section of the reaction ^{27}Al(p,p'), E_p=62 MeV. Full lines: from eq.(1). Dashed curves: second-order DWBA calculation of ref./8/. The data points are taken from ref./7/.

3. Non-equilibrium statistical operator approach : The intranuclear relaxation process in nucleon-induced reactions is investigated in a Fermi gas model /4,9/ utilizing a statistical operator for the non-equilibrium state /10/ which contains energy, particle number and linear momentum as relevant observables. The phase space is subdivided in subspaces assumed to be in a time-dependent quasi-equilibrium. A set of non-linear equations for the time developement of the inverse temperature, chemical potential and mean velocity in each subspace coupled via the kinetic coefficient and generalized suszeptibility matrices (the former containing two-body matrix elements) has been derived and solved numerically taking into account the depletion of the system due to emission of nucleons. The initial conditions are fixed in accordance with the momentum distribution of both

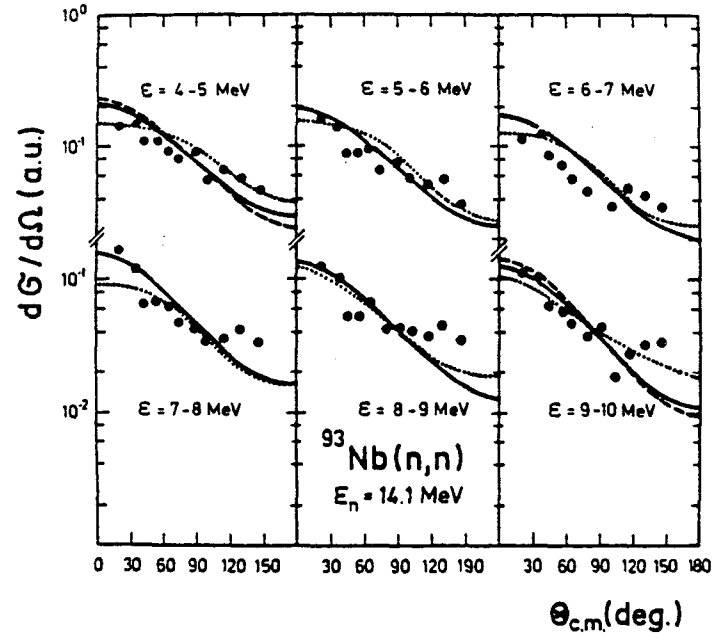

Fig. 2 :
Differential cross section of the reaction ^{93}Nb(n,n') at E_n = 14.1 MeV. Full curves : our result /4/ without taking into account depletion of the system. Dashed curves : with depletion. Dotted curves : generalized exciton model of /11/. The data are also from /11/.

particles occupying states above the Fermi surface after the first collision event. The proposed equations yield a time-dependent description of both preequilibrium and equilibrium stages of the deexcitation process without additionally weighting their relative contributions. The results of the equilibrium stage are consistent with the common evaporation theory. Spectra and angular distributions are in good agreement with experiment even for bombarding energies around 15 MeV. The numerical solution is, however, much more time consuming than for the generalized exciton model. For much higher incident energies the number of subspaces must be increased in order to better describe the early stages of the reaction. Fig. 2 as an example shows the preequilibrium fraction of angular distributions for $^{93}Nb(n,n')$, E_n = 14.1 MeV, calculated with only 2 subspaces ($\mathcal{E} \gtrsim \mathcal{E}_F$) of the compound system phase space. The experimental points as well as a model calculation taking into account angular momentum conservation are taken from ref. /11/.

References :

/1/ H. Feshbach, A. Kerman and S. Koonin, Ann. Phys. 125 (1980) 429

/2/ R. Bonetti et al., Phys. Rev. C24 (1981) 71; C26 (1982) 2417

/3/ P. Mädler and R. Reif, Nucl. Phys. A337 (1980) 445

/4/ P. Mädler and R. Reif, Nucl. Phys. A373 (1982) 27

/5/ G. Mantzouranis, D. Agassi and H.A. Weidenmüller, Phys. Lett. 57B (1975) 220; G. Mantzouranis, H.A. Weidenmüller and D. Agassi, Z. Phys. A276 (1976) 145

/6/ P. Mädler, TU-Information 05-42-80, Dresden, 1980

/7/ F.E. Bertrand and R.W. Peelle, Phys. Rev. C8 (1973) 1; Oak Ridge National Laboratory reports ORNL-4455 (1969) and ORNL-4638 (1971)

/8/ T. Tamura et al., Phys. Lett. 66B (1977) 109; T. Tamura, T. Udagawa and H. Lenske, Phys. Rev. C26 (1982) 379

/9/ P. Mädler et al., Phys. Lett. 61B (1976) 427

/10/ D.N. Zubarev, Statistische Theorie des Nichtgleichgewichts, Akademieverlag, Berlin, 1976

/11/ Y. Irie et al., J. Phys. Soc. Japan 39 (1975) 537; Phys. Lett. 62B (1976) 9

Recoil Proton Pulse Height Spectrometry, applied to a Pb Sphere Leakage Spectrum

D. Albert, W. Hansen, W. Vogel,
Akademie der Wissenschaften der DDR, Zentralinstitut für Kernforschung, Rossendorf bei Dresden,
DDR-8051 Dresden, PSF 19, GDR

In Rossendorf the pulse height spectrometry using hydrogen filled proportional counters /1/ and stilbene scintillators /2/ was established in order to measure neutron spectra in fast critical assemblies /3/. Here the methods are briefly described and an application to a Pb sphere leakage spectrum is mentioned.
Spherical and cylindrical counters are used, with diameters of 3...4 cm and H_2 pressures of 100 kPa ... 1 MPa. The energy range of 2 keV ... 1.5 MeV can be covered. The evaluation consists mainly of differentiation and an unfolding taking into account the downscattering of recoil protons created by high energy neutrons and the wall effect. Small stilbene cylinders are used, with diameters of 1...3 cm. The evaluation takes into account differentiation as well as light efficiency and nonisotropic response. For all detectors both the accuracy of relative neutron spectrum measurements and the energy resolution are 5...10%.
In addition to the time of flight spectrometry the recoil proton pulse height methods should be used in order to measure leakage spectra at 14 MeV neutron driven onedimensional benchmarks. We applied recoil proton spectrometry at the 14 MeV neutron generator of the Technical University Dresden, Department of Nuclear Physics (Prof. Dr. D. Seeliger), with the target at the centre of a 4.1 mfp Pb sphere, and the detector on the top of the sphere, in order to measure the scalar neutron flux spectrum $\Phi(u)$ and to have a minimal amount of floor backscattered neutrons only.
A calculation has been carried out using ANISN code and ENDF-B/III data. Normalizing in the peak region the trends of deviations in the experiment-calculation comparison are as follows:

1. Fair agreement in 50 keV ... 700 keV range.
2. Approximately 50% more neutrons measured in 700 keV ... 5 MeV range.
3. Remarkably more neutrons measured in 5 MeV ... 12 MeV range.

The deviations could be roughly explained by inadequate ENDF-B/III secondary neutron emission spectra as far as (n,2n) and (n,n') reactions are concerned.
The investigations will be continued.

References

/1/ D. Albert et al., Kernenergie 21(1978)82
/2/ D. Albert et al., Nucl. Instr. Meth. 200(1982)397
/3/ D. Albert et al., Kernenergie 23(1980)89

The $^{12}C(n,\alpha)$ Reaction at E_n = 14.1 MeV*

R. C. Haight, S. M. Grimes, R. G. Johnson, and H. H. Barschall
Lawrence Livermore National Laboratory
University of California
Livermore, CA 94550

As part of the Coodinated Research Program on Measurement and Analysis of 14-MeV Neutron Nuclear Data Needed for Fission and Fusion Reactor Technology, we have investigated the $^{12}C(n,\alpha)$ reaction at 14.1 MeV.[1] Our approach is to measure the number and energy of charged particles produced when a target, carbon in this case, is bombarded with 14.1-MeV neutrons. The spectrometer consists of a magnetic quadrupole triplet lens that serves to transport the charged particles to a counter telescope placed approximately 2.8 m from the target foil. Background events are greatly reduced with this technique and consequently we can detect alpha particles with energies down to 1 MeV.

In the present experiment, energy and angular distributions of α-particles from the bombardment of carbon foils with 14.1-MeV neutrons were measured with the quadrupole spectrometer. The observations included α-particles with energies above 1 MeV emitted at angles between 19° and 135°. The measured spectra are given in Fig. 1. The cross section for α-particle emission obtained by integrating over emission angle is 402 ± 46 mb. From these data and from evaluations of the elastic and inelastic scattering cross sections a kerma factor (energy deposition) of $1.84 \pm 0.16 \times 10^{-9}$ cGy cm^2 is deduced. The present cross section for the $^{12}C(n,n'3\alpha)$ reaction is much lower than previous measurements.

*Work performed under the auspices of the U.S. Department of Energy by the Lawrence Livermore National Laboratory under contract number W-7405-ENG-48.

[1] R. C. Haight, S. M. Grimes, R. G. Johnson, and H. H. Barschall, Nucl. Sci. Eng. (to be published).

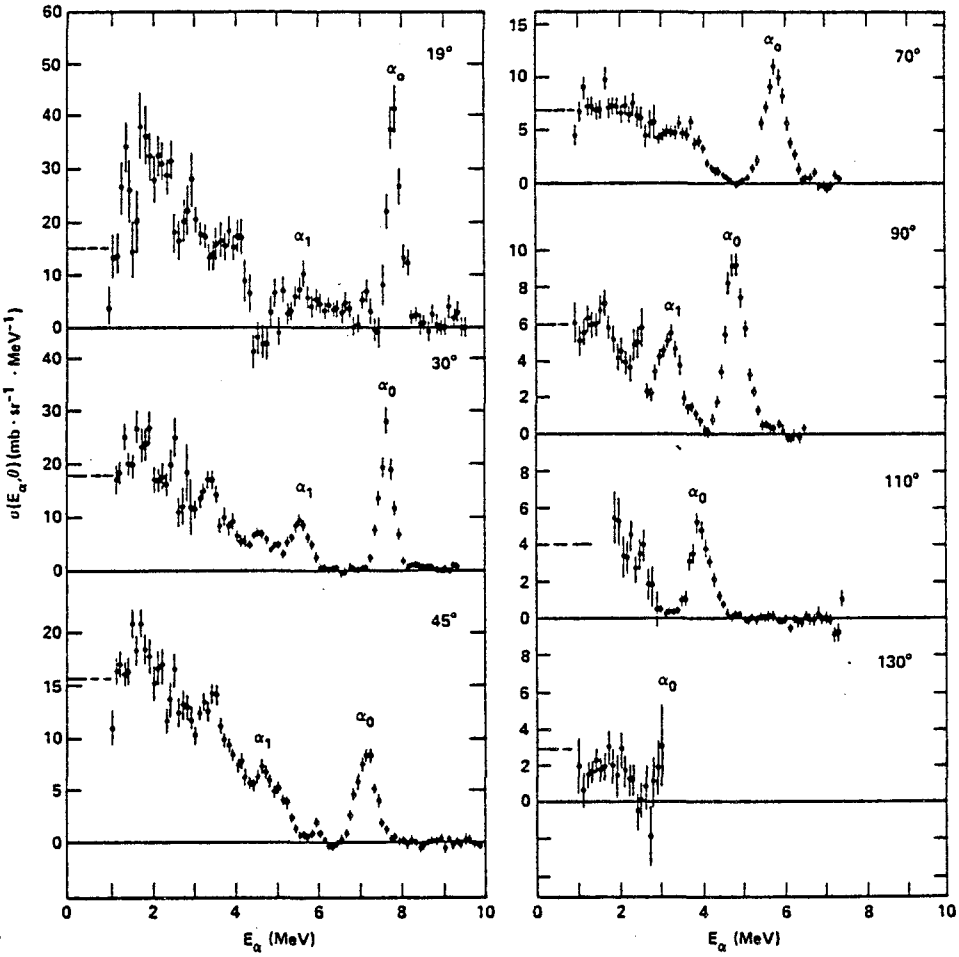

Figure 1. Energy spectra of alpha particles emitted from carbon under bombardment by 14.1-MeV neutrons. The α_0 peak is from the $^{12}C(n,\alpha)^9Be$(ground state) reaction; the α_1 peak is from the $^{12}C(n,\alpha)^9Be$ (2.4 MeV) reaction.

Cross section measurements by the activation technique using gamma ray and X ray spectrometry

A. REGGOUG ; A. AIT HADDOU ; M. BOUFRAQECH ; A. CHIADLI ; A. CHOUAK ; M. ERRADI ; M. VIENNOT and M. BERRADA.
Laboratoire de Physique Nucléaire, Faculté des Sciences, B.P. 1014, Rabat - Morocco.

1. Introduction

The activation method for the cross sections measurements of 14 MeV neutron induced reactions uses principally the gamma ray spectrometry of the residual radioactive nuclei. But, when these nuclei decay by electron capture or isomeric transitions which are partially or totally converted , some vacancies are created in the internal electronic shells, resulting in the emission of characteristics X-rays[1]. The X-ray spectrometry is very useful when the X absolute intensity of the residual nucleus is much higher than its gamma intensity. It is complementary to the gamma spectrometry when the X, and gamma intensities are comparable. Then, the simultaneous utilization of the two methods reduces the measures errors, and allows to check the nuclear data which are used. The X ray method will be illustrated by the detailed study of the 14 MeV neutrons induced reactions on natural Indium, and will be applied to the cross sections measurements of other reactions induced on Silver and Gold and Tin. The results will be compared to those of the gamma spectrometry which was used parallely. The classical gamma spectrometry using an Aluminium comparator $^{27}Al(n,\alpha)^{24}Na$; σ-(En = 14.7 MeV) = (113 $\pm$ 0.4)mb has been also applied to the determination of various excitation functions around 14 MeV bombarding neutron energy (Table 6)

Table 1 : Decay modes of the n + natural In reaction products ; X and gamma rays used with teir associated nuclear data.

Reactions 1 and 1' : (6)

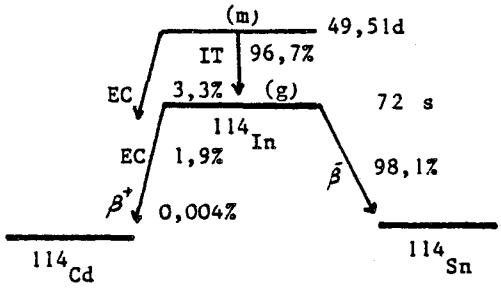

Reactions 3 & 3' (6)

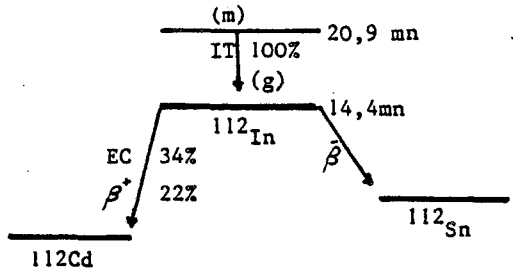

Notation	Reactions	$T_{1/2}$ (6)	Observed In KX	Observed Cd KX	α_K used (7)	α_K (6)	I_ε(%)	ε_K calcul from (6)	E_γ (KeV)	I_γ (%) used (7)	I_γ (%) (6)
1	$^{115}In(n,2n)^{114m}In$	49,51d	Yes	Yes	2,57	$2,37_{31}$	$3,3_2$	0,877	190,29 with IT	15,64	15,64 17,82
						$1,95_{29}$					
1'	$^{115}In(n,2n)^{114g}In$	72 s		Yes			1,9	0,877			
2	$^{115}In(n,n')^{115m}In$	4,49 h	Yes		0,862	$0,843_{12}$			336,23 with IT	45,28	$45,9_1$
3	$^{113}In(n,2n)^{112m}In$	20,9mn	Yes		5,27	$5,8_{12}$			155 with IT	12,66	$45,9_1$
3'	$^{113}In(n,2n)^{112g}In$	14,4mn		Yes			34	0,86	511 with EC+ β^+	44 (6)	44
4	$^{113}In(n,n')^{113m}In$	99,5mn	Yes		0,448	$0,437_7$ $0,441_{13}$ $0,431_7$ $0,454_{12}$			391,69 with IT	64,14	64_1

Reaction 2 : (6)

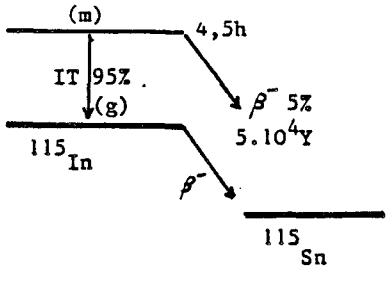

Reaction 4 : (6)

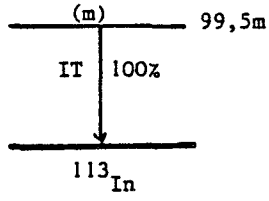

2. Typical experiment : n + In

Two natural In samples 0.1 mm thick and 1 cm diameter were irriated with an Aluminium foil 0.1 mm thick, in a sandwich between Cd foils, 7 mm far from the tritium target of a S.A.M.E.S. T 400 neutron generator. The mean neutron energy was estimated (2) to be (14.7 $\pm$ 0.15) MeV. The small thickness of the foils was choosen for several reasons :

1) to minimize the X ray absorption

2) to minimize the X ray fluorescence of the foil induced by $\beta^{\pm}$, conversion electrons[3] and soft gamma rays[4].

The first In foil was placed, after irradiation, on an Hyperpure Ge detector of 7mm active depth, 16 mm diameter and 125μm Be window, which detected the X rays. An off line counting in subsequent time intervals was used with a multichannel analyzer working in a programmed mode in association with a rapid data storage system. The X ray peaks were integrated and stored after 10 mn of cooling time and for different counting times : 12 measures of 5 mn, 12 of 1 hour, 12 of 4 hours and the last one of 8h 30 mn.

The second foil was placed on a Ge(Li) detector of 67 cm^3 active volume, for the gamma spectrometry. The aluminium foil was used as a comparator for the absolute measurements of the cross section by the gamma method.

The different nuclear reactions mentionned in Table 1 were identified by their gamma lines. The origin of the observed X rays is also indicated in Table 1. Cd was used to avoid the $^{113}In(n,\gamma)^{114m,g}In$ reactions which could be induced by the weak thermal neutron component of the beam, giving thus an interference with the $^{115}In(n,2n)^{114m,g}In$ reactions. Fig.1 shows one of the X rays spectra obtained. The identification of the reactions involved is done also by the decay curve corresponding to each X-ray peak observed. Fig.2 and 3 show the decay curves of the In K_α and Cd K_α peaks[5].

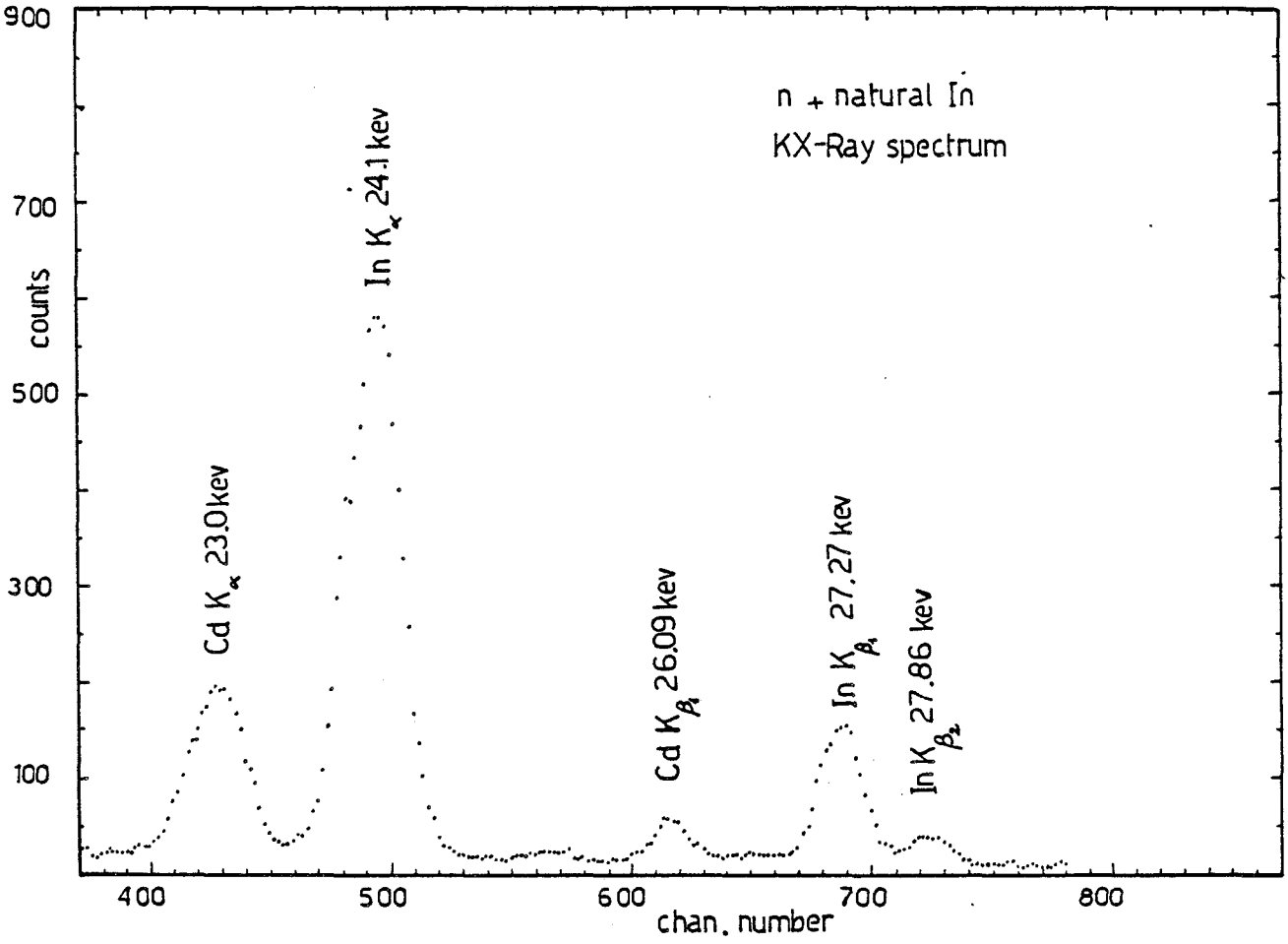

Figure 1 .: X-ray spectrum obtained for the n + natural In reactions ; Irradiation time = 30 mn ; cooling time = 47 mn ; counting time = 5 mn.

3. Calculations : n + In

The In K_α peak comes from the reactions 1, 2, 3, 4 indicated on Table 1. Its decay equation has been calculated from the decay schemes of the residual nuclei which have been involved. By fitting this equation to the experimental decay curve using a linear optimization code, the cross sections ratios σ_1/σ_2 ; σ_2/σ_3 ; σ_4/σ_3, have been found.

The Cd K_α peak comes from the reactions 1, 1', 3 and 3'. Its decay equation has been fitted in the same manner, to its experimental decay curve, giving thus the cross sections ratios σ_1/σ_3 ; and $\sigma_{3'}/\sigma_3$.

The results are given in Table 2, the errors are standard deviations they don't include the errors on the nuclear data used.

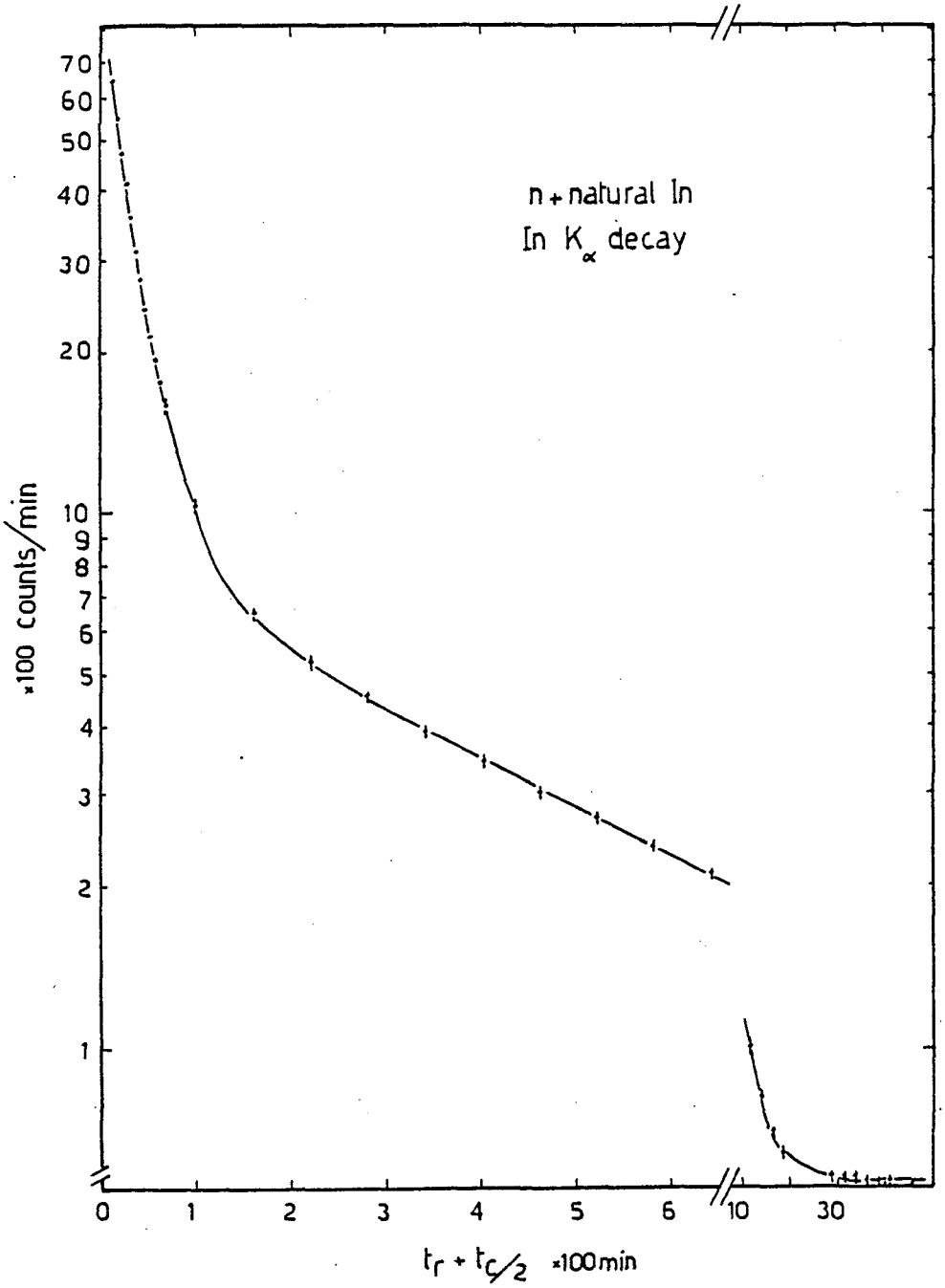

Figure 2 : Decay curve of the In K_α peak coming from the reactions 1, 2, 3, 4. The solid line represents the fit with the decay equations.

In the X-ray spectrometry method, the self-absorption and the detector efficiency factors are eliminated in the cross section ratios formulas, as the same peak is used for their calculations. The σ_3'/σ_3 ratio has been obtained without any data concerning the X intensity. Its precision is due only to the quality of the fit and the precision on C_3'/C_3.

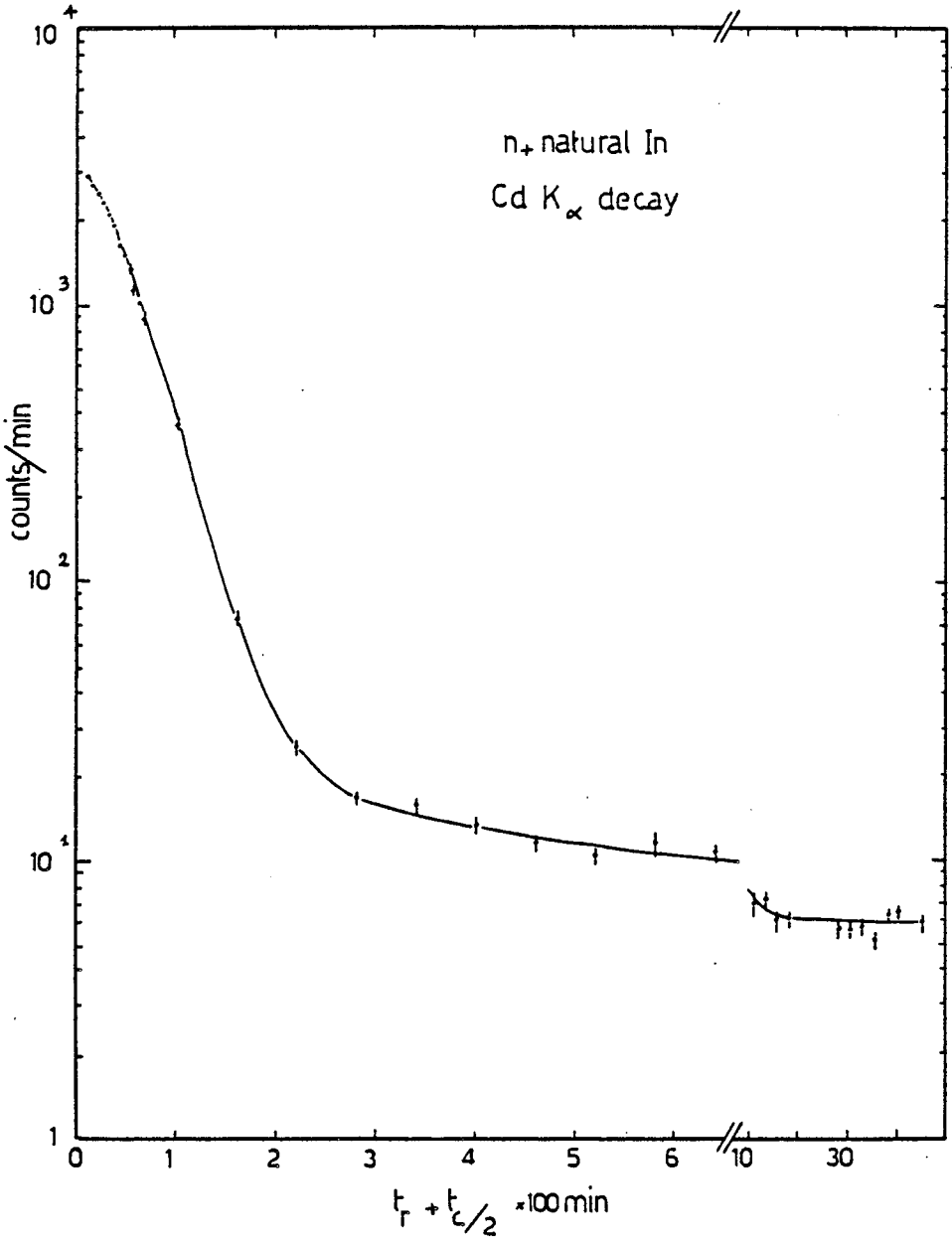

Figure 3 : Decay curve of the Cd K_α peak coming from the reactions 1, 3, 3'. The solid line represents the fit with eq. (7).

The σ_1/σ_3 ratio is given twice in the X-ray spectrometry method, because of the utilization of each X-ray peak. The small difference between the two results is not due to experimental errors but rather to systematical errors in the nuclear data used ; concerning the X intensities. The weak precision on the σ_4/σ_3 ratio is due to the weak isotopic abundance of ^{113}In, the relatively weak cross section of the reaction 4, and the weak X intensity of ^{113m}In (Table 1).

Table 2 : Comparison of the cross sections ratios measured with the X-ray spectrometry and the γ-ray spectrometry.

		σ_1/σ_3	σ_2/σ_3	σ_4/σ_3	$\sigma_{3'}/\sigma_3$
X-Method	In K_α	1,160 ± 0,008	0,0641 ± 0,0004	0,050 ± 0,010	
	Cd K_α	1, 12 ± 0,02			0,23 ± 0,05
γ-Method		1,16 ± 0,09	0,060 ± 0,004	0,058 ± 0,004	0,23 ± 0,01

Table 3 : Absolute cross sections obtained from the ratios of table 2 and the value of σ_3 measured by γ-ray spectrometry. Comparison with ather values from the litterature.

	Reactions	σ (mb) this work (X-ray spect.)	σ (mb) Litterature
1	$^{115}In(n,2n)^{114m}In$	1543 ± 57	(1515 ± 100)[11]; (1390 ± 110)[12]
2	$^{115}In(n,n')^{115m}In$	85 ± 3	(78,6 ± 3,6)[13]; (63 ± 6)[11]; (69 ± 5)[12]
3	$^{113}In(n,2n)^{112m}In$	1330 ± 48	(1317 ± 200)[11]; (1290)[14]; (1450 ± 100)[15]
3'	$^{113}In(n,2n)^{112g}In$	306 ± 67	(313 ± 40)[11]; (320 ± 25)[15]; (1240 and 360)[14]
4	$^{113}In(n,n')^{113m}In$	67 ± 13	(42 ± 9)[11]

Compared to the gamma spectrometry method, the results are coherent, which indicates the global coherence of all the nuclear data used. These results confirm and complete those obtained in a previous work (9).

By measuring absolute σ_3, with the classical gamma method, using the aluminium comparator $^{27}Al(n,\alpha)^{24}Na$; $\sigma(E_n = 14.7\ MeV) = (113.1 \pm 0.4)mb$ (10) it has been possible to calculate the absolute cross section σ_1, σ_2, σ_3, σ_4, by means of the measured ratios (Table 2). These values are given in Table 3 with other values of the litterature.

Table 4 : Other cross section ratios measured with X-ray and γ-ray spectrometry : $^{107}Ag(n,2n)^{106m,g}Ag$, $^{197}Au(n,2n)^{196m,g}Au$.

Reactions	Target	Method	X or γ Rays (keV) and absolute intensity (%)	Statistical errors	Results
$^{107}Ag(n,2n)^{106m}Ag$ and $^{107}Ag(n,2n)^{106g}Ag$	enriched ^{107}Ag	X	Pd K_{α} (I_{Xm} = 71.19) (16) Pd K_{α} (I_{Xg} = 29.3) (16)	1.5 %	$\frac{\sigma_m}{\sigma_g} = 0.658 \pm 0.010$
		γ	512($I_{\gamma m}$ = 88) (16) 511 + 512($I_{\gamma g}$ = 135.1) (16)	1 %	$\frac{\sigma_m}{\sigma_g} = 0.676 \pm 0.007$
$^{197}Au(n,2n)^{196m}Au$ and $^{197m}Au(n,2n)^{196g}Au$	Natural Au	X	Pt K_{α_2} (I_{Xm} and I_{Xg} not needed) Eq. 13	14 %	$\frac{\sigma_m}{\sigma_g} = 0.064 \pm 0.010$
		X	Pt K_{α_1} (I_{Xg} = 38.8) + (17) Au K_{α_2} (I_{Xm} = 39.4) (17)	1.2 %	$\frac{\sigma_m}{\sigma_g} = 0.081 \pm 0.001$

Table 5 : Cross sections measured with X-ray spectrometry

$^{114}Sn(n,2n)^{113m}Sn$; $^{124}Sn(n,2n)^{123m}Sn$; $^{112}Sn(n,2n)^{111}Sn$.

	Reactions	Target	En (MeV)	X ray (absolute intensity)	Results (σ in mb)	Litterature (σ in mb).
1	$^{114}Sn(n,2n)^{113m}Sn$	natural Sn	14.70 ± 0.15	Sn K_{α} (58 %)	$\sigma_1/\sigma_2 = 2.16 \pm 0.2$	$\sigma_2 = 547 \pm 23$
2	$^{124}Sn(n,2n)^{123m}Sn$			Sb K_{α} (13 %)	$\sigma_1/\sigma_3 = 0.86 \pm 0.08$	$\sigma_3 = 1275 \pm 100$
3	$^{112}Sn(n,2n)^{111}Sn$			In K_{α} (71 %)	$\sigma_1 = 1180 \pm 130$ $\sigma_1 = 1100 \pm 130$	

Table 6 : Cross sections measured with γ ray spectrometry.

Reactions	Target	En (MeV)	γray in keV; abs. intensity (%)	σ (mb)	Litterature (mb) (11)
$^{58}Ni(n,2n)^{57}Ni$	nat.foil	13.75 ± 0.15	1378 (77.6 %)	13.6 ± 0.4	ref. 11
		14.10 ± 0.15		20.2 ± 0.6	
		14.80 ± 0.15		31.0 ± 0.9	35 ± 3
$^{59}Co(n,2n)^{58m}Co$	nat.foil	13.75 ± 0.15	811 (99.44 %)	277	
		14.10 ± "		387	
		14.50 ± "		460	402 ± 41
		14.70 ± "		531	
		14.80 ± "		532	
$^{59}Co(n,2n)^{58g}Co$	nat.foil	13.75 ± "	811 (99.44 %)	559	
		14.10 ± "		684	
		14.50 ± "		690	720 ± 50
		14.70 ± "		793	
		14.80 ± "		877	
$^{90}Zr(n,2n)^{89m+g}Zr$	nat.foil	14.8 ± 0.3	909 (99,01 %)	889 ± 57	848 ± 82
$^{93}Nb(n,2n)^{92m}Nb$	nat.foil	14.8 ± 0.3	943 (99.2 %)	472 ± 30	512 ± 46
$^{59}Co(n,\alpha)^{56}Mn$	nat.foil	13.75 ± 0.15	847 (98,87 %)	25.0 ± 0.8	
		14.10 ± "		27.6 ± 0.8	
		14.50 ± "		27.7 ± 0.9	30 ± 2
		14.70 ± "		30.0 ± 0.9	
		14.80 ± "		28.4 ± 0.9	
$^{59}Co(n,p)^{59}Fe$	nat.foil	13.75 ± 0.15	1099.(56,5 %)	46.9 ± 1,6	
		14.10 ± 0.15		47.7 ± 1.7	
		14.50 ± 0.15		44.5 ± 1.6	73 ± 10
		14.70 ± 0.15		44.0 ± 1.4	
		14.80 ± 0.15		43.3 ± 1.5	

4. Other cross section ratios

The X-ray spectrometry method has been applied to the measurement of some cross section ratios of other 14 MeV neutron induced reactions. The same energy (14.7 ± 0.15) MeV ; was used. Table 4 gives the results

which were obtained, and the comparison with the gamma spectrometry method which was used parallely. As the X-ray method has given good results for the reactions which have been studied till now, it is interesting to apply it for other reactions where the residual nuclei have a low gamma intensity, but a high X intensity. The reaction $^{114}Sn(n,2n)^{113m}Sn$ is an example of this last case. Its cross section has not been measured till now because probably of its very low γ intensity. Table 5 gives the results obtained with the X-ray method. Our value is σ_1(1140 $\pm$ 130)mb for this last reaction, it is the first value known in the litterature.

5. Reactions studied with the gamma method.

The classical gamma method was used for some (n,2n), (n,p) and (n,α) reactions, using as comparator an aluminium foil. Some excitation functions around 14 MeV have been also determined Table 6 gives our results and the comparison with other authors.

REFERENCES

(1) J. Janczyszyn et al., rapport INT 133/I, Institute of Physics and Nuclear Techniques KRAKOW (1978).

(2) A. Chiadli D.E.S. 3ème cycle, Faculté des Sciences de Rabat - Université Mohammed V 3/7/1982.

(3) E. Casnati et al., J. Phys. B : At. Mol. Phys. 15(1982) 155-167.

(4) J.H. Hubbell. National Nureau of Standards (U.S) NSRDS - NBS 29 (1969).

(5) D. De Soete, et al., Neutron Activation Analysis, vol.34, Chap. 11 page 522 (1972), wiley intersciences ed.

(6) C.M. Lederer et al., Table of Isotopes, Seventh ed. wiley Intersciences (1978).

(7) Rösel et al., Atomic Data and Nuclear Data Tables, vol. 21, n° 2-3 Feb-Mar. 1978.

(8) D. De Soete et al. Neutron Activation Analysis, vol.34, Chap.5, page 130, wiley intersciences (1972).

(9) A. Reggoug et al. Nuclear Data for Science and Technology, 873 - 874, K.H. Bôckhoffed. (1983).

(10) Vonach INDC/NEANDC 1980.

(11) S.M. Qaim ; Handbook of spectroscopy, vol.3, p.141, CRC Press, Inc. Florida (1981).

(12) R.C. Barrall et al., Nucl. Phys. A 138, 387-391 (1969).

(13) I. Garlea et al. INDC (ROM) 15/GI INT (1983) - 2 I.A.E.A. Nuclear Data section.

(14) J. Csikai, Proc. interregional advanced training course on applications of nuclear theory to nuclear data calculations, Trieste, 28 Janv. - 22 Feb. 1980.

NUCLEAR PHYSICS STUDIES ON NEUTRON GENERATORS

A.I. Abramov
Physics and Energy Institute (FEhI), Obninsk, USSR

This paper constitutes a brief review of the main work done in recent years at different institutes in the USSR on low-voltage neutron generators in order to study the interaction of neutrons with atomic nuclei at energies of 14-15 MeV.

Physics and Energy Institute (FEhI). By 1970 a broad cycle of measurements of inelastically scattered neutron spectra using the time-of-flight method had been completed for a large group of nuclei [1-4]. Although these measurements were done almost 20 years ago, they agree well with results published relatively recently by a group of Austrian physicists working with modern experimental technology [5]. Similar measurements have subsequently been performed at the FEhI on improved apparatus: the path length has been increased and more up-to-date equipment has been used, so that the time resolution has been brought down to 1.2-0.6 ns/m [6,7]. The measurements done on neutron inelastic scattering spectra for iron nuclei at angles of 45°, 60°, 75°, 90°, 120° and 150° have shown that the angular distribution of neutrons at the peak corresponding to excitation of a nucleus with an energy of 4.5 MeV is such that this peak can be ascribed to a single-photon 3^- state [6]. In the same paper the conclusion is reached that the inelastically scattered neutron spectrum can be characterized by the sum of the evaporative spectrum and the spectrum from direct inelastic scattering without the concept of the pre-equilibrium state needing to be involved. Refs [8,9] give the spectra for inelastically scattered neutrons with niobium nuclei measured at angles of between 30° and 135° at E_o = 14.3 MeV. A theoretical analysis has resulted in the identification of the spectra of the first and second neutrons and in determination of the (n,2n) reaction cross-section. At the end of the neutron spectrum a peak is noted which was not found in previous studies.

With a maximum (high) resolution of 0.6 ns/m, measurements have been made of scattered neutron spectra, of elastic scattering cross-sections of hydrogen (54 ± 5 mb/sr) and of inelastic scattering cross-sections of carbon with excitation of the level 4.43 MeV (13.3 ± 2.0 mb/sr) and 9.6 MeV (7.2 ± 1.5 mb) [7].

The time-of-flight method was also used for measuring the prompt neutron spectrum from fission of uranium-238 by neutrons with an energy of 14.3 MeV [10]. The main difficulty with such measurements is associated with the need to identify neutrons from side reactions such as (n,n'), (n,2n) and (n,nf). The

result obtained is $\nu = 5.07 \pm 0.13$, and it is found that the shape of the fission neutron spectrum cannot be described by a Maxwellian distribution with one temperature. The conclusion reached earlier that 20% of the neutrons are emitted from non-equilibrium states (direct and pre-equilibrium processes) was confirmed.

A theoretical analysis of experimental data on the (n,p) and (n,2n) reactions has produced relationships linking the cross-sections of these reactions at a neutron energy of 14.5 MeV with the parameter (N-Z)/A [11].

Leningrad Institute of Technology. In the 1970s a cycle of studies was carried out on the (n,p) and (n,α) reactions with the nuclei of relatively light elements, for which a counter telescope was used at angles of 7°, 45°, 60° and 80° to measure the spectra of protons produced in the interaction between 14.1 MeV neutrons and ^{27}Al, ^{28}Si, ^{31}P, ^{35}Cl, ^{39}K and ^{52}Cr nuclei [12]. The nuclear temperatures and level density parameters were also determined. During a further theoretical analysis [13] it became clear that neither the statistical theory nor the pre-equilibrium disintegration theory describes the hard part of the proton spectrum well, since the concept of level densities ceases to be meaningful near the ground state of a nucleus. The cross-sections of these reactions were also measured [14]. The energy spectra of α-particles from (n,α) reactions with nuclei of ^{28}Si and ^{29}Si were measured with a sodium-lithium drift detector, which also served as target [15]. In this study, up to five groups of α-particles corresponding to transitions to the different levels of the final product were identified and the reaction cross-section was determined for each group. Together with research workers from the Radium Institute, the fine structure of fragments produced in the fission of ^{232}Th, ^{235}U, ^{237}Np and ^{239}Pu by 14.7 MeV neutrons was studied using a mass spectrometer to identify isotopes of xenon with A = 131-136 [16,17]. The results show that the fine structure (with an increased fission fragment yield where A = 134) is preserved right up to compound nucleus excitation energies of 21 MeV, which can be explained by the large contribution from the (n,nf) and (n,2nf) reactions, leading to rapid "cooling" of the nucleus.

In recent years a more detailed study of reactions with emission of charged particles has continued. The counter telescope method (two gas and one sodium) was used to measure energy and angular distributions of protons from the (n,p) and (n,np) reactions with ^{27}Al, ^{50}Cr and ^{54}Fe nuclei [18]. It was found that the angular distributions of protons for ^{50}Cr and ^{54}Fe are approximately symmetrical, while that for ^{27}Al is asymmetrical. The cross-sections of the (n,p) and (n,np) reactions were found and nuclear temperatures were determined. The proton spectra measured by the authors of this paper

were later analysed using a non-linear least-squares method [19], whereby it became possible to distinguish between proton spectra from non-equilibrium processes (direct and pre-equilibrium) and protons evaporating from the compound nucleus separately in the (n,p) and (n,np) reactions. Here, account was taken of distortions in the energy spectrum of charged particles in targets of finite thickness [20]. For the time-of-flight method of measuring neutron spectra from the (n,n), (n,n'γ) and (n,2n) reactions, a technique was developed involving the introduction in sequence of corrections for the differential non-linearity in the scales of analysers, for finite geometry etc. [21]. A method was also developed for analysing the response function of a time-of-flight spectrometer for fast neutrons [22].

Kiev State University. A space-time neutron selection method was developed representing a combination of the time-of-flight method with detection of the energy spectra of gamma quanta accompanying neutron emission [23]. This method can be used in conditions of limited time resolution when studying the transitions between low-lying nuclear levels, for example for identifying transitions of the $4^+ \rightarrow 2^+$ type etc. Together with a representative of the Physics Institute of Bratislava, Czechoslovakia, measurements were made of the interaction cross-section of 14.6 MeV neutrons with ^{56}Fe nuclei leading to the formation of only one secondary neutron in the energy range $0.3 \leq E' \leq 1.1$ MeV. It was not possible to describe the cross-section obtained of $\sigma = 46 \pm 24$ mbn within the framework of the statistical model, which indicates the possibility of a (n,γn') process with the emission of a gamma quantum at a pre-equilibrium stage [24]. At the same time, differences in the angular distributions of gamma quanta discovered in measurements of the differential cross-sections for the emission of certain gamma lines in the ^{115}In (n,xnγ) and $^{64,66,68}Zn$ (n,n'γ) reactions can be examined on the basis of the simple model of a statistical cascade of the population of low-lying levels [25].

Using a spectrometer based on detection of recoil protons by a scintillation counter with stilbene, measurements were made of the spectra of neutron leakage from an aluminium sphere and a uranium sphere surrounding the neutron generator target [26]. The secondary neutron spectra were measured in the energy range between 0.6 and 9 MeV for uranium and between 3 and 14 MeV for aluminium. The results are shown in the form of tables and a good agreement with theory is noted.

Using the time-of-flight method in the range of angles between 5° and 175°, the angular distributions of secondary neutrons formed in the interaction of 14.6 MeV neutrons with ^{56}Fe, ^{59}Co, ^{93}Nb, ^{115}In, ^{205}Bi and ^{238}U

nuclei were measured [27,28]. The results are analysed within the framework of a generalized exiton model taking into account pre-equilibrium disintegration of nuclei and interference of channels with fixed J but different values of ℓ. Altogether, the calculations give a qualitative picture of the fundamental features of the behaviour of differential cross-sections and, in particular, show a marked preponderance of forward neutron emission. At the same time, calculations for iron within the framework of the microscopic approach [29] do not give the anticipated quantitative agreement with experimental results and predict the existance of a structure in the form of angular distributions which is not in fact observed.

The activation method with detection of gamma quanta by a germanium-lithium counter was used to measure the cross-sections of the ^{115}In (n,γ) $^{116}In^{m}$ reaction [30]. Here, the intensity of gamma lines with E_γ = 416 keV from the disintegration of $^{116}In^{m}$ was compared with 319 keV lines from the ^{113}In (n,n') $^{113}In^{m}$ reaction and with the 336 keV line from the ^{115}In (n,n') $^{115}In^{m}$ reaction, for which the cross-sections were then determined in terms of the known (n,p) and (n,α) reaction cross-sections for aluminium. The results are shown in a table.

Reference reaction	Cross-section of reference reaction, mb	$\sigma_{n\gamma}(^{115}In)$, mb
$^{113}In(n,n')^{113}In^{m}$	56.0 ± 3.6	1.27 ± 0.20
$^{115}In(n,n')^{115}In^{m}$	62.1 ± 3.9	1.08 ± 0.18

A powerful new neutron generator with an ion source of the duoplasmatron type and a power of 5 kW was constructed in order to produce 14 MeV neutrons [31]. The generator can produce deuterons with an energy of 150 keV; the beam current is up to 10 mA. At E_o = 135 keV and I = 4.5 mA a neutron yield of $\simeq 10^{11}$ n/s was achieved.

Radium Institute (Leningrad). Together with physicists from the Technical University of Dresden (German Democratic Republic), measurements were made of the fission cross-sections for the $^{235,238}U$, ^{237}Np and ^{239}Pu nuclei [32]. Here, the associated particle technique for obtaining absolute cross-sections was used. For the measurements a deuteron beam with E = 130 keV and I = 10-30 μA struck a T+Ti target affixed to a copper backing. 14.7 MeV neutrons were detected at an angle of 15° to the axis of the deuteron beam. The results are as follows: $\sigma_f(^{235}U)$ = 2.085 ± 0.023 b, $\sigma_f(^{238}U)$ = 1.166 ± 0.021 b, $\sigma_f(^{237}Np)$ = 2.226 ± 0.024 b and $\sigma_f(^{239}Pu)$ = 2.394 ± 0.024 b.

I.V. Kurchatov Atomic Energy Institute (Moscow). Measurements were made of the spectra of gamma quanta and the formation cross-sections of discrete gamma lines occurring as a result of inelastic interaction of 14 MeV neutrons with magnesium, sodium, phosphorus, sulphur, titanium and zinc nuclei [33]. The measurements were performed using spherical samples surrounding the neutron generator target. The gamma quanta were detected by a scintillation counter with a NaI(Tl) crystal 200 mm in diameter and 100 mm thick which was placed behind a concrete shield 4 m from the sample. Sharply defined peaks corresponding to the 2^+ levels were observed in the spectra obtained. Using a similar method, the same authors measured the cross-sections of the yield of individual gamma lines and group-averaged cross-sections of the formation of gamma quanta in decimal energy ranges for copper, uranium-235, uranium-238 and plutonium-239 [34]. The results are given in tables and a linear dependence of σ_γ on $A^{1/3}$ is discovered.

Nuclear Physics Institute of the Kazakh Academy of Sciences (Alma-Ata). The activation method involving a semi-conductor gamma spectrometer was used to measure the cross-sections of the (n,p) and (n,α) reactions with nuclei of 19 nuclides at E_n = 14.8 MeV [35]. The measurements were performed for the cross-sections of the reactions ^{65}Cu (n,2n) ^{64}Cu and ^{27}Al (n,α) ^{24}Na. The results are shown in the form of tables.

Khar'kov Institute of Physics and Technology of the Ukrainian Academy of Sciences. During the 1970s a cycle of measurements was carried out on differential cross-sections of the (n,α) reaction at neutron energies of 14.7 MeV with the nuclei ^{51}V, ^{55}Mn, ^{59}Co [36], ^{50,52,53,54}Cr, ^{54,56,57,58}Fe, ^{60,62}Ni [37,38] and ^{40,42,43,44}Ca [39]. A correlation was found between the integral cross-sections of the (n,α) and (n,p) reactions as a function of mass number. The experimental differential cross-sections are satisfactorily approximated by calculations within the framework of the statistical model with level density parameters near those of theory.

The transmission beam method was used to measure the total interaction cross-sections of neutrons with Ni, Mo, Sn, W and Bi nuclei [40]. The results are as follows: σ_t(Ni) = 2.74 ± 0.03 b, σ_t(Mo) = 4.06 ± 0.03 b, σ_t(Sn) = 4.67 ± 0.04 b, σ_t(W) = 5.06 ± 0.04 b and σ_t(Bi) = 5.37 ± 0.05 b.

Some conclusions. From the above it will be seen that a very wide range of studies is being performed at different institutes in the Soviet Union on processes of interaction between 14–15 MeV neutrons and atomic nuclei: studies are being made of different reactions (elastic and inelastic scattering of neutrons, reactions with charged particle and gamma quantum emission and

fission) and measurements are being made of their different characteristics (cross-sections, secondary particle spectra and angular distributions); for this, use is being made of a variety of resources (time-of-flight method, scintillation spectrometers, counter telescopes and activation). In parallel, theoretical studies are being performed on different mechanisms of nuclear processes. All these studies are yielding numerous experimental data which are being incorporated into the EXFOR system. Nevertheless, the considerable difficulties arising in studies with 14 MeV neutrons, associated to a large extent with the need for distinguishing between a considerable number of possible processes, mean that the accuracy of measurement being attained at present is still not sufficient to satisfy requirements for the corresponding nuclear data. Such studies will therefore be continued.

REFERENCES

[1] ANUFIRIENKO, V.B., et al., Yad. Fiz. 2 (5) (1965) 826.

[2] SAL'NIKOV, O.A., et al., Yad. Fiz. 4 (6) (1966) 1154.

[3] SAL'NIKOV, O.A., et al., Yad. Fiz. 12 (6) (1970) 1132.

[4] SAL'NIKOV, O.A., et al., Preprint FEhI-216 (1970).

[5] CHALUPKA, A., et al., ZfK-410 (1980) 23.

[6] LYCHAGIN, A.A., et al., Preprint FEhI-923 (1979).

[7] LYCHAGIN, A.A., et al., Preprint FEhI-1406 (1983).

[8] LYCHAGIN, A.A., et al., Preprint FEhI-1385 (1982).

[9] LYCHAGIN, A.A., et al., Programme of the VIth All-Union Conference on Neutron Physics, Kiev, 1983, p. 38, para. 13.

[10] BARYBA, V.Ya., KORNILOV, N.V., SAL'NIKOV, O.A., Preprint FEhI-947 (1979).

[11] BYCHKOV, V.M., PASHCHENKO, A.B., PLYASKIN, V.I., in: Nejtronnaya fizika (Neutron Physics), Pt. 3, TsNIIatominform, Moscow (1980) 291.

[12] KOVRIGIN, B.S., KLOCHKOVA, L.I., Yad. Fiz. 19 (4) (1974) 715.

[13] ALEKSANDROV, D.V., KLOCHKOVA, L.I., KOVRIGIN, B.S., Yad. Fiz. 22 (6) (1975) 1146.

[14] ALEKSANDROV, D.V., KLOCHKOVA, L.I., KOVRIGIN, B.S., At. Ehnerg. 39 (2) (1975) 137.

[15] KLOCHKOVA, L.I., KOVRIGIN, B.S., At. Ehnerg. 42 (2) (1977) 141.

[16] PETRZHAK, K.A., PLATYGINA, E.V., TEPLYKH, V.F., At. Ehnerg. 42 (4)(1977) 337.

[17] TEPLYKH, V.F., et al., Yad. Fiz. 29 (2) (1979) 293.

[18] KLOCHKOVA, L.I., KOVRIGIN, B.S., et al., in: Nejtronnaya fizika (Neutron Physics), Pt. 2, TsNIIatominform, Moscow (1980) 58.

[19] KLOCHKOVA, L.I., KOVRIGIN, B.S., Programme of the VIth All-Union Conference on Neutron Physics, Kiev, 1983, p. 22, para. 23.

[20] KURITSYN, V.N., SHIBAEV, V.A., Programme of the VIth All-Union Conference on Neutron Physics, Kiev, 1983, p. 23, para. 38.

[21] ALEKSANDROV, D.V., KOVRIGIN, B.S., Programme of the VIth All-Union Conference on Neutron Physics, Kiev, 1983, p. 22, para. 27.

[22] ALEKSANDROV, D.V., KOVRIGIN, B.S., Programme of the VIth All-Union Conference on Neutron Physics, Kiev, 1983, p. 23, para. 37.

[23] ANDREEV, E.A., et al., Programme of the VIth All-Union Conference on Neutron Physics, Kiev, 1983, p. 23, para. 45.

[24] GLAVACH, S., DEGTYAREV, A.P., PROKOPETS, G.A., Yad. Fiz. 31 (5) (1980) 1121.

[25] GLAVACH, S., DEGTYAREV, A.P., PROKOPETS, G.A., in: Nejtronnaya fizika (Neutron Physics), Pt. 2, TsNIIatominform, Moscow (1980) 13.

[26] BRODER, D.L., et al., Programme of the VIth All-Union Conference on Neutron Physics, Kiev, 1983, p. 19, para. 24.

[27] DEGTYAREV, A.P., PROKOPETS, G.A., in: Nejtronnaya fizika (Neutron Physics), Pt. 2, TsNIIatominform, Moscow (1980) 50.

[28] DEGTYAREV, A.P., et al., Yad. Fiz. 34 (2) (1981) 299.

[29] IGNATYUK, A.V., LUNEV, V.P., PRONYAEV, V.G., Izv. Akad. Nauk SSSR, Ser. Fiz. 39 (10) (1975) 2144.

[30] DEMEKHIN, V.L., LESHCHENKO, B.E., MAJDANYUK, V.K., PETO, G., Programme of the VIth All-Union Conference on Neutron Physics, Kiev, 1983, p. 27, para. 10.

[31] KUKHLENKO, A.S., et al., Programme of the VIth All-Union Conference on Neutron Physics, Kiev, 1983, p. 22, para. 33.

[32] ARLT, R., et al., Nuclear Cross-Sections for Technology (Proc. Knoxville Conf.), NBS, United States (1980) 990.

[33] BEZOTOSNYJ, V.M., GORBACHEV, V.M., SHVETSOV, M.S., SUROV, L.M., in: Nejtronnaya fizika (Neutron Physics), Pt. 2, TsNIIatominform, Moscow (1980) 21.

[34] BEZOTOSNYJ, V.M., GORBACHEV, V.M., SHVETSOV, M.S., SUROV, L.M., At. Ehnerg. 49 (4) (1980) 239.

[35] ARTEM'EV, O.I., KAZACHEVSKIJ, I.V., et al., At. Ehnerg. 49 (3) (1980) 195.

[36] DOLYA, G.P., et al., in: Voprosy atomnoj nauki i tekhniki, Ser. "Fizika vysokikh ehnergij i atomnogo yadra", 1 (18) Khar'kov (1977) 15.

[37] DOLYA, G.P., et al., in: Nejtronnaya fizika (Neutron Physics), Pt. 2, Moscow (1977) 68.

[38] DOLYA, G.P., BOZHKO, V.P., et al., KFTI 76-50, Khar'kov (1976).

[39] DOLYA, G.P., OLEJNIK, S.N., SAVCHUK, O.G., Voprosy atomnoj nauki i tekhniki, seriya "Obshchaya i yadernaya fizika" 2 (16) (1981) 31.

[40] TUTUBALIN, A.I., BOZHKO, V.P., DAKHNO, D.D., DOLYA, G.P., in: Nejtronnaya fizika (Neutron Physics), Pt. 2, Moscow (1977) 65.

CROSS SECTIONS OF SOME REACTIONS INDUCED BY 14 MEV NEUTRONS

I.Gârlea,C.Miron,D.Dobrea,C.Roth,H.N.Roşu,S.Răpeanu

Central Institute of Physics,Bucharest,POB MG-6

Romania

Abstract

The activation cross sections for $^{58}Ni(n,p)$, $^{58}Ni(n,2n)$, $^{59}Co(n,2n)$, $^{59}Co(n,\ )$, $^{48}Ti(n,p)$, $^{27}Al(n,p)$ and $^{98}Mo(n,p)$ reactions have been obtained from reaction rates measured by high resolution gamma spectrometry (Ge-Li). The Ge-Li crystal has been calibrated in the absolute efficiency . The cross section of $^{235}U(n,f)$ reaction has been taken as reference.

The reported cross sections have been measured by using TEXAS-9900 neutron generator of Central Institute of Physics. The energy of neutrons incident on the targets have been of 14.80 MeV, with a dispersion lower than 65 keV. The neutron flux has been monitored by a system of 3 absolutely calibrated fission chambers.

1. INTRODUCTION

The results here reported have been achieved under the contract TA/INT/018 of the Interregional Project[1] initiated by International Atomic Energy Agency-Vienna. The experimental procedure has been set in reference[2] by tacking into account the statistical limits suggested by Agency and the admitted errors for the absolute calibration installations. These works are performed in the frame of the international effort for covering of major requirements nuclear data used in the fusion reactor technology and shielding calculations. The activation reactions here tested have an important role in the neutron dosimetry for fusion reactors and in the fast reactor design.

2. RUN-TO-RUN MONITOR LEVELS

The neutron flux has been monitored by means of 3 parallel plate sealed fission chambers , made at Saclay[3], of 12 mm diameter, set up at 120° in the plane of the Tritium target, around

the generator tube, perpendicular to the deuteron beam. These chambers, of which characteristics are given in Table 1, are designated as follows:

FC 6 - 1st monitor (MON1)

FC 7 - 2nd monitor (MON2)

FC 18 - 3rd monitor (MON3)

These chamber have been absolutely calibrated by exposure in the reference spectrum $\Sigma\Sigma$-ITN[4] and in standard thermal spectrum[5]. The used procedure and results concerning the calibration of fissionable deposit masses contained in fission chambers, are given in reference[6].

The beam spot on the Tritium target has a diameter of about 1 cm and its position changes during an irradiation and from an irradiation to the next one. The displacement of the beam alters neutron source parameters. The spot displacement could be inferred from the indications of the 3 permanent monitors by tacking into account the masses of fissionable deposits and cross sections, accurately determined. The spot position for every recording is calculated by means of computer code POZ[7] from the indications of MON3 to that of MON1 and indications of MON2 to that of MON1. Code POZ also calculates the neutron intensity in this determined spot position. Once know the position, a Monte-Carlo computer program[8] calculates the neutron intensity incident on the detector. That program also gives the neutron energy dispersion, caused by coolant and structure materials.

The main operation parameters of TEXAS generator are, for the reported measurements, as follows:

- high voltage : 120 kV
- current : about 450 μA
- neutron intensity : about 10^{10} n/s.

The Tritium targets have:

- Molybdenum backing of 0.4 mm thickness
- deposit: Titanium , about 10 mg/cm^2

- total activity : 1o Ci Tritium
- water cooling.

The distance target-sample is 13.4 mm.

3. REACTION RATES MEASURING

The cahracteristics of fission chambers used as reference and permanent monitors are given in TABLE 1. The fission chambers No.23 (containing ^{235}U) and No.24 (containing ^{239}Pu) have been irradiated in a central position on the window screen of TEXAS generator. Simultaneously, have been recorded and the indications of the monitors. An electronic chain set as suggested by J.Grundl[9] has been used for the both central chamber and monitors. The experimental set up is that presented in ref.[2].

The Nickel, Molybdenum ,Titanium ,Aluminium and Cobalt activation detectors have been irradiated on the generator window screen , in a central position, together with the fission chamber No.23. The characteristics of these activation foils are given in Table 2, cf.supplier's material data sheets. All materials are natural, not enriched.

The gamma activities of the isotopes produced in the reactions induced by 14.8o MeV neutrons have been determined by a Ge-Li(1oocm^3) crystal spectrometer, calibrated in absolute efficiency[1o]. The source-crystal distance has been of 5 cm and crystal resolution of 2.98 keV. The calibration factor for the ND442o analyzer is o.35625 keV/channel. The analyzer is provided with an ADC-1oo MHz module.

The PDP15 version of the computer code SAMPO[11] has been used to calculate gamma rays peak areas. The reaction rates have been calculated from these results by using the RATREA program and nuclear constants from references[12,13].

The indications of fission chamber No.23, irradiated simultaneously with activation foils or independently, have been used to calculate the average flux for each irradiation.

TABLE 1 : Fission chamber characteristics

Chamber identification	Contain	Main isotope mass ($x10^{17}$ nuclei)	Aditional isotope mass ($x10^{15}$ nuclei)	Impurities (%)
CF 23	^{235}U	2.281±1.6%		99.89 ^{235}U, o.o2 ^{234}U, o.o7 ^{238}U o.o4 ^{236}U
CF 24	^{239}Pu	2.367±1.8%		99.88 ^{239}Pu, o.12 ^{240}Pu
CF 7	^{238}U+1% ^{239}Pu	2.865±2.8%	3.o26± 2.7%	
CF 6	^{238}U+1% ^{233}U	2.488±2.6%	2.294±2.6%	
CF 18	^{238}U	1.7o5±2.8%		loo ^{238}U, 2oo ppm ^{235}U

TABLE 2 : The caharacteristics of activation foils

Material	Foil	Diameter (mm)	Weight (g)	Purity (%)	Impurities (%)
Nickel	Ni-AB	12.7	o.562630	99.981	C(o.ool),Mn(o.ool),Co(o.ool),
	Ni-1	2o	2.377288		Fe,S,Si,Cu,Cr,Ti,Mg(o.ool)
	Ni-2	2o	1.o971o8		
Titanium	Ti-1	2o	1.716185	99.729	Cu o.oo5, Si,Sn(o.oo5),Al(o.7o)
	Ti-2	2o	1.7o1297		Fe(o.12o),V(o.o2o),Cr(o.o4o)
					Mn,Mg(o.ool),Ni(o.oo4)
Aluminium	Al-C	19.o5	o.575o29	99.994	Mg o.ool, Fe o.oo2, Cu o.ool
					Ca(o.oo2)
Cobalt	Co-1	2o	1.366940	99.9o88	Fe(o.ol),Ni(o.o3),Mn(o.oo8),
	Co-2	2o	1.362115		Mg(o.oo3),Ca(o.ooo2),Cu,Si(o.o2)
Molybdenum	Mo-1	2o	3.242999	99.9995	
	Mo-2	2o	3.215952		

TABLE 3 : Results

Reaction	Detector	Reaction rate	F	d (mm)	f	G	I	Cross section (mb)	Error (%)
$^{27}Al(n,p)$	Al-C	6.518E-17	0.9894	2.413	0.974	0.998	0.99994	79.2	±5.0
$^{59}Co(n,2n)$	Co-2	2.312E-16	1.0	2.152	0.979	0.993	0.99908	828.0	±7.3
	Co-1	1.178E-16	1.0	2.573	0.970	0.993	0.99908		
$^{59}Co(n,\ )$	Co-1	1.023E-19	1.017	2.573	0.970	0.993	0.99908	35.0	±5.8
	Co-2	1.420E-19	1.004	2.152	0.979	0.993	0.99908		
$^{58}Ni(n,2n)$	Ni-AB	3.579E-19	1.001	1.427	0.982	0.993	0.99981	40.3	±4.9
	Ni-2	5.630E-19	1.001	2.751	0.966	0.993	0.99981		
$^{58}Ni(n,p)$	Ni-AB	3.789E-17	1.0	1.427	0.982	0.997	0.99981	392.0	±5.2
	Ni-2	6.270E-17	1.0	2.751	0.966	0.997	0.99981		
$^{98}Mo(n,p)$	Mo-1	7.736E-19	1.030	1.504	0.989	0.987	0.9995	5.4	±6.3
	Mo-2	1.091E-18	1.022	0.335	0.975	0.987	0.9995		
$^{48}Ti(n,p)$	Ti-1	1.554E-17	1.001	2.324	0.976	0.998	0.99729	73.0	±4.8
	Ti-2	1.060E-17	1.001	3.00	0.960	0.998	0.99729		

Note: The value for Titanium includes and that for $^{49}Ti(n,np)$.

In TABLE 3 there are gathered the results concerning cross sections measurements. The reaction rate is determined per nucleus, using the absolute values of activities. The corrections applied to reaction rates there are presented in the same table and they are:

F - correction for time variation of neutron source intensity;

d -correction for spot displacement, in mm, averaged for all time of irradiation;

f - correction for neutron source displacement;

G- correction for gamma selfabsorbtion;

I - impurity correction.

The cross sections are calculating taking as reference that of $^{235}U(n,f)$ reaction. The associated errors are:

- statistics error	0.4 - 1.2 %
- error in the absolute efficiency calibration	1.5 - 2.1 %
- background substraction error	0.5 - 0.9 %
- error in the absolute flux determination	2.0 - 2.3 %.

REFERENCES

1. N.Kocherov,JJ.Schmidt, - Interregional Project for Training in Basic Techniques for the Generation on Nuclear Data Required for the Development and Applications of Nuclear Science and Technology.,IAEA-Viena,NDS,(1980)

2. I.Gârlea et al - Measuring of the integral cross sections at 14 MeV for reactions: $^{115}In(n,n')$, $^{197}Au(n,2n)$, $^{93}Nb(n,2n)$, $^{27}Al(n,\alpha)$, $^{56}Fe(n,p)$, $^{239}Pu(n,f)$, $^{238}U(n,f)$, $^{232}Th(n,f)$ and $^{237}Np(n,f)$. (1983)

3. M.Guerry,A.Jarrige - Rev.Phys.Appl.,No.6,p.121, (1975)

4. I.Gârlea et al - Studii Cercet.Fizică, No.6, (1978)

5. I.Gârlea - Doctor thesis, Bucureşti, (1979)

6. I.Gârlea et al - R.I. IRNE 1386 (1983)

7. C.Roth - Description of code POZ (1983)

8. D.Dobrea - Calculator programe F1 (1983)
9. J.Grundl et al- Nucl.Technology, No.25,p.237, (1975)
1o. I.Gârlea et al - Studii Cercet.Fizică, No.1o, (1981)
11. J.T.Routti - Rep.UCRL-19452 (1969)
12. *** - Die gamma Einien der Radionuclide (197o)
13. N.G.Gusev,P.P.Dimitriev - Spravocinik, Moskva Atomizdat, (1977)

A PROPOSAL TO DETERMINE NEUTRON FLUX-SPECTRA AT ROMANIAN PLASMA FOCUS INSTALLATIONS, BY SSTR METHOD

C.Miron, I.Gârlea, C.Dumitrescu, V.Zoiţa
Central Institute of Physics, Bucharest, POB MG-6, ROMANIA

Abstract

A procedure of measuring of flux fast neutrons emitted by the plasma focus installations of Central Institute of Physics, by using the solid state track recorders (SSTR) is suggested. The method is based on the analysis of the tracks recorded in Makrofol KG, tracks due to the fission fragments appeared by neutron irradiations of fissionable deposits.

The absolute calibration of fissionable deposits in the reference spectrum $\Sigma\Sigma$ -ITN and in the thermal standard spectrum (SST) and also techniques of sample preparation and image analysis are described.

The absolutely measured fission rates serve to obtaining of the absolute values of neutron flux and to spectral characterization of the fields, being used as input data in the unfolding code SANDII.

1. INTRODUCTION

The fast neutrons emitted by hot plasmas produced in controlled fusion devices can provide informations regarding some characteristics of the source plasma, such as temperature or energy distribution of interacting particles , plasma confinement and lifetime .

The neutron diagnostics methods have therefore become standard measuring techniques for various fusion plasmas. Their application to the investigation of the performances of plasma focus devices - one of the most efficient plasma neutron generators- presents a particular interest : it is expected that by making sufficiently accurate measurements on the fusion neutrons (yield, energy spectrum flux anisotropy), one can derive relevant informa-

tion on the energetic characteristics of the plasma particles. This represents a basic requirement for identifying the physical processes involved in energy transport in the focused plasma, a matter of major interest in the extrapolation of plasma focus devices to higher energies and currents.

The plasma focus installations operate in pulses, so the neutron flux measuring techniques have to involve an integration, independently by time. The emission intensities achieved by these devices make requirement of the integrating large number of pulses to get a resonable statistics. Thus, it is very attractive to use the integral recorders, SSTR type, associated with fissionable disks, to characterize the neutron flux-spectrum in these facilities.

2. FLUX-SPECTRA MEASUREMENTS

For the purpose of improving the accuracy of flux-spectrum measurements the plasma focus neutron emission, a proposal is made for using the solid state track detectors. The fluence range that such a technique could be applied (if using Deuterium in devices) is $5x10^{8}$ - $5x10^{11}$ n/cm^{2} . This range is currently used in the measure points from the plasma focus facilities (outside the reaction chambers). Preliminary measurements have been performed on the IPF-2/2o and IPF-3/5o plasma focus devices in operation in the Central Institute of Physics, Bucharest.[1,2,3]

The fissionable deposits used in our works there are Aluminium alloys : ^{235}U 2o% and 1o% , ^{239}Pu 1o% and 5% and pure metalic disks of ^{238}U. For reaction rate obtaining it is necessary to know the number of nuclei in deposit, and more precisely , this value in a "sensible volume", placed on the sample surface.[4] This volume produces fission fragments detected by plastic foils, being a cylinder with height equal to one half of path length in the fissionable samples. The rest of fission fragments are absorbed in fissionable material and does not impress Makrofol detector.

By exposure in the reference spectrum $\Sigma\Sigma$-ITN[5] and in thermal standard spectrum (SST)[6] and tacking into account the abso-

lute cross sections for $^{235}U(n,f)$, $^{238}U(n,f)$, $^{239}Pu(n,f)$ reactions (accurately measured and averaged on these spectra)[7], there were determined the following values:

- for ^{235}U 2o% $6.572 \times 10^{17} \pm 1.9\%$ nuclei/cm^2
  Aluminium alloy
- for ^{239}Pu 1o% $3.oo8 \times 10^{17} \pm 2.3\%$ nuclei/cm^2
  Aluminium alloy
- for ^{238}U $8.323 \times 10^{18} \pm 2.7\%$ nuclei/cm^2
  pure metal

These values have used to determine the absolute fission rates. The solid state track recorders impressed by fission fragments have been prepared for microscope examination by technology described in references[8,9].

For flux-spectra measurements there were exposed at IPF-3/5o installation calibrated fissionable deposits associated with Makrofol foils (6o μm thickness), in two positions: 0° and 90°, refering to plasma positioning. The measured reaction rates, with their associated errors, are given in Tabla 1. These absolute values have been used as input data in unfolding code SANDII[10,11]. The spectral forms, for the two irradiation positions, have been determined by nuclear emulsions method[12]. The nuclear data library used by code is ENDF/B V- Dosimetry file. The neutronic flux-spectra obtained by this calculation, are described in 62o energy groups (in the range o-18 MeV). They are characterized by the follows: 1st position o°

- average energy : 2.7 MeV
- fluence : 7.14×10^7 neutron/cm^2
- neutrons with energy under o.5 MeV : o.1%

2nd position (90°)

- average energy : 2.14 MeV
- fluence : $4.o4 \times 10^7$ neutron/cm^2
- neutrons with energy under o.5 MeV : o.3% .

TABLE 1

ISOTOPE	DENSITY (track/cm^2)	REACTION RATE (per cm^2, per nucleus, per s)	ERROR (%)
1st position 0^o			
^{238}U	322.78	3.878×10^{-17}	± 5.1
^{235}U	90.13	1.371×10^{-16}	± 7.7
^{239}Pu	125.05	4.157×10^{-16}	± 7.3
2nd position 90^o			
^{238}U	151.85	1.824×10^{-17}	± 6.9
^{235}U	92.98	1.415×10^{-16}	± 8.9
^{239}Pu	122.61	3.744×10^{-16}	± 7.6

We suggest the utilization of solid state track recorders for spectral characterization of neutronic fields generated by plasma focus devices, because this method completes the description of neutronic spectra obtained by time-of-flight and nuclear emulsions methods, giving and the absolute values of flux.

REFERENCES

1. C.Miron, I.Gârlea - R.I. IRNE 1145 (1982)
2. I.Gârlea, C.Miron, C.Roth - R.I. IRNE 1149 (1982)
3. V.Zoiţa et al - Plasma Physics and Controlled Nuclear Fusion Research. IAEA, vol.II, p.197, (1981)
4. C.Miron, I.Gârlea - R.I. IRNE 1192 (1982)
5. I.Gârlea et al - Studii Cercet.Fizică, Nr.6, (1978)
6. I.Gârlea - Doctor thesis, Bucharest , (1979)
7. I.Gârlea et al - Rev.Roum.Physique ,No.4,p.409, (1978)
8. R.Richmond,R,Rügger - Nucl.Technology, No.10, p.213, (1971)
9. I.Gârlea et al - Studii Cercet.Fizică, No.5, (1978)
10. I.Gârlea et al - Studii Cercet.Fizică, No.1, (1979)
11. W.N.McElroy et al - Nucl.Sci.Eng., vol.36,No.15, (1969)
12. A.Mihul - Private communication , (1983)

Gamma ray spectra and multiplicities from ^{52}Cr bombarded with 14.6 MeV neutrons +

P.Obložinský, S.Hlaváč, R.Antalík and E.Běták
Institute of Physics, Electro-Physical Research Centre of the Slovak Academy of Sciences, 842 28 Bratislava, Czechoslovakia

Present study with enriched ^{52}Cr is a part of our systematic effort to obtain more comprehensive and new data as well as physical insight about γ decay of highly excited fp shell nuclei. γ ray production cross sections on a number of these nuclei is of interest for fusion/fission reactor technology. Recently, we completed results for another enriched sample, ^{58}Ni, and reported them to the Agency [1].

Measurements were carried out with the multidetector system described in ref.[2]. It makes use of the associated α particle technique and includes NaI(Tl) and Ge(Li) γ ray spectrometers as well as NE 213 neutron tof spectrometer. The sample of ^{52}Cr enriched to 99.8%, weight 120g and thickness 0.0123 at/b, was irradiated 210 hours. The following data were taken:

(i) NaI(Tl) singles γ ray spectrum in the spectral energies $E_\gamma \approx$ 0.2-25 MeV at 70 deg towards the neutron beam,

(ii) Ge(Li) singles spectra in the region $E_\gamma \approx$ 0.3-2.5 MeV at 40, 61, 90, 103, 134 and 158 deg,

(iii) singles neutron tof spectra in the region $E_n \approx$ 1.5-14 MeV at 30,60, 90, 101, 123 and 149 deg,

(iv) Ge(Li) spectrum in coincidence with open NaI(Tl) and

(v) full matrix of neutron tof spectrum versus NaI(Tl) γ ray spectrum.

The task of data reduction has been already started.

Experimental results including cross sections, angular distributions as well as γ ray multiplicities are partial and preliminary . Among them are angular distributions for 10 discrete transitions in the $(n,n'\gamma)$ channel and for 2 transitions in the $(n,2n\gamma)$ channel. The neutron spectrum gated

+) Work performed under the IAEA Research Agreement No 3436/CF

Tab.1. Average γ ray multiplicities observed in $^{52}Cr(n,n'\gamma)$.

Transition	E_γ (keV)	$\overline{M}$
(3+)→4+	704.6	7.2(.8)
4+ →4+	647.4	5.8(.7)
6+ →4+	744.2	6.2(.7)
4+ →2+	1333.6	3.9(.5)
4+ →2+	935.5	3.8(.4)
2+ →0+	1434.1	3.8(.2)

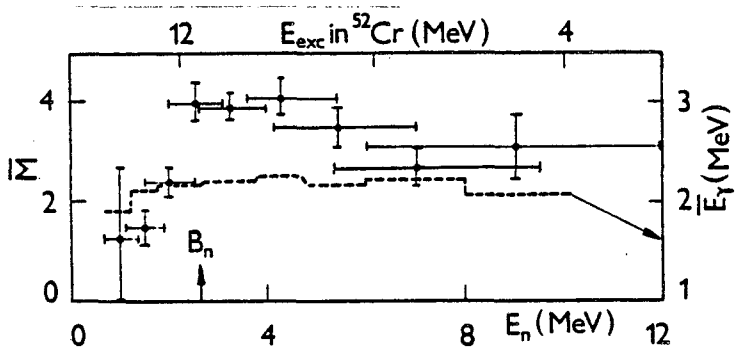

Fig.1. Average γ ray multiplicites observed in $^{52}Cr+n$ as a function of energy of emitted neutrons. Also shown are average γ ray energies.

with strong 1434 keV line in the $(n,n'\gamma)$ channel is of special interest. Average γ ray multiplicities including specific discrete transition are given in tab.1 and those following emitted neutrons in fig. 1.

Theoretical analysis was initiated using advanced statistical code STAPRE[3] as well as relatively simple, but fully preequilibrium PEQGM[4] with multiple particle and multiple γ emission included. More sophisticated calculations concentrate on high energy parts of neutron spectra in frame of the DWBA formalism with macroscopic form factors, where excitation strenghts are computed in the random phase approximation [5].

References

1) S.Hlaváč and P.Obložinský, Report for NDS IAEA (October 1983)
2) S.Hlaváč and P.Obložinský, Nucl.Instr.Meth. 206(1983)127
3) M.Uhl and B.Strohmaier, Code STAPRE, Report IRK Vienna 76/1
4) E.Běták and J.Dobeš, Report IP EPRC SAS (Bratislava 1983)
5) R.Antalík, Thesis (Bratislava 1983), unpublished

MEASUREMENT OF DOUBLE DIFFERENTIAL NEUTRON EMISSION CROSS SECTIONS BY THE 14 MEV NEUTRON SOURCE OKTAVIAN

A. Takahashi, J. Yamamoto, M. Ueda, M. Fukazawa, Y. Yanagi,
J. Miyaguchi and K. Sumita

Department of Nuclear Engineering, Osaka University, Japan

Abstract: Using the intense 14 MeV neutron source facility OKTAVIAN, experimental system has been established to measure double differential neutron emission cross sections of fusion reactor candidate elements. Measured data for D, Li, F and Pb are compared with ENDF/B-IV and other calculations. Secondary neutron energy range 14 MeV to 50 KeV is covered.

INTRODUCTION

Double differential neutron emission cross sections (DDX) are useful for fusion neutronics calculations/1/. However DDX can not be sufficiently reproduced/2/ from currently available nuclear data libraries like ENDF/B-IV and JENDL-2, which give single differential data base. Experimental DDX data and re-evaluation of the nuclear data libraries are needed. For high accuracy measurement of DDX, time of flight technique with long flight path is very useful. At OKTAVIAN Facility/3/ of Osaka University, many DDX measurements have been carried out since 1981 and some of results were reported/4/,/5/. In the present paper are shown new results for D, Li, F and Pb. Measurement for a wide secondary neutron energy range 14 MeV to 50 KeV is carried out to observe (n,n't) and (n,2n) neutron distributions. The detail of experimental and other new results for O, Si, Ti, Mn, Bi and Be are shown in Ref./6/.

EXPERIMENTAL

By pulse operation of OKTAVIAN, DT neutron burst is generated at a 2 cm dia. 10 Ci TiT target bombarded with 245 KeV deuteron ion beam of which pulse width and peak current are 1.5 ns and 20 mA, respectively. In the present TOF experiment, repetition of DT neutron burst is 250 KHz or 500 KHz. By using 1 mm thick SS304 target support tube and air cooling, the lower energy part of source neutron spectrum than 10 MeV is 5 % (integral value) of nominal 14 Mev peak, so that the contamination for DDX spectra is very small. Angular dependence of source neutron energy and yield are determined experimentally/4/ by measuring elastically scattered neutron peaks from many ring samples and Al(n,alpha) activations, respectively.

For DDX measurement, the ring-sample-TOF method/4/ is applied. Ring samples with 20 cm major diameter and 2 cm minor diameter are used. A ring sample suspended with three pieces of 0.5 mm dia. steel string can be moved along the axis of deuteron beam to change scattering angle. A 5"dia. 2" NE213 detector positioned at 9.5 m from the target counts scattered neutrons from the ring. Direct injection of source neutrons into the detector is removed with a 9 cm dia. 110 cm long shadow bar. Room-returned neutrons are shielded with the pre- and main-collimator shielding system/4/. For deuterium and fluorine experiments, ring samples of compound materials were used.

Block diagram of the measuring system is shown in Ref./6/. Two parallel n-gamma pulse shape discrimination systems are used to widen the covering neutron energy range. Two kinds of setting for pulse height threshold are used in the present work; 50 KeV and 300 KeV. For the determination of energy-dependent detector efficiency, the following three methods are used; polyethylene ring TOF experiment (14 MeV to 6 MeV), Cf-252 TOF experiment (8 MeV to 300 KeV) and carbon sphere leakage spectrum measurement (1 MeV to 50 KeV in the case of 50 KeV setting)/6/.

For multiple scattering corrections, one-point transport calculations using an approximate collision probability function of ring scatterer were carried out with 64 angular points and 135 energy groups, based on ENDF/B-IV cross sections. Estimated systematic errors in DDX experiment are about 5 % in energy distribution and about 5 % in absolute values of DDX. In many cases, most prominent error source is statistical one.

SOME RESULTS AND DISCUSSIONS

In Fig.1 the result for D(n,2n) is shown. Energy-angular distributions given in ENDF/B-IV are very differed from experiment/4/. New evaluation by Young(LANL) fits fairly well to experiment. Calculation by Faddeev theory shows the best fitting to experiment.

In Fig.2 the result for F is shown. Significant disagreements are seen between experiment and ENDF/B-IV, in the lower energy range than about 8 MeV for forward angles and at level-inelastic scattering peaks for backward angles.

In Fig.3 is shown the secondary neutron spectrum of natural lithium, in comparison with two calculations. Solid curves show the results of modified ENDF/B-IV data with (n,n't) and (n,2n) kinematics. Original ENDF/B-IV data (broken) underestimate experiments at both forward and backward angle. Modified calculation shows better agreement at forward angle, but underestimates largely at backward angle, for the low energy range where (n,2n) is dominant. Experiment shows larger (n,2n) cross sections than ENDF/B-IV.

In Fig.4 the result for Pb is shown in comparison with ENDF/B-IV. Measured spectrum is much harder than that of ENDF/B-IV, (n,3n) cross section in ENDF/B-IV is too high.

Acknowledgment: The present work has been financially supported by Grant-in-Aid, Ministry of Education, Science and Culture, Japan.

References

/1/ Constantine, G. : IAEA-TECDOC-223 (1979)
/2/ Takahashi, A., Rusch, D. : KFK-2832 (1979)
/3/ Sumita, K., et al : Proc. 12th SOFT (1982)
/4/ Takahashi, A., et al : Proc. Conf. Nucl. Data Sci. Technol., Antwerp (1982)
/5/ Takahashi, A., et al : OKTAVIAN-Report A-8301 (1983)
/6/ Takahashi, A., et al : ibid., A-8303 (1983)

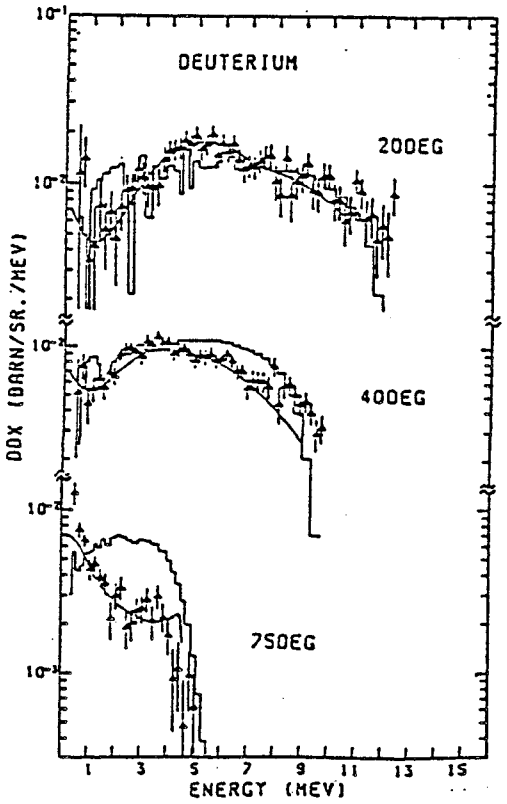

Fig.1 DDX for D(n,2n),
solid; Faddeev, broken; Young

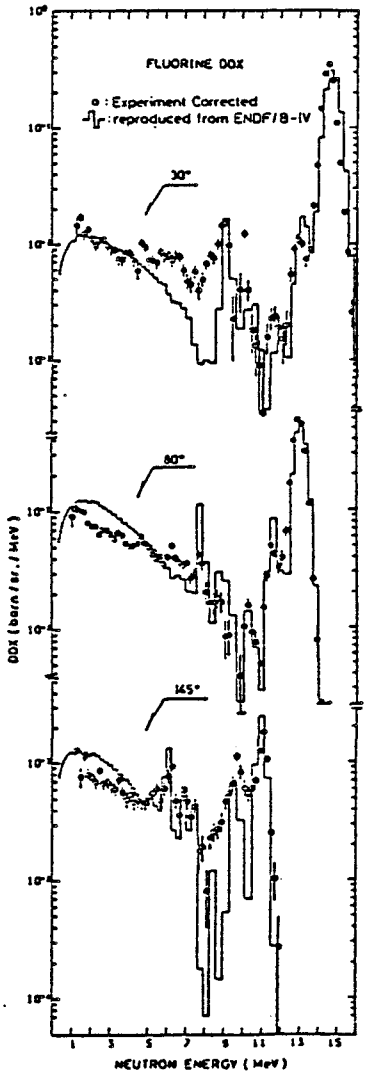

Fig.2 DDX for fluorine, c.f. ENDF/B-IV

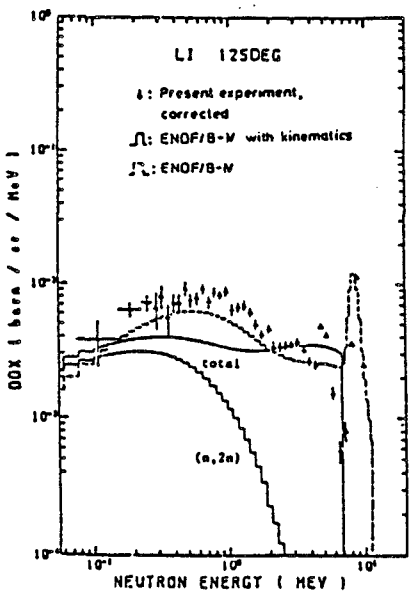

Fig.3 Secondary neutron spectrum for lithium

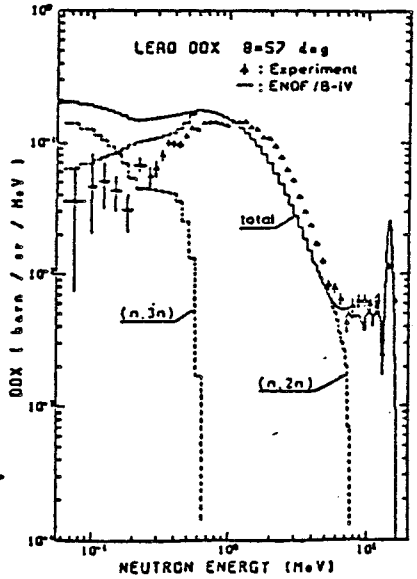

Fig.4 Secondary neutron spectrum for lead

RECENT INVESTIGATIONS OF NUCLEAR REACTIONS BY 14 MeV NEUTRONS AT THE NEUTRON LABORATORY OF THE EÖTVÖS UNIVERSITY /BUDAPEST/

F. Deák, S. Gueth, Á. Kiss, J. Kecskeméti
and P.N.Ngoc

Department of Atomic Physics
Roland Eötvös University
Budapest, Hungary

H-1088.Budapest,Puskin u. 5-7.

Results of two, recently finished works on the field of the reactions induced by 14 MeV fast neutrons are briefly reviewed:

1. Excitation Function Measurements of the $^{56}Fe(n,p)$, $^{58}Ni(n,p)$, $^{58}Ni(n,2n)$, $^{65}Cn(n,p)$ and $^{65}Cu(n,2n)$ Reactions at $13,5MeV \leq E \leq 14,7MeV$.

The excitation functions of the (n,p) and (n,2n) reactions for iron, nickel and copper have been measured by the activation method. The aim of the experiment was to provide consistent and (as far as possible) reliable cross section data for these neighbouring nuclei around the proton magic shell z=28 in order to investigate possible shell effects, (n,2n) threshold effects and energetically allowed gamma-neutron competition.

The experimental procedure was that of the standard activation method. The targets were of natural iron,nickel, and copper foils. The typical neutron production was about 5.10^{9} /sec in the whole solid angle and it was stabilized during the irradiation by computer control. The $^{27}Al(n,\alpha)$ reaction was used as monitor for the evaluation. The targets are positioned at six different angles corresponding to incident neutron energies between 13,55MeV and 14,71MeV. Special care was taken to design the target holder system in order to avoid bulks of materials with big solid angles for the target foils. The induced gamma activities were determined by Ge(Li) detector inside a $\sim$ 1m low background lead cube.

The results are summarized in Table 1. The quoted errors correspond to the statistical uncertainties added to the guessed upper limits of the ambiguities of the whole procedure.

Table 1.

	Cross sections (mb)				
Reaction	$^{56}Fe(n,p)$	$^{58}Ni(n,p)$	$^{58}Ni(n,2n)$	$^{65}Cu(n,p)$	$^{65}Cu(n,2n)$
Energy (MeV					
$13,55\pm0,12$	$107,0\pm9,5$	411 ± 29	$11,9\pm1,1$	$27,9\pm3,4$	841 ± 54
$13,77\pm0,12$	$100,4\pm8,6$	386 ± 35	$15,9\pm1,2$	$26,2\pm2,4$	843 ± 54
$14,08\pm0,13$	$99,0\pm7,7$	352 ± 33	$20,8\pm1,8$	$25,3\pm3,2$	875 ± 59
$14,40\pm0,13$	$101,6\pm9,0$	340 ± 31	$27,0\pm2,1$	$24,6\pm3,1$	908 ± 52
$14,62\pm0,14$	$96,6\pm8,2$	318 ± 26	$30,1\pm2,4$	$24,1\pm2,6$	930 ± 62
$14,71\pm0,14$	$91,3\pm7,3$	295 ± 23	$31,2\pm2,3$	$23,0\pm2,2$	954 ± 58

The experimental excitation functions have been compared with results of Hauser-Fesbach type calculations. There was a good agreement with the no-free parameter one-shot calculations in all but the ^{58}Ni(n,2n) case. - The analysis did not reveal any direct appearance of shell effects around z =28. The disagreement in the ^{58}Ni(n,2n) case may be an evidence that the gamma deexcitation mode might effectively compete with particle emission in cases where only few levels of the finite nucleus could be populated after the emission of the last particle.

2. Neutron-deuteron break-up in collinear geometry at E_n =14,7MeV with ϑ_n=0° .

The 14,7 MeV fast neutron induced break-up of the deuteron has been investigated in order to provide conclusions of enhanced reliability on the existence of the theoretically proposed collinearity effects in the three nucleon interactions.

A special arrangement has been used which made possible to cover a big part of the phase space for collinear geometry with ϑ_n=0 in a single experiment.

The energy of the neutrons was measured by time-of-flight neutron spectrometer. The target was a deuterized organic scintillator, which served as the proton detector at the same time. The neutron and the proton detectors were in coincidence, the zero of time was provided by the associated alpha particles from the neutron producing T(d,α)n reaction.

The analysis of the data has shown that the present results significantly contradict to the existence of the proposed strong cross section enhancement in the collinearity region and no evidence is seen for any prominent collinearity behaviour of the deuteron break-up cross sections. (Fig. 1.)

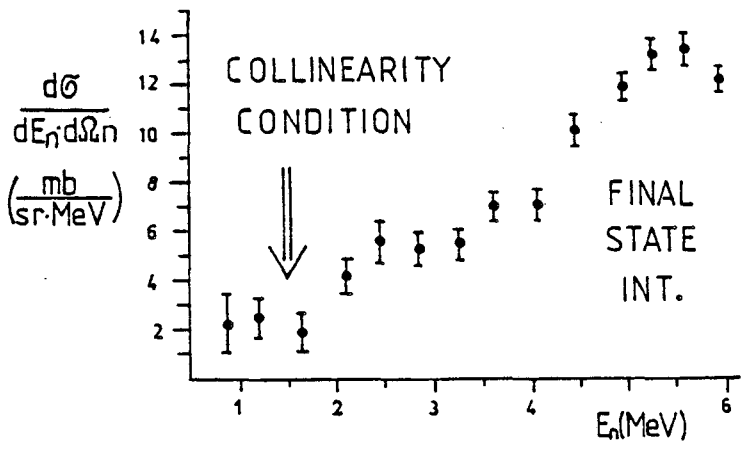

Fig. 1.
Experimental cross sections of the ^{2}H(n,pn)n reaction with ϑ_n=0°, integrated for E ≤ 5 MeV

PERFORMANCE OF A PROTOTYPE LARGE VOLUME FAST NEUTRON SPECTROMETER*

T.VILAITHONG, N. CHIRAPATPIMOL, G.G.HOYES, S.NA CHIANGMAI
S.SINGKARAT, V.TEEYASOONTRANON
Department of Physics, Faculty of Science, Chiang Mai University
Chiang Mai 50002, THAILAND

A prototype (4.5 cm diam x 28 cm) large volume liquid scintillation detector equipted with two photomultipliers has been constructed. Its principle characteristics with respect to timining uncertainty, pulse height distribution and n-γ pulse shape discrimination have been studied and are presented herein.

1. Introduction

In order to achieve an energy resolution of a few hundreds keV for high resolution neutron time-of-flight (TOF) measurements, a large volume detector with sub-nanosecond time dispersion is needed at the end of a long (>10 m) flight path. The detector described is intended to be used at the Chiang Mai 14-MeV fast neutron facility which will be operational in 1984. The purpose of this work is to evaluate the oxygen removal facility and associated fast electronic modules constructed at this laboratory.

2. Prototype detector and electronics

A 4.5 cm diam by 28 cm long pyrex glass tube was filled with BC 501 liquid scintillator.(i) Oxygen was removed by slowly bubbling high purity nitrogen gas through the scintillator. Figure 1 displays the oxygen removal facility. The scintillator is viewed from both ends by RCA 8575 photomultiplier tubes (PMT).

---

*This work has been supported in part by the International Atomic Energy Agency, Vienna, under contract no. 3226/RB and the International Seminar in Physics, Uppsala University, Sweden.

(i) manufactured by Bicron Corporation, Chio, U.S.A.

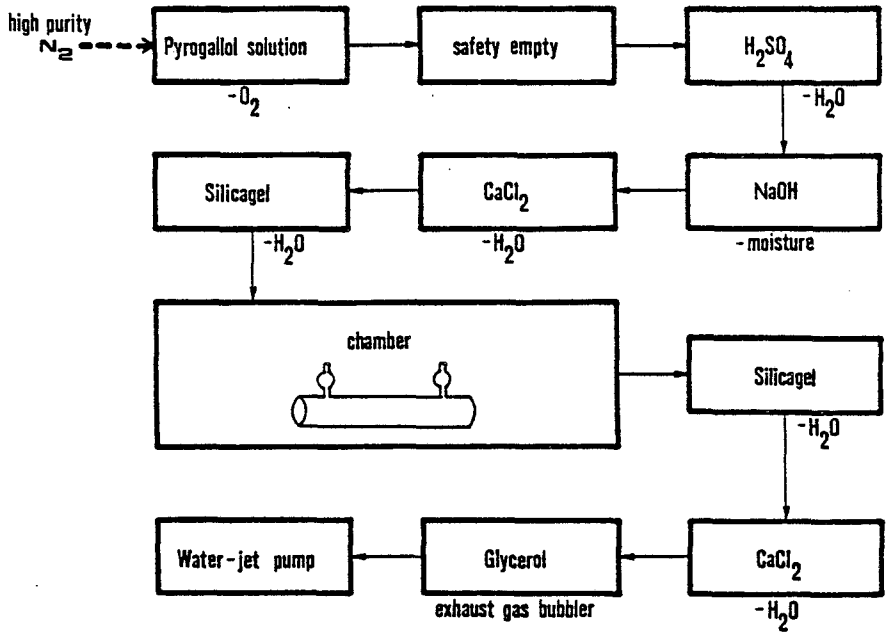

Figure 1 Oxygen removal facility

The anode signal from each PMT is fanned out into a constant-fraction discriminator (CFD) and a linear summing module (LSM). The outputs from the two discriminators feed the mean-timer module (MT).

We constructed a mean-timer module and a linear summing module based on a design by the Kent State nuclear group.[1,2] The pulse shape discriminator (PSD) was constructed based on a designed by Sperr et al[3] and incorporating the modification of Bialkowski and Szezepankowski[4] as well as some of our own. The PSD circuit has been described elsewhere.[5]

3. Performance of the prototype spectrometer

Figure 2 shows the pulse height variation as a function of the location of the incident radiation. Except for the position near the PMT the light attenuation is about a factor of 3 over the entire scintillator length for a single PMT. The sum of the light outputs is practically constant over the region far from the photomultiplier tubes. A pulse height variation of about 20 % is observed over the whole scintillator length.

Figure 3 displays the transit time taken by the photons to reach each photocathode. With the mean timing method the average of the photon transit times is independent of the position of the event.

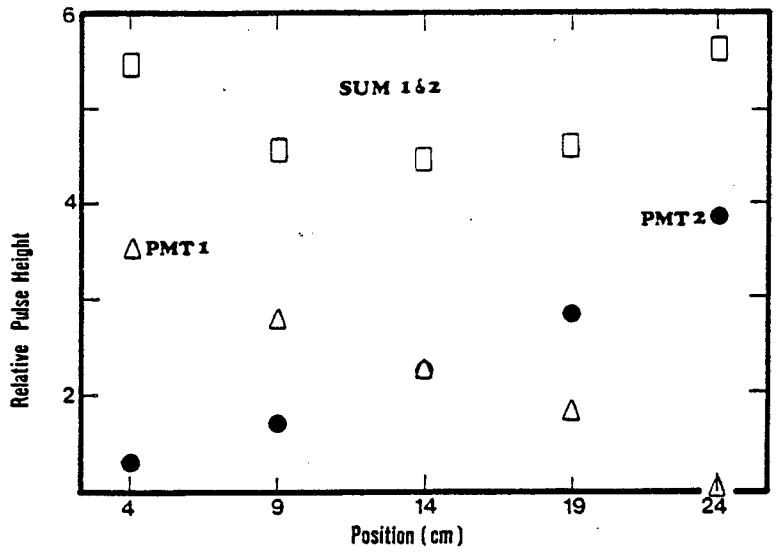

Figure 2 Pulse height variation within the scintillator

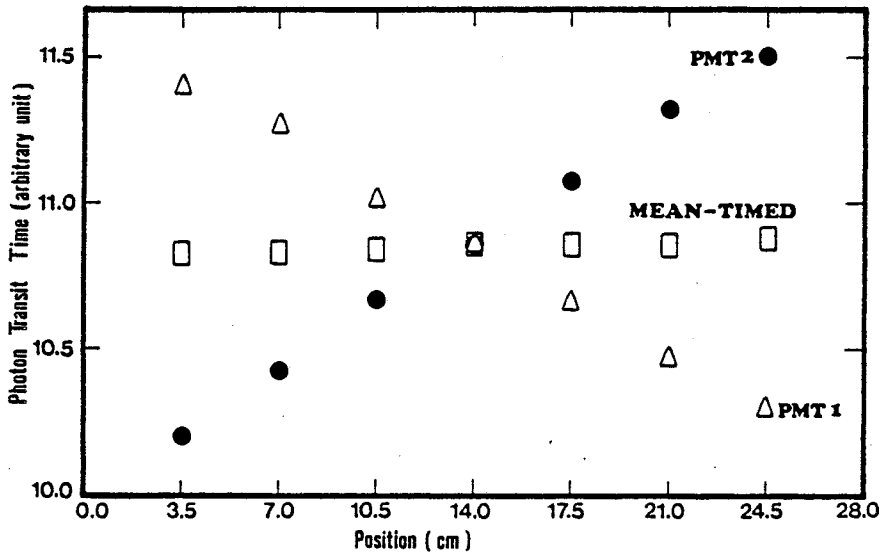

Figure 3 Variation of mean photon transit time within the scintillator

The PSD characteristic of the prototype detector was investigated using an Am-Be source. As shown in Figure 4 the best results were obtained by operating on the sum of the anode signals which confirms the finding of Carlson et al.[6]

We are now planning construction of a larger volume detector. The choice of scintillator material (liquid or plastic) deserves further study.

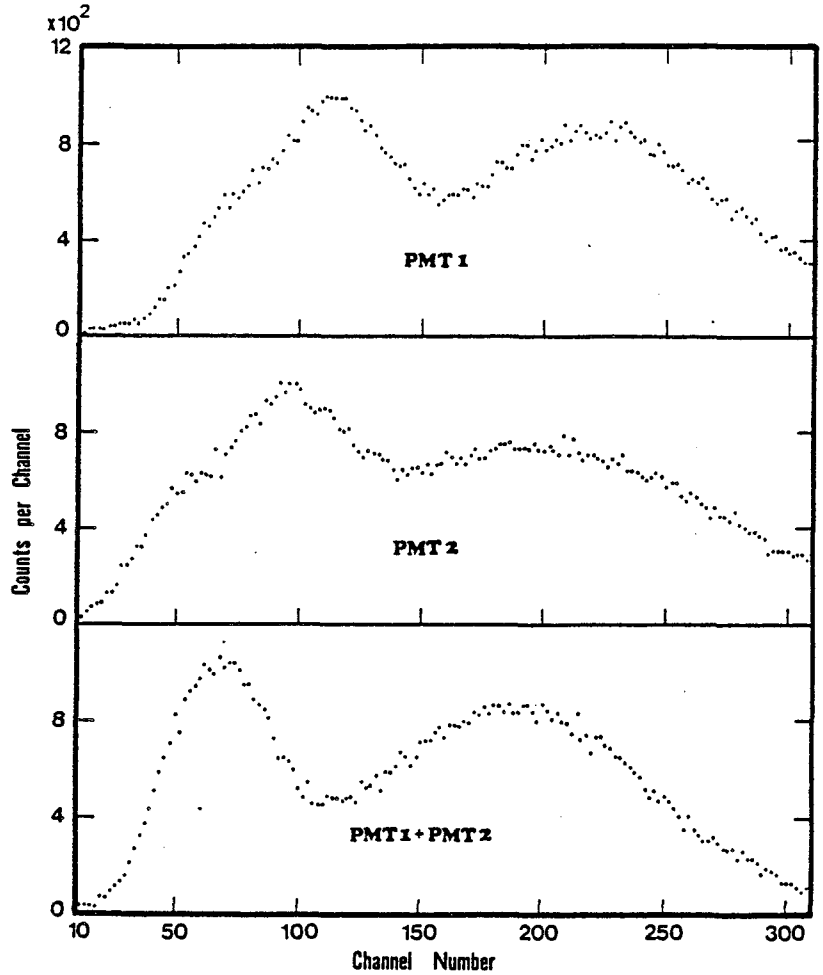

Figure 4 Pulse shape spectra with Am-Be source for a threshold setting at half the height of ^{60}Co peak

References

1. A.R. Balwin and R. Madey, Nucl. Instr. and Meth. 171(1980)149.
2. R. Madey and A.R. Balwin, Private communication.
3. P. Sperr, H. Spicler, M.R. Maier, and D. Evers, Nucl. Intr. and Meth. 116(1974)55.
4. J. Bialkowski and J. Szezepankowski, Nucl. Instr. and Meth 152(1978)589.
5. G.G. Hoyes, T. Vilaithong, and N. Chirapatpimol, INDC(TAI)-002/GI (1982).
6. J.D. Carlson, R.W. Finley, and D.E. Bainum, Nucl. Instr. and Meth. 147(1977)353.

The Calculations of Neutron and Photon Emission Cross Sections in Nonelastic Interaction of 14.5 MeV Neutrons with Mo Isotopes

A.Marcinkowski and M.Herman
Institute for Nuclear Studies, Warsaw

This work has been advanced under the Research Contract No 3241/RB of the International Atomic Energy Agency. The spectra of inelastically scattered neutrons and the accompanying gamma-ray spectra have been requested, for fusion research purposes, in WRENDA 81/82 /requests No 741-753/. Such data are also used in calculations of properties of the shielding materials. The cross sections have been calculated with use of the EMPIRE code [1], which accounts for the evaporation of neutrons, protons and alphas, as well as for the preequilibrium emission of nucleons. The full gamma-deexcitation cascades between and from the continuum of states were also contained in the calculations.

The compound nucleus contribution was calculated according to the standard Hauser-Feshbach formulation of the statistical model of nuclear reactions, with level densities by Cameron and Gilbert [2], parametrised by Reffo [3], partial wave transmission coefficients calculated from the optical potentials for neutrons [4,5], protons [6] and alphas [7], and gamma-ray cascades assuming E1, E2 and M1 transitions, with GDR effects included.

The calculation of the precompound contribution was based on the geometry dependent hybrid model [8], with the intranuclear transition rates calculated from the imaginary optical potential [6]. Both the precompound and compound nucleus components of the cross section are added incoherently. For more detailes the reader is referred to refs. [1,9]. The EMPIRE code takes part in the International

Table I

Calculated Cross Sections at 14.5 MeV

for ^{92}Mo in mb/MeV

Neutron Energy Bin	/n,n'//E_n,/	/n,nem//E_n,/	Gamma Energy Bin	/n,n'γ//E_γ/	/n,totalγ//E_γ/
0.5	314.8	531.8	0.25	20.9	554.3
1.5	346.1	417.7	1.0	139.4	759.0
2.5	245.4	251.8	2.0	246.3	724.2
3.5	142.2	142.5	3.0	247.0	402.1
4.5	81.5	81.5	4.0	187.0	260.1
5.5	49.5	49.5	5.0	118.3	162.5
6.5	33.5	33.5	6.0	67.0	81.2
7.5	25.9	25.9	7.0	35.3	40.8
8.5	22.5	22.5	8.0	17.5	19.2
9.5	21.2	21.2	9.0	8.5	8.6
10.5	19.8	19.8	10.0	3.9	3.9
11.5	18.5	18.5	11.0	1.3	1.3
12.5	15.1	15.1	12.0	0.4	0.4
13.5			13.0	0.1	0.1
14.5			14.0	0.05	0.05
Integrated	1335.9	1631.1		1092.7	3017.7

Table II

Calculated Cross Sections at 14.5 MeV

for ^{94}Mo in mb/MeV

Neutron Energy Bin	/n,n'//E_n,/	/n,nem//E_n,/	Gamma Energy Bin	/n,n'γ//E_γ/	/n,totalγ//E_γ/
0.5	251.8	881.6	0.25		156.8
1.5	458.4	819.8	1.0	99.3	1776.0
2.5	327.9	498.5	2.0	202.6	371.7
3.5	194.5	233.1	3.0	238.5	410.1
4.5	103.4	111.6	4.0	125.6	162.5
5.5	62.5	62.5	5.0	58.2	61.6
6.5	42.5	42.5	6.0	23.7	24.7
7.5	33.6	33.6	7.0	11.3	11.4
8.5	29.9	29.9	8.0	4.6	4.6
9.5	28.5	28.5	9.0	1.2	1.2
10.5	26.9	26.9	10.0	0.3	0.3
11.5	25.2	25.2	11.0	0.1	0.1
12.5	20.6	20.6	12.0	0.07	0.07
13.5	0.002	0.002	13.0		
Integrated	1605.7	2814.3		765.6	2981.1

Table III

Calculated Cross Sections at 14.5 MeV

for ^{95}Mo in mb/MeV

Neutron Energy Bin	/n,n'//E_n,/	/n,nem//E_n,/	Gamma Energy Bin	/n,n'γ//E_γ/	/n,totalγ//E_γ/
0.5	307.0	492.5	0.25		133.8
1.5	488.6	1296.1	1.0	114.7	3079.1
2.5	336.9	630.5	2.0	208.4	784.1
3.5	190.5	263.1	3.0	124.6	426.8
4.5	94.8	113.6	4.0	69.8	148.1
5.5	53.6	55.6	5.0	36.2	56.1
6.5	33.5	33.7	6.0	16.6	18.4
7.5	24.8	24.8	7.0	7.3	8.2
8.5	21.3	21.3	8.0	2.6	3.1
9.5	20.0	20.0	9.0	0.8	1.1
10.5	18.8	18.8	10.0	0.3	0.5
11.5	17.8	17.8	11.0	0.2	0.3
12.5	14.5	14.5	12.0	0.1	0.2
13.5	0.002	0.002	13.0	0.05	0.1
14.5			14.0	0.003	0.003
Integrated	1622.2	3002.4		581.6	4659.9

Table IV

Calculated Cross Sections at 14.5 MeV

for ^{96}Mo in mb/MeV

Neutron Energy Bin	/n,n'//E_n,/	/n,nem//E_n,/	Gamma Energy Bin	/n,n'γ//E_γ/	/n,totalγ//E_γ/
0.5	318.8	598.2	0.25	122.6	902.1
1.5	507.0	1272.5	1.0	174.2	2066.7
2.5	326.9	626.2	2.0	130.6	329.0
3.5	173.1	275.5	3.0	69.7	126.2
4.5	84.0	121.1	4.0	32.7	45.4
5.5	48.7	50.4	5.0	13.3	13.5
6.5	32.7	32.7	6.0	5.2	5.3
7.5	26.2	26.2	7.0	1.9	1.9
8.5	23.8	23.8	8.0	0.4	0.4
9.5	22.7	22.7	9.0	0.1	0.1
10.5	21.4	21.4	10.0	0.05	0.05
11.5	20.2	20.2	11.0	0.03	0.03
12.5	16.4	16.4	12.0	0.01	0.01
13.5	0.0005	0.0005	13.0		
Integrated	1684.9	3096.9		550.8	3490.6

Table V

Calculated Cross Sections at 14.5 MeV

for ^{97}Mo in mb/MeV

Neutron Energy Bin	/n,n'//E_n,/	/n,nem//E_n,/	Gamma Energy Bin	/n,n'γ//E_γ/	/n,totalγ//E_γ/
0.5	402.2	1337.4	0.25		232.5
1.5	497.5	893.0	1.0	86.8	3367.2
2.5	325.5	470.2	2.0	127.3	890.8
3.5	171.0	212.7	3.0	71.8	513.4
4.5	82.6	95.8	4.0	35.6	239.8
5.5	47.1	50.0	5.0	15.8	79.3
6.5	30.5	31.0	6.0	6.4	19.0
7.5	23.7	23.8	7.0	2.3	3.9
8.5	21.2	21.2	8.0	0.8	0.8
9.5	20.2	20.2	9.0	0.3	0.8
10.5	19.2	19.2	10.0	0.2	0.2
11.5	18.2	18.2	11.0	0.1	0.1
12.5	14.9	14.9	12.0		
13.5	0.001	0.001	13.0		
Integrated	1673.5	3207.3		347.3	5347.8

Table VI

Calculated Cross Section at 14.5 MeV

for ^{98}Mo in mb/MeV

Neutron Energy Bin	/n,n'//E_n,/	/n,nem//E_n,/	Gamma Energy Bin	/n,n'γ//E_γ/	/n,totalγ//E_γ/
0.5	460.1	1424.6	0.25		134.0
1.5	498.3	847.6	1.0	94.2	2095.1
2.5	306.2	420.3	2.0	149.3	892.6
3.5	151.5	181.6	3.0	102.5	434.0
4.5	74.1	82.4	4.0	48.3	67.6
5.5	44.9	45.6	5.0	20.5	20.5
6.5	32.2	32.2	6.0	7.3	7.3
7.5	27.2	27.2	7.0	2.9	2.9
8.5	25.2	25.2	8.0	1.0	1.0
9.5	24.1	24.1	9.0	0.2	0.2
10.5	22.8	22.8	10.0	0.1	0.1
11.5	21.5	21.5	11.0	0.03	0.03
12.5	17.5	17.5	12.0	0.02	0.02
13.5			13.0	0.01	0.01
Integrated	1706.3	3173.3		426.1	3655.4

Table VII

Calculated Cross Sections at 14.5 MeV

for ^{100}Mo in mb/MeV

Neutron Energy Bin	/n,n'//E_n,/	/n,nem//E_n,/	Gamma Energy Bin	/n,n'γ//E_γ/	/n,totalγ//E_γ/
0.5	484.5	1485.8	0.25		2091.8
1.5	497.6	862.4	1.0	140.3	2105.2
2.5	305.9	424.0	2.0	150.9	899.1
3.5	149.1	179.9	3.0	78.9	506.3
4.5	74.9	83.1	4.0	36.4	215.2
5.5	46.7	48.4	5.0	14.8	63.2
6.5	33.8	33.8	6.0	5.1	5.9
7.5	28.5	28.5	7.0	1.4	1.4
8.5	26.4	26.4	8.0	0.4	0.4
9.5	25.2	25.2	9.0	0.1	0.1
10.5	23.8	23.8	10.0	0.05	0.05
11.5	22.5	22.5	11.0	0.02	0.02
12.5	18.3	18.3	12.0		
13.5	0.0002	0.0002	13.0		
Integrated	1737.1	3261.9		428.4	5889.3

Nuclear Model Code Intercomparison, Spherical Optical Model Study at the NEA Data Bank, Saclay, with good results [9].

The calculated inclusive neutron and gamma-ray spectra following the nonelastic interaction of 14.5 MeV neutrons with ^{92,94,95,96,97,98,100}Mo contain contributions from the reaction channels /n,n/, /n,2n/, /n,p/, /n,pn/, /n,alpha/. In some cases the /n,np/ or /n,alpha n/ channel contributions have been calculated too. The neutron capture gamma-ray spectra following the compound nucleus decay have been found to be negligible at 14.5 MeV neutron energy. Thus the resulting gamma-ray spectra dont contain only the semidirect component due to neutron capture.

As a byproduct of the calculations described the activation cross sections for the /n,p/, /n,n/, /n,2n/ and some /n,alpha/ reactions have been obtained. These data could be refined by comparison with the results of measurements currently going on in the frame of the CRP. Such analysis seems highly desireable for impro-

ving the parametrisation of the preequilibrium model, which still contains at least one not too well recognized parameter, the fraction of particles in the initial exciton configuration being neutrons.

The numerical data are contained in tables I - VII.

References

1/ M.Herman, A.Marcinkowski and K.Stankiewicz, Comput. Phys. Commun., 1984 in press

2/ A.G.W.Cameron and G.Gilbert, Can. J. Phys. 43/1965/1446

3/ G.Reffo, CNEN Report RT/FI/78/11, Bologna 1978

4/ P.Moldauer, Nucl. Phys. 47/1963/65

5/ F.Björklund and S.Fernbach, Conf. on Nucl. Optical Model /Florida State University Studies No 32, Tallahassee, 1958/

6/ F.D.Becchetti and G.W.Greenlees, Phys. Rev. 182/1969/1190

7/ L.McFadden and G.R.Satchler, Nucl. Phys. 84/1966/177

8/ M.Blann, Nucl. Phys. A213/1973/570; Report COO-3494, 1974

9/ A.Prince, G.Reffo and E.Sartori, NEANDC-152"A", INDC/NEA/4 1983

Calculation of Cross Sections for Neutron Induced Reactions on Mo Isotopes at 14.5 MeV Energy

A.Marcinkowski and M.Herman
Institute for Nuclear Studies, Warsaw

Cross Sections of /n,n'/,/n,p/,/n,2n/ and /n,pn/ reactions for the isotopes ^{92,94,95,96,97,98,100}Mo have been calculated with use of the EMPIRE code [1,2], which is based on the standard, angular momentum dependent, formulation of the statistical model of nuclear reactions by Hauser and Feshbach. The preequilibrium emission was calculated according to the geometry dependent hybrid model [3], which has been extended in order to include the angular momentum effects. The calculated total reaction cross sections and cross sections for population of metastable states in the residual nuclei are intended for comparison with activation cross sections measured by the participants of the CRP. Such analysis should result in improving the parametrisation of the model and the calculational scheme itself. The results of calculations are presented in the following tables.

References

[1] M.Herman, A.Marcinkowski and K.Stankiewicz, Comput. Phys. Commun., 1984 in press

[2] G.Reffo, CNEN Report RT/FI/78/11, Bologna 1978

[3] M.Blann, Nucl. Phys. A213/1973/570; Report COO-3494, 1974

Table I

Comparison of the calculated cross sections in mb with experimental results

Reaction	/n,n'/	/n,p/			/n,alpha/			
Target	calc.	calc.	exper.	ref.	calc.	exper.	ref.	misc.
^{92}Mo	497	97			35	18.7±1.5	a	
						22.0±3	c	
						24.0±6	f	
						25.0±3	d	
						28.1±2	e	
		66	60±10	h	8.6	2.5±0.3	k	isomers
			62.5±4	a		3.6±0.6	c	+2, 10.2d
						7.4±0.6	g	-0.5,4.2m
						9.4±0.9	a	
^{94}Mo	393	44						
		29	6.0±1.5	h				isomer
^{95}Mo	174	41	37.0±6	c	4.2			
		5						isomer
^{96}Mo	239	20	16.0±3.0	m	1.2			
			19.2±2.1	d				
			21 ±7	l				
			21.3±1.5	a				
^{97}Mo	170	34	15.9±1.3	a				
			17.7±1.5	m				
			68.0±14	l				
		10	5.0±1.1	f				isomer
			7.4±0.8	a				-0.5, 1m
^{98}Mo	240	12			0.6	8.1±1	a	72m
		6	4.1±0.5	a				isomer
			6.7±0.6	m				+5, 51m
			7.3±0.8	i				
			9±2	h				
^{100}Mo	214	6	9±1	f	0.3	14.0±6	l	

Table II

Comparison of the calculated cross sections in mb with the experimental results

Reaction	/n,2n/			/n,pn+np/			
Target	calc.	exper.	ref.	calc.	exper.	ref.	misc.
^{92}Mo	157	132±21	b	93+680	112	h	15.5m
		158±5	m				
		161±1.5	n				
		211±16	g				
		226±11	f				
	11	7±2	r	21+159			isomer
		16.2±1.2	p				-0.5, 66s
		17.4±3.2	j				
		19±3	f				
		22.1±1.6	g				
^{94}Mo	1174			35			
	14	3.5±0.5	f				isomer
^{95}Mo	1368			9			
^{96}Mo	1407			3.7+1.3			
				0.3+0.3			isomer
^{97}Mo	1503			23			
^{98}Mo	1466			0.4			
^{100}Mo	1522	1389±84	p	1.2			66h
		1390±60	j				
		1510±180	m				

a Phys. Rev. C1/1970/358, b J. Phys. Soc. Jap. 12/1957/443, c Proceed. Conf. Chem. Nucl. Data Canterbury 1971, d Proceed. 8th Conf. Fusion Techn. 1974, e Phys. Rev. C4/1971/1173, f Physica Scripta 24/1981/935, g J. Inorg. Nucl. Chem. 37/1975/631, h Phys. Rev. 131/1963/2649, i BARC Conf. Chandigarh-India 2/1972/115, j Nucl. Phys. A185/1972/614, k Nucl. Phys. A181/1972/101, l Nucl. Phys. 30/1962/49, m Nucl. Phys. A103/1967/616, n Nucl. Phys. A139/1969/42, p Phys. Rev. C1/1970/350, r Proceed. Conf. Small Accelerators, Oak Ridge 1960

Studies of (n,^{3}He), (n,tα), (n,2n) and (n,d) reactions at 14 MeV

Đuro Miljanić
Rudjer Bošković Institute, Zagreb, Yugoslavia

In the period November 1982 - November 1983 the following work was done

1. Study of (n,^{3}He) reactions

Data from the measurement of the ^{40}Ca(n,^{3}He)^{38}Ar reaction (the first measurement of any (n,^{3}He) reaction angular distribution ever done at $E_n \leq 15$ MeV) were compared with DWBA calculations. The agreement of the calculations with the data supports the assumption that in this case direct reaction mechanism is still dominant at these energies. Measured cross section is much higher than all other cross sections measured by activation technique. From the data on (n,^{3}He) and (^{3}He,n) reactions on different nuclei it was concluded that the differences in (n,^{3}He) cross sections for $E_n \approx 14$ MeV could be attributed mainly to Coulomb effects. This is best seen in Fig.1. Fig. 1a shows available data on

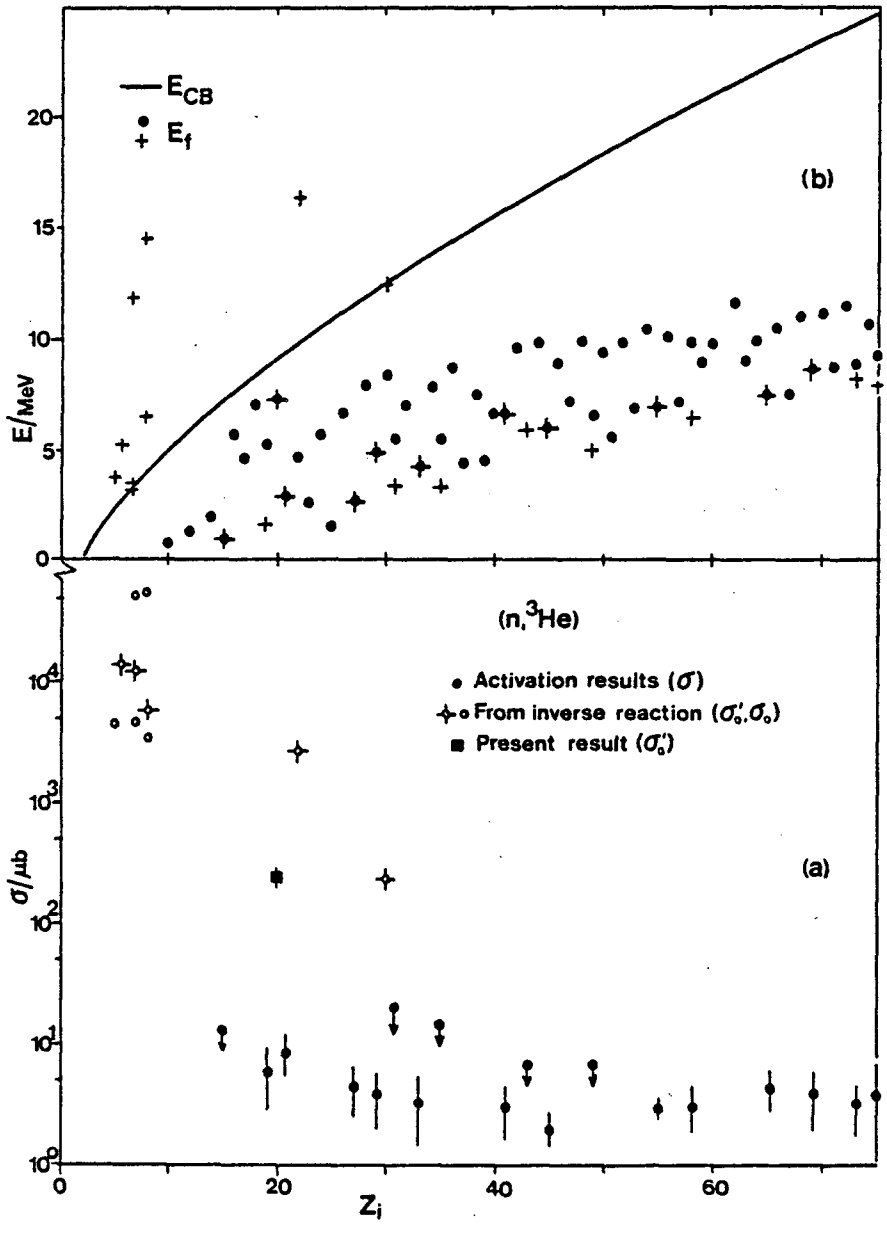

Fig. 1.

($n,^3He$) reactions. The curve on Fig. 1b represents Coulomb barrier height for ^3He, while crosses are centrum-of-mass energies available in ^3He channel of the ($n,^3He$) reaction for E_n= 14.6 MeV and for the nuclides, for which ($n,^3He$) data exist. Correlation of the cross section values and the positions of these energies in respect to Coulomb barrier is obvious. More information on this study will be found in [1].

2. Study of the $^7Li(n,t\alpha)n$ reaction

Measurements of the $^7Li(n,t\alpha)n$ reaction are in progress. Special kinematical condition had to be used in order to shorten the time of the experiment. Outgoing tritons and α-particles are detected in coincidence in 3 solid state detectors. Alternative approach using 3 proportional counters and 1 solid state detector will also be used.

3. Study of (n,2n) reactions

Theoretical and experimental work was done in this study. It was estimated direct ($n,^2n^*$) reaction contribution to the (n,2n) reaction cross section ($^2n^*$ - $^1S_0$ neutron-neutron final state interaction). It was concluded, that these contributions are not large, but they could be observed anyway due to energy and space correlation of two neutrons from $^2n^*$. A more detailed information on these calculations can be found in [2]. A system for 2n coincident measurement was completed. It consists of 2 liquid scintilator neutron detectors and 1 associated particle detector with associated electronics. With this system two neutrons will be detected in coincidence and their energies will be determined by the time-of-flight method.

4. Measurement of the $^{27}Al(n,d)^{26}Mg$ reaction cross section

A preliminary measurement of the $^{27}Al(n,d)^{26}Mg$ reaction was done using a standard counter telescope consisting of proportional counters and a solid state detector.

[1] Đ. Miljanić, M. Zadro and D. Rendić, Nucl. Phys. A, to be published

[2] M. Zadro and Đ. Miljanić, Z. Phys. A - Atoms and Nuclei, 312 (1983) 257

Fine structure in the neutron emission spectrum from 14 MeV neutron bombardment of Fe

K. Gul
Pakistan Institute of Nuclear Science and Technology
Nilore, Rawalpindi - Pakistan

The Neutron generator Laboratory at PINSTECH, Pakistan, has been participating in the IAEA coordinated research programme since October 1982. The Neutron Generator is of transformer type having a 150 KV power supply capable of 1 milliampere current. However it being about 20 years old, it is providing a maximum current of 300 microamperes only. It is sufficient for on line neutron spectroscopy work. The neutron generator is housed in a hall measuring 13.3 meters long, 5.6 meters wide and 3.2 meters high. The neutron producing target is about 1 meter above the floor. For gamma-rays production cross section measurements, another small room of size 2.9 meter in length, 2.3 m in width and 3.2 meters in height has been erected. This has resulted in aggravating the general neutron background in the hall. However now the neutron detector along with its shielding has been shifted into this small room and the neutron generator is rotated rather than the detector for angular distribution measurements.

We have repeated measurements on Fe and Al under different conditions than before with better energy resolution and better signal to background ratio. The neutron detector along with its shielding was placed in the small room built in the neutron generator hall and a 3 m flight path was used. In the last few months our efforts were mainly centered on the identification of fine structure in the neutron emission cross-sections. Evaporation and pre-equilibrium models cannot explain fine structure in the neutron emission cross-sections and thus the presence of fine structure demonstrates the contribution

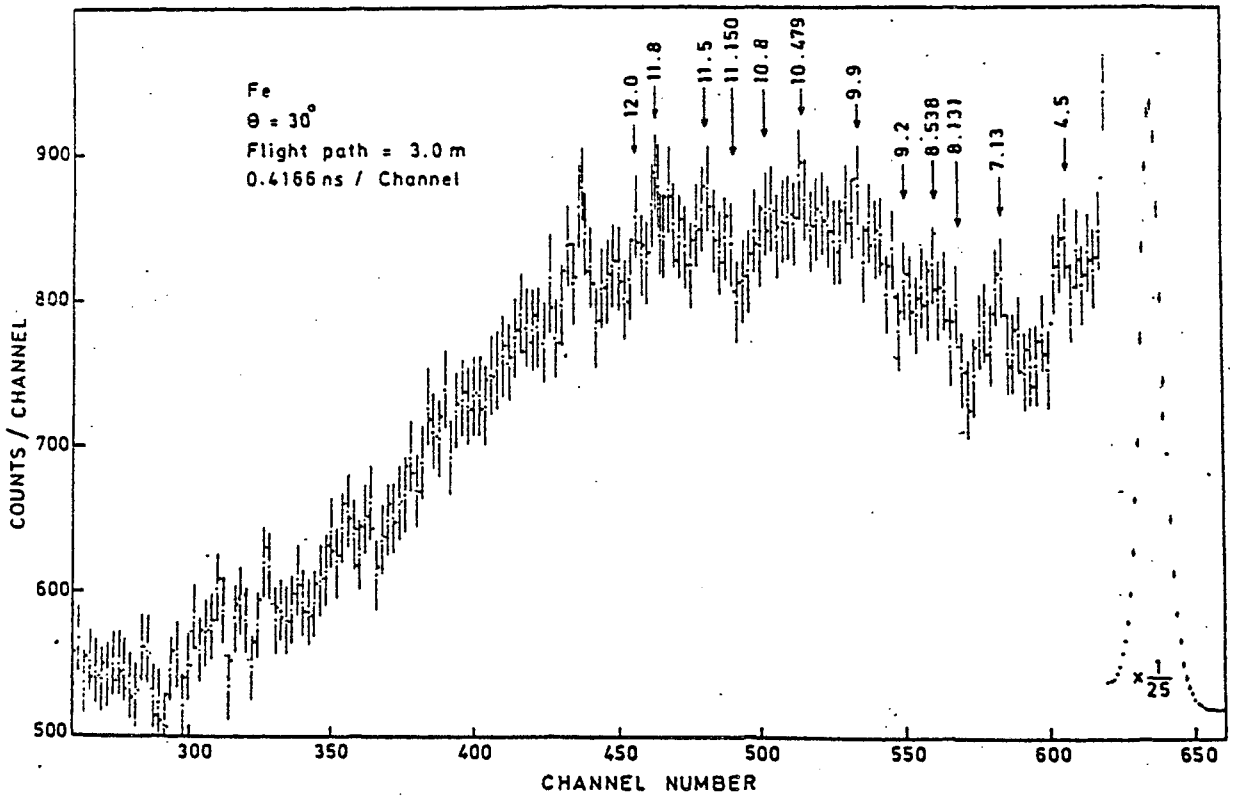
Fe
θ = 30°
Flight path = 3.0 m
0.4166 ns / Channel
12.0
11.8
11.5
11.150
10.8
10.479
9.9
9.2
8.538
8.131
7.13
4.5
×1/25
COUNTS / CHANNEL
CHANNEL NUMBER

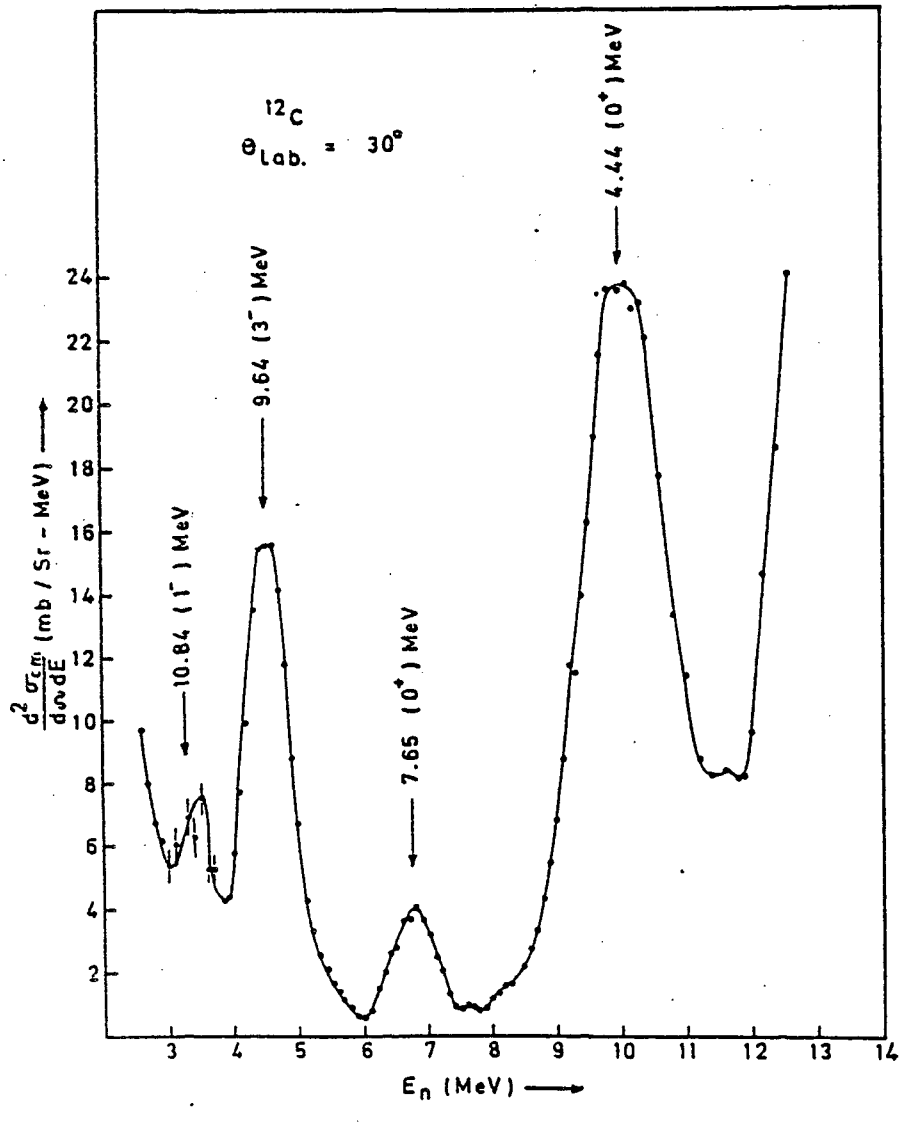
12C
θLab. = 30°
4.44 (0+) MeV
9.64 (3-) MeV
10.84 (1-) MeV
7.65 (0+) MeV
d²σc.m./dΩdE (mb / Sr - MeV)
En (MeV)

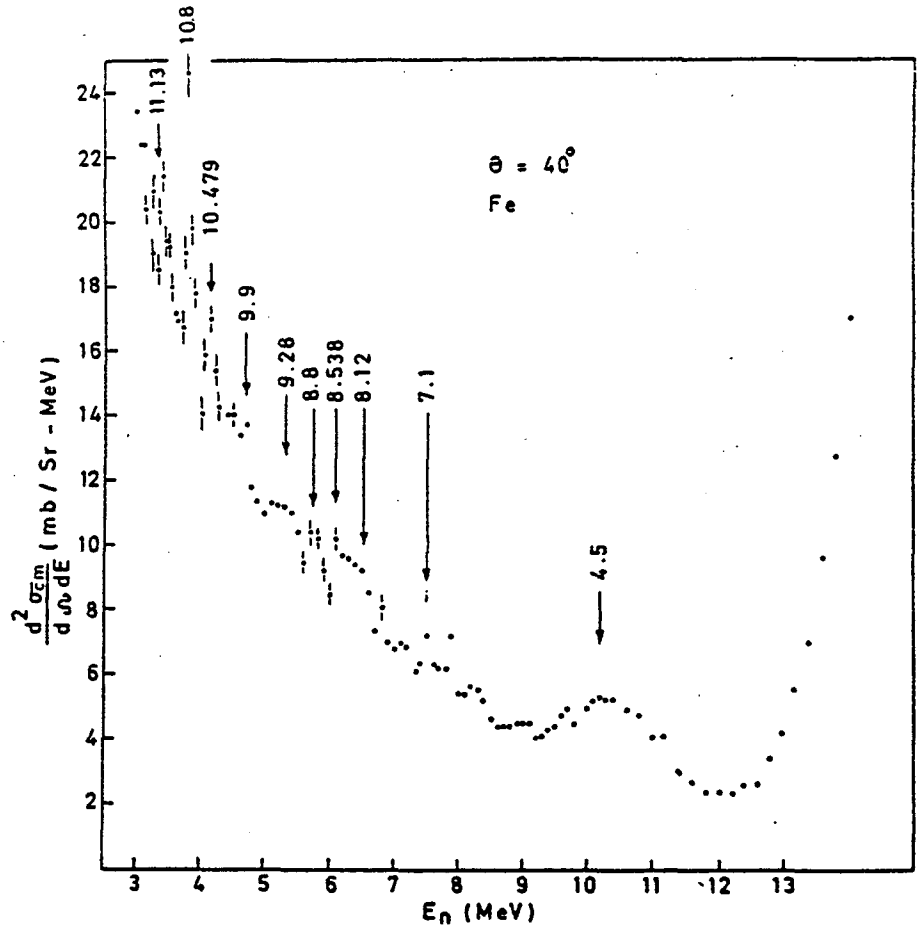
θ = 40°
Fe
11.13
10.8
10.479
9.9
9.28
8.8
8.538
8.12
7.1
4.5
$\frac{d^2\sigma_{cm}}{d\omega dE}$ (mb / Sr - MeV)
E_n (MeV)

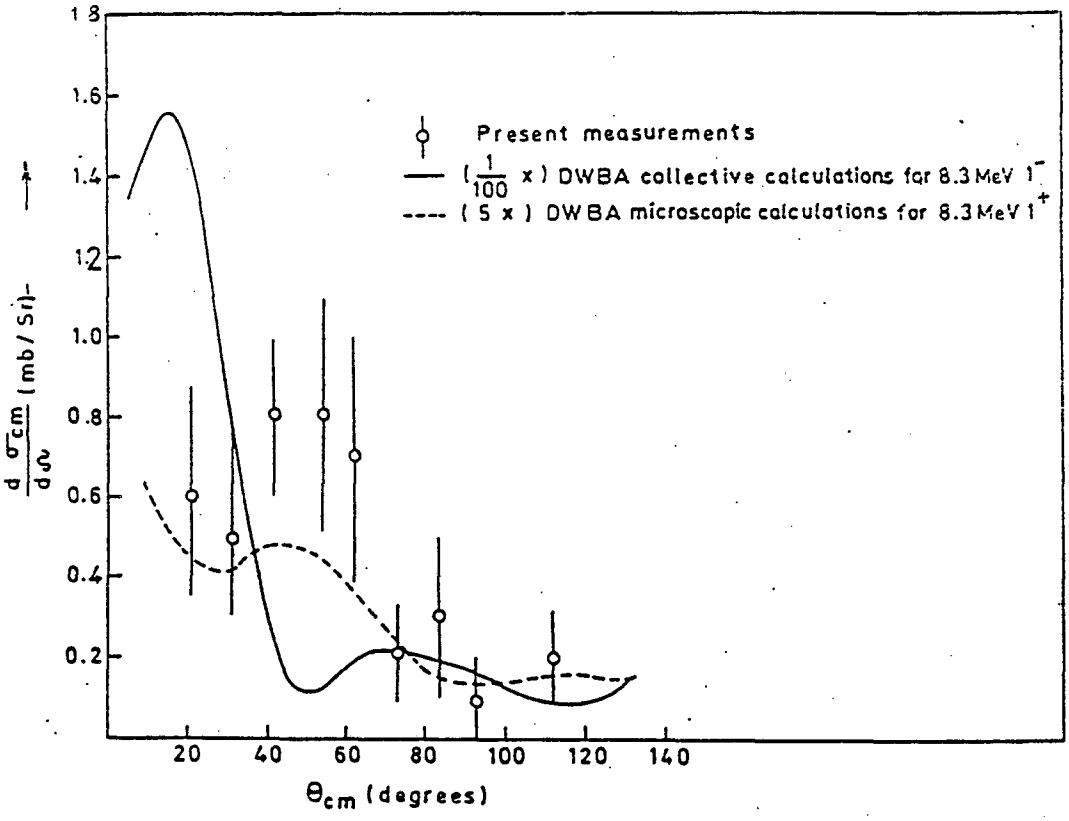
Present measurements
($\frac{1}{100}$ x) DWBA collective calculations for 8.3 MeV 1⁻
(5 x) DWBA microscopic calculations for 8.3 MeV 1⁺
$\frac{d\sigma_{cm}}{d\omega}$ (mb / Sr)
θ_{cm} (degrees)

of direct reactions to the neutron emission mechanism. Figure 1 shows a time-of-flight spectrum of 14.7 MeV neutrons scattered from Fe at 30°. In Figure 2 is shown similar spectrum for ^{12}C. The neutron emission spectrum for Fe at 40° is shown in Figure 3 which shows structure in neutron emission cross-sections and its correlation to levels in ^{56}Fe. In Figure 4 is shown the angular distribution of 8.3 MeV excitation group and calculations for two values of spin-parity i.e. 1^- and 1^+. An enhancement factor of 1936 has been included in the microscopic DWBA calculation for 1^+ spin-parity value.

For the measurements of the production of gamma-rays we intend to use Ge(Li) detectors for precise energy measurements of the gamma-rays. Our first job was to measure the gamma-ray detection efficiencies of 100 CC Ge(Li) detector and an intrinsic germanium detector. This we have done on our 5 Mega-Watt research reactor using ^{35}Cl (n, γ) ^{36}Cl and ^{14}N (n, γ) ^{15}N reactions.

MEASUREMENTS OF THE TOTAL PROTON EMISSION CROSS SECTION FOR NEUTRON INDUCED REACTION ON ^{58}Ni AT 18.5 MeV.

B.Mariański, J.Rondio, A.Korman

Institut for Nuclear Science, Warsaw, Poland

The ^{58}Ni/n,p/ reaction for 2-25 MeV neutron energy range plays an important role in the dosimetry [1]. Thus, the precise determination of the proton emission cross section for this reaction is needed. The available data for that reaction are very scarce above 15 MeV [2]. They are all obtained by activation method.

The differential proton emission cross sections for neutron induced reaction on ^{58}Ni were measured in this work at 18.5 MeV. Neutrons were produced in the ^{3}T/d,n/^{4}He reaction, the deuterons being accelerated to 2,3 MeV in a Van de Graaff accelerator. The neutron energy spread, due to the deuteron energy loss in T-Ti target and the geometrical conditions, was about ± 150 KeV. The experiment was carried out with the help of the eight-telescope chamber [3]. Proton spectra were obtained for 14 angles from 10° to 150° in 10° step. The absolute normalization of the cross sections was provided by measuring the protons recoiled from the poliethylene target.

The angle-integrated proton spectrum obtained in this work is shown in fig.1 and compared with the results of the combined preequilibrium /Hybrid model/ and multistep nuclear reaction Hauser-Feshbach calculations. The calculations were made with the help of the "EMPIRE" code [4] and included the contributions from the /n,p/ and /n,np/ reactions, and the preequilibrium contribution in the first step of the reaction. The calculated σ/n,p/ contains also σ/n,pn/, σ/n,2p/ and cross sections of other reactions in which the proton is emitted as a first particle. The optical model parameters used in this calculation were those proposed by Beechetti and Greenleess [5] for protons and neutrons and by Satchler and Mc Fadden [6] for α-particles. Level density parameters were taken from ref.[7]

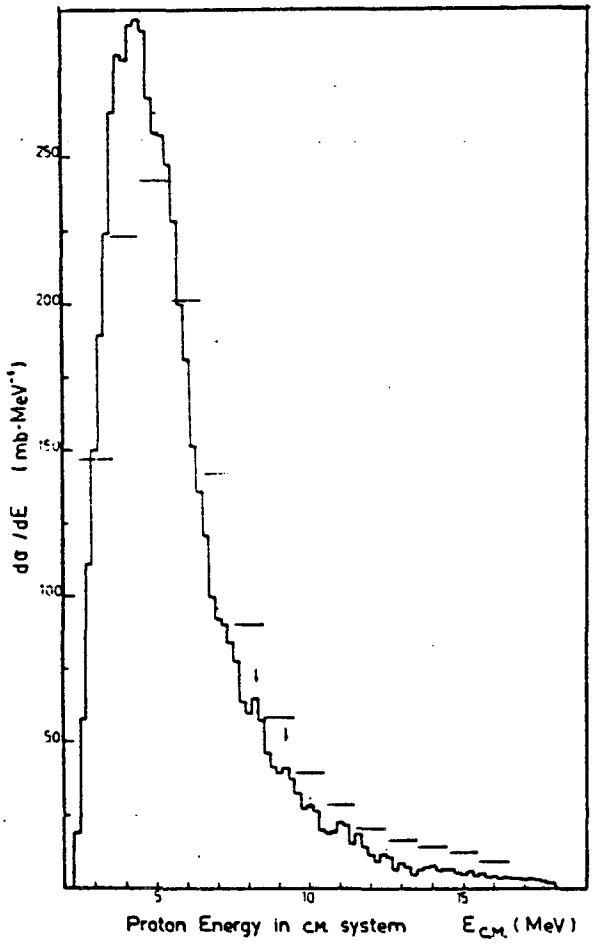

Fig.1. The angle integrated spectrum of protons from the neutron induced reaction on ^{58}Ni at 18.5 MeV. The horizontal bars represent the results of combined preequilibrium multistep Hauser-Feshbach calculations.

We see that, in general, there is agreement as regards the shape and the "EMPIRE" results, although the latter exceeded our data, especially in the high energy region of the spectrum. We believe, however, that the shape of the compound /n,p/ and /n,np/ spectra given by the "EMPIRE" code are properly described and can be used to determine σ/n,p/ and σ/n,np/. The total proton emission cross section $\sigma_{\pi}^{p} = \sigma$/n,p/ + σ/n,np/ cannot be obtained by integrating the experimental spectrum because below about 5 MeV there are additional protons due to the /n,p/ reaction induced by neutrons from D/d,n/^{3}He reaction on deuterons gathered in the Ti-T target during the measuring.

Thus the angle integrated experimental spectrum was fitted by the sum of /n,p/ and /n,np/ compound spectra the ratio σ/n,p/$/\sigma$/n,np/ being suitably adjusted. The compound σ/n,p/ has been obtained by integrating the normalized /n,p/ "EMPIRE" spectrum in the whole energy range. Then the cross sections of noncompound processes have been added to the above one. Those are transitions which excite the analogs of E1 GDR seen in the proton spectra about 8-10 MeV and direct processes dominating in the high energy part of the spectrum. The obtained σ/n,p/ for ^{58}Ni is 604 mb. The estimated error is about 15% and arises mainly from the uncertainty in the determination of the σ/n,p/$/\sigma$/n,np/ ratio. The σ/n,np/ obtained in the same way is 369 mb but the error is twice that for the σ/n,p/. The σ_{π}^{p} is 973 mb and the error only about 10% because the influence of uncertainty as to the σ/n,p/$/\sigma$/n,np/ ratio is in this case much smaller.

The cross sections for neutron induced reactions on ^{58}Ni obtained by the activation method are:
σ/n,p/ = 220 mb [8] or 328 mb [9] and σ/n,pn/ + σ/n,np/ = 230 mb [10].
The last value was evaluated by Guenter et al [11], in view of the probable systematic error at 800 mb. Our σ_{π}^{p} can be compared with the sum of the above cross sections, because the cross sections of other reactions which give contribution are negligible. Reasonable agreement is obtained when the evaluated value of σ/n,np/ + σ/n.pn/ is taken.

References:

1. Symposium on Neutron Cross-Sections from 10 to 40 MeV 1977, ed, M.R.Bhat and S.Pearlstein, BNL-NCS-5068
2. Handbook on Nuclear Activation Cross-Sections IAEA 1974
3. A.Korman, B.Mariański, J.Rondio, Nucl. Instr. Meth. 206 /1983/ 421
4. M.Herman, A.Marcinkowski, and K.Stankiewicz, Computer physics communications, to be published.
5. F.D.Becchetti, Jr., and G.W.Greenless, Phys.Rev. 182 /1969/ 1190
6. W.R.Mc Faden and G.R.Satchler, Nucl. Phys. A84 /1966/ 177
7. A.Gilbert and A.G.W.Cameron, Can. J.Phys. 43/1965/1146
8. M.Bormann, F.Dreyer, U.Zieliński, Rep. EANDC /E/ 66 "U", NEA, Paris /1966/ 42
9. P.Decowski, W.Grochulski, A.Marcinkowski, K.Siwek, J.Śledzińska, Z.Wilhelmi, Nucl. Phys. A112 /1968/ 513
10. J.M.F.Jeronymo, G.S.Mani, J.Olkowsky, A.Sadeghi and C.F.Williamson, Nucl. Phys. 47 /1963/ 157
11. P.Guenther, A.Smith, D.Smith, J.Whalen, and R.Howerton, Argonne National Laboratory Report No ANL/NDM - 11, 1975 /unpublished/.

"THE MULTISTEP COMPOUND MECHANISM CONTRIBUTION TO INELASTIC SCATTERING OF 14.6 MeV NEUTRONS FROM ^{181}Ta."

M.Herman, A.Marcinkowski - Institute for Nuclear Studies, Warsaw
K.Stankiewicz - Institute of Nuclear Energy, Świerk

The problem of the quantum approach to precompound emission, for the first time, was addressed in the work of Agassi et al. [1], which up to now appears to be a most general formulation of the process, known as the multistep compound MSC mechanism. The next step toward applicable model, was made by Feshbach, Kerman and Koonin [2], who introduced two separate mechanism to account for a precompound emission. The one, refered as multistep compound , describes the flow of the flux through the series of doorways of increasing complexity, each of them containing only bound nucleons. The characteristic feature of the MSC mechanism is a symetric angular distribution, which results from the fundamental random phase approximation. The formulation of Feshbach et al. differs from that of Agasi et al. in additional assumptions, which significantly simplify the cross section formula, and make calculations feasible. Recently some papers, concerning /p,n/; /n,p/ and /^{3}He,p/ reactions have been published by Milan-Naples group [3]. Their conclusions are in favour of MSC mechanism, which reproduced correctly the particle spectra as well as doorway state widths. These results motivated us to incorporate MSC formalism into the statistical model code "EMPIRE" [4].

The precompound part of the calculations was programmed and executed according to the example contained in the original paper of Feshbach et al [2]. An exciton representation for the partition of Hilbert space was adopted. The spin distribution of exciton levels was derived from shell model combinatorial calculations by Reffo and Herman [5]. The two-body residual interaction, was taken in the form of the δ-function. Following Feshbach et al. all radial wave functions were taken constant inside the nuclear volume, so that radial overlap integrals could be easily calculated. The three exit modes, altering exciton numbers by -2, 0 or +2, were allowed for particles escapeing the composite system. For each exit mode the strict angular momentum coupling was performed. The energy independent parts of X-matrices, containing angular momentum coupling coefficients, were prepared in advance, stored and used throughout the calculations. For the purpose of the present work, the strength function for the formation of the first doorway state was approximated by optical model transmission coefficient.It should be pointed out that due to this approximation, the formulation does not depend on the residual interaction strength. The distinction between neutrons and protons was not carried out explicitely, but appropriate coefficients, reflecting the contribution of the given kind of nucleons to the considered configuration, were taken into account in the calculations of the escape widths.As far as a treatment of the r-space is concerned, we used the standard Hauser-Feshbach theory which is expected to be equivalent to the MSC r-space contribution, being at the same time much better parametrized and easier to handle.

The calculations were performed for inelastic scattering of neutrons from ^{181}Ta. The neutron scattering was chosen because of its importance

for reactor and dosimetry applications and since it was not included in the previous analyses done by the Milan-Naples group. The incident neutron energy was set at 14.6 MeV to fit experimental data of Hermsdorf et al. [6]. It was assumed, that an entrance channel couples to the first doorway, which has a three exciton structure. Two further steps, characterized by 5 and 7 excitons respectively, were allowed for in the equilibration chain. The results of the calculations are displayed in Fig.1,2 and 3. In Fig. 1 the relative values of the damping width and of the escape width are shown for different stage numbers N /exciton number equals 2N + 1/ as the function of spin. In the case of $\Gamma^{\downarrow}$ a good agreement with the results of Bonetti [3] is found, in contradiction to the results of Feshbach et al.[2]. On the other hand, our predictions for $\Gamma^{\uparrow}$ are in disagreement with those

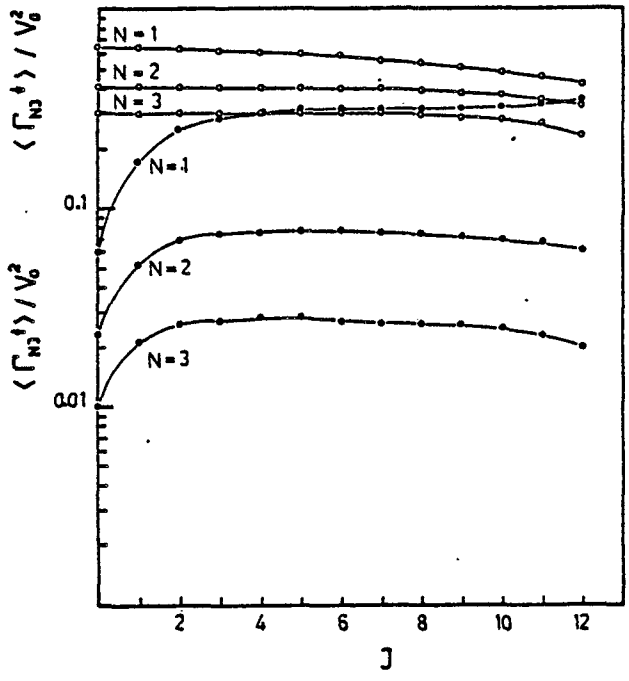

Fig. 1 Damping widths /open circles/ and escape widths /closed circles/ relative to the residual interaction strength as a function of spin.

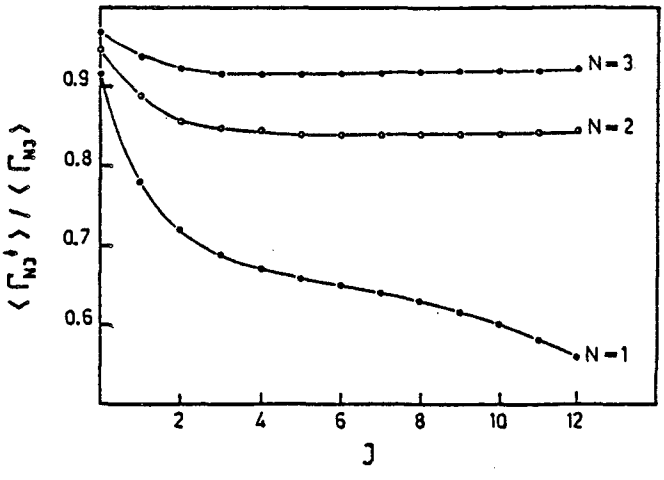

Fig. 2. Transmission probability as a function of spin.

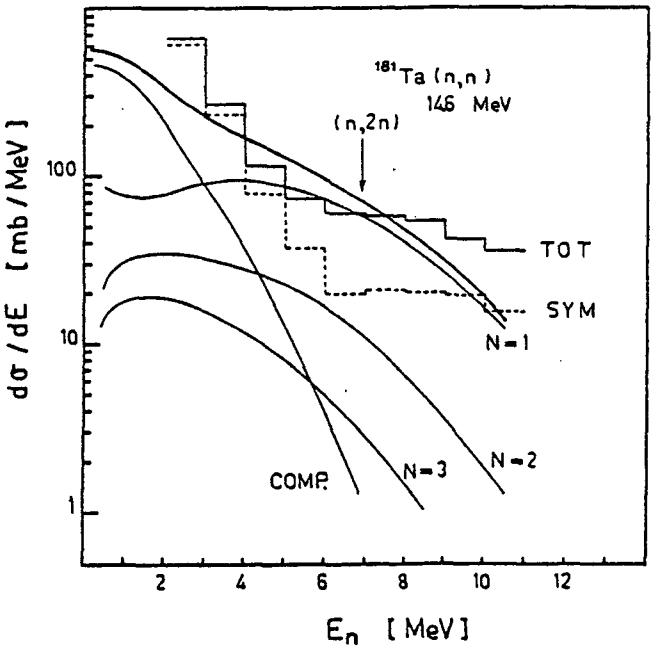

Fig. 3. Experimental and calculated neutron spectrum. Solid line histogram represents angle integrated data of Hermsdorf [6], while dashed line histograms shows symetric part of the spectrum. Solid curve displays present calculations. The contributions from different stages are also presented. An arrow marks /n,2n/ threshold.

of Bonetti et al., who made the calculations however for much lighter nuclei. One can conclude from Fig. 1 that $\Gamma^{\downarrow}$ and $\Gamma^{\uparrow}$, both show a slight spin dependence, and that escape widths decrease much faster with N than damping widths do. The following figure presents transmission probability for stages with given N as a function of spin. In this case all three papers disagree rather. Our results, at higher spins and N = 1 resemble those of Feshbach, but in general our emission is greater by a factor of 3.

In order to compare the calculated spectra with the experimental data of Hermsdorf [6] the latter ones were angle integrated. Because of the nature of the MSC mechanism, which provides symetric angular distribution for emitted particles, the symetric portion was extracted from the experimental data for comparison. This was done under the assumption of no direct process contribution to the backward angles. The analysis showed, that the symetric part, which may be connected with the MSC mechanism, amounts to about 80% of the total spectra, and this factor was applied to reduce the reaction cross section used in the present calculations. The results are compared in Fig. 3. The total calculated spectrum /heavy solid line/ is shown together with the contributions from subsequent stages of the reaction. It appears, that the predicted spectrum overestimates the symetric portion of experimental data /dashed line histogram/ in the energy range from 4 to 10 MeV. To achieve an agreement the reduction of MSC emission by a factor 3 would be required. There is some indication that adequate densities of accessible states , accounting for the bound particles only,

might result in lower cross section in agreement with experiment. Further improvements on this preliminary calculations are in progress.

References

1. D.Agassi, H.A.Weidenmüller and G.Mantzouranis, Phys. Rep. 22 /1975/ 145
2. H.Fashbach, A.Kerman and S.Koonin, Ann of Phys. 125 /1980/ 429
3. R.Bonetti, L.Colli Milazzo and M.Melanotte, Phys. Rev. C27 /1983/ 1003, and ref. therein.
4. M.Herman, A.Marcinkowski,and K.Stankiewicz Comp. Phys. Comm. to be published.
5. G.Reffo and M.Herman, Nuovo Cim. Lett. 34 /1982/ 261
6. Ditrich Hermsdorf, Andreas Meister, Sasson Sassonoff, Dieter Seeliger, Klaus Seidel, Fayez Shahin, report ZfK - 277 /U/ 1975.